Michael A. Hunter
Candidate

Psychology
Department

This dissertation is approved, and it is acceptable in quality and form for publication:

Approved by the Dissertation Committee:

Vincent P. Clark , Chairperson

Katie Witkiewitz

Vince Calhoun

Eric Schumacher

Expanding Your Cognitive Capacity: An Assessment of the Neuroplastic Changes Associated with Mindfulness Training and Transcranial Stimulation

by

Michael A. Hunter

B.A., Philosophy, The University of New Mexico, 2009
B.S., Psychology, The University of New Mexico, 2009
M.S., Psychology, The University of New Mexico, 2013

DISSERTATION

Submitted in Partial Fulfillment of the
Requirements for the Degree of

Doctor of Philosophy

Psychology

The University of New Mexico
Albuquerque, New Mexico

May 2016

DEDICATION

I dedicate this dissertation to my beautiful wife, Joanna Hunter, and our newborn baby girl, Lilyann Hunter. Your love and presence in my life is the greatest accomplishment and gift of all. In memory of my father, Eric D. Hunter, and my grandparents, Bobby and Maryann Hunter, I dedicate this dissertation to you as well: Through the struggle and hardships of living on without your presence, I have strengthened a will toward the selfless pursuit of truth.

ACKNOWLEDGEMENTS

I would like to acknowledge and express my gratitude to my dissertation committee, Vincent P. Clark (Advisor), Katie Witkiewitz, Vince D. Calhoun, and Eric Schumacher, who have always been supportive and willing to offer their knowledge and expertise to benefit my graduate education. I would also like to thank Jose Cañive, Gerardo Villarreal, and Terran Lane for the continual mentorship and contributions to my career. I am grateful to have mentors who keep my long term goals in mind and who help me succeed.

I would also like to extend my gratitude to the National Science Foundation Graduate Research Fellowship Program (DGE-0903444) for their financial support, and to the National Academies Ford Pre-Doctoral Fellowship for their academic resources and financial support. I would also like to thank the Intelligence Advanced Research Projects Activity (IARPA) via contract #2014-131270006 and Charles River Analytics (CRA) for supporting this project (see disclosure below)

I also want to extend my appreciation to research assistants, Mika Armenta, Tristin Collar, Melanie Lueras, Tessa Frohe, and David Brown for their help with data collection and study coordination, and to Janet Vowels for her administrative support related to this project. I would also like to thank my fellow graduate students, Mike Trumbo, Sam Robinson, Aaron Jones, AJ O'Sickley, and Elizabeth McCallion, along with our previous post-docs, Brian Coffman, Greg Lieberman, and Matt Bezdek for their help with implementing the study and providing a solid support system for me throughout graduate school. I would also like to thank the personnel at CRA for their software and website development and design, and to our MRI technicians, Diana South and Catherine

Smith for their help, and many thanks to countless others who made this possible, including the participants who enrolled into the study.

Special thanks to my mother Lola Coca for her words of wisdom and to my brother Eric for reminding me of my long term goals, and to my wife Joanna who was always there for me when I needed her most. To my Father, I know you would be proud.

Disclosure: this research was supported by the Intelligence Advanced Research Projects Activity (IARPA) via contract #2014-131270006. The United States Government is authorized to reproduce and distribute reprints for Governmental purposes notwithstanding any copyright annotation thereon. The funders had no role in study design, data collection, analysis, decision to publish, or preparation of the manuscript. The views and conclusions contained herein are those of the authors and should not be interpreted as necessarily representing the official policies or endorsements, either expressed or implied, of IARPA, the Office of the Director of National Intelligence, or the U.S. Government.

EXPANDING YOUR COGNITIVE CAPACITY: AN ASSESSMENT OF THE NEUROPLASTIC CHANGES ASSOCIATED WITH MINDFULNESS TRAINING AND TRANSCRANIAL STIMULATION

by

Michael A. Hunter

B.A., Philosophy, The University of New Mexico, 2009

B.S., Psychology, The University of New Mexico, 2009

M.S., Psychology, The University of New Mexico, 2013

ABSTRACT

Given that mindfulness-based training techniques (MBT) stimulates and pushes one's core cognitive control capacity limits, brain stimulation techniques, such as transcranial direct current stimulation (tDCS), can be used to facilitate the ongoing neural patterns of functional connectivity toward long-lasting neuroplastic change. The current study assessed the combined effects of MBT with right frontal tDCS on cognitive control abilities and their corresponding brain patterns of activation using electroencephalography (EEG) and functional magnetic resonance imaging (fMRI). This study found an enhancement in working memory and sustained attention performance along with changes in the attention-related P3 component and its theta and alpha oscillatory profiles recorded by EEG. Furthermore, a reconfiguration in the chronnectome of large-scale resting-state networks was observed using resting-state fMRI, in addition to task-related changes in the polymodal neural architecture associated with encoding and adaptation, which may bridge the necessary connections from near to far transfer gains.

TABLE OF CONTENTS

LIST OF FIGURES

LIST OF TABLES

CHAPTER 1: INTRODUCTION

Cognitive and neuroscientific research over the past 60 years has shown that cognitive abilities, and their underlying neural architectures, change depending upon the experience of learning itself (Raisman, 1969; Cicchetti and Blender, 2006). Indeed, while neural plasticity refers to the brain's capacity for implementing reactive changes in response to one's environmental demands (Lövdén et al., 2010), cognitive plasticity refers to the enduring alterations in one's functional architecture, resulting in acquired "adaptive skills" (Mercado, 2008), or "sets of habits" (James, 1890). Knowing that neural and cognitive plasticity are interactive and dynamic processes (Thelen and Smith, 1996; Stiles, 2000), researchers can now intentionally shape the direction of "plasticity" by targeting core cognitive capacities using novel neuro- and cognitive enhancement techniques. Certainly, neuroplasticity-based interventions can be applied in various settings, providing benefits for those suffering from various cognitive and neurological impairments, or for those working under extreme, high-stress circumstances (e.g., military personnel, medical professionals, etc.), or even for individuals seeking their very own individualized self-improvement programs. Thus, the continual development in novel, individualized interventions, harnessed by the interplay of cognitive and neuroscientific methodologies, will soon lead a new era of cognitive enhancement and remediation within medicine, academia and the work industry.

The necessary ingredients for inducing cognitive and neural plasticity

A necessary condition to induce alterations in one's neural architecture is a substantial environmental (i.e., training) demand imposed upon one's cognitive capacity (Mercado, 2008; Lövdén et al., 2010). That is, in order to induce neuroplastic changes, a given system must be challenged beyond his or her asymptotic levels of performance, i.e., one's dynamic equilibrium, or baseline, as depicted in Figure 1 below. This framework is analogous to the typical learning curve: an initial rapid learning within a task—observed as increases in performance, which then approaches an asymptotic trajectory (Lövdén et al., 2010). Thus, prolonged deviations from one's baseline ability, which challenges one's current range of functional supply and cognitive system (yellow background in Figure 1), constitute the range by which change, or learning, that can be accrued (distance between dotted lines on the y-axis). Furthermore, this interval of time must be long enough in order to sufficiently push the system toward a new dynamic equilibrium, or baseline, with measurable changes in one's neural architecture and cognitive capacity.

Figure 1: Schematic model of induced plasticity between cognitive capacity and training (i.e., experienced environmental demands).

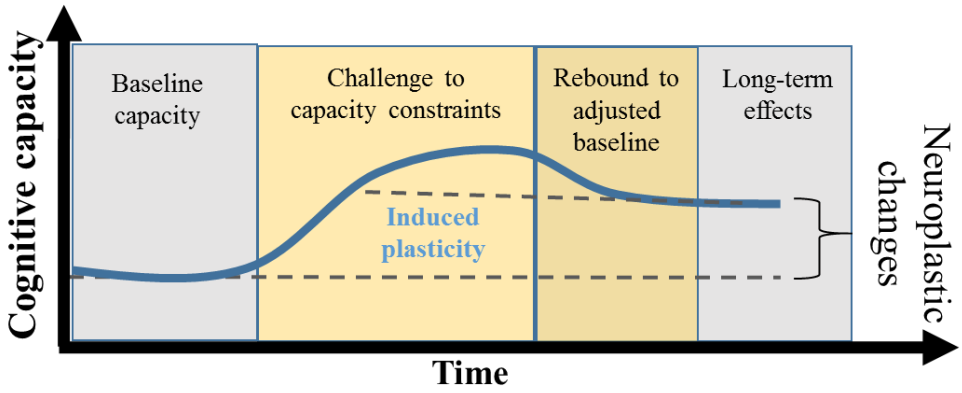

The induction of neuroplastic change requires a challenge to one's existing capacity constraints, which can be assessed at baseline and rebounds to an adjusted baseline, reflecting long-lasting training-related effects. Note that the y-axis represents units relative to the individualized range of possible functional and performance gains (e.g., working memory performance and its corresponding neural architecture).

Another central aspect of this model is the emphasis on learning constraints set forth by the intrinsic potential for plastic changes in one's existing neural architecture (i.e., individual differences in gross neural circuitry), which is largely determined by the previous manifestations of one's learning history (Kolb and Muhammad, 2014). There are several metrics that can be employed to assess these intrinsic functional characteristics, such as, resting-state metabolic supply through vascular integrity, volume conduction of white matter, and the gross neuroelectric signatures in response to particularly challenging tasks. To this end, experiments that directly assess these various

aspects of one's intrinsic potential for change (i.e., using the appropriate neuroimaging techniques) are necessary in order to assess the magnitude of changes due to learning (Jorgenson, 2015) and/or overall cognitive capacity (Mercado, 2008).

The need for assessing transfer effects

Central to the context of learning and the methods by which to evaluate cognitive training interventions is the concept of transfer (Cormier and Hagman, 1987). The notion of "transfer" is generally used to make the distinction between near and far transfer effects (Woodworth and Thorndike, 1901). Near transfer refers to training-induced effects on tasks close to those trained—as they share similar elemental properties. For example, a near transfer effect would be detected if improvements were observed on a visuospatial working memory task following training on a verbal working memory task. Conversely, far-transfer effects refer to improvements on tasks "elementally" different from those trained; for example, improvements on fluid IQ tasks following training on working memory tasks.

In regard to assessing the efficacy of the existing neuroplasticity-based interventions, there have been mixed results in the scientific community, suggesting that the currently established interventions do not produce effects that extend beyond the tests used to train and evaluate them. For example, there has been a rapid increase in the number of working memory training (WMT) studies published in the past decade, with the primary objective to establish far transfer of working memory performance to fluid intelligence. Although there have been some positive results in healthy (Klingberg, 2002;

Jaeggi et al., 2008) and psychiatric populations (see Lawlor-Savage & Goghari, 2014 for review), there have been other studies using identical WMT methods, but controlling for crucial methodological confounds, which failed to replicate (Redick et al. 2012; Thompson et al., 2013; Richmond et al., 2014). In addition, several recent comprehensive reviews (Chein and Morrison, 2010; Shipstead et al., 2012), and an extensive meta-analysis (Melby-Lervag & Hulme, 2013), concluded that WMT may enhance near transfer performance, but far transfer to other reasoning tasks have yet to be fully demonstrated, suggesting that training is only beneficial when performing the training-specific tasks.

Thus, in order to control for general practice-related performance gains due to task specific stimulus-response mappings, the assessment of performance gains on separate tasks that measure an overlapping construct must be employed (Lövdén et al., 2010). Furthermore, recent studies have confirmed the important role of baseline individual differences (assessed prior to training), such as resting-state functional connectivity as a possible measure of intrinsic capacity constraints, and personality measures as moderators of significant gains throughout the training intervention (Shapiro et l., 2011; Hill et al., 2014; Jaeggi et al., 2014; Zheng et al., 2015).

Targeting the domain-general capacity of cognitive control within mindfulness training

In order to produce changes across individuals that persists outside of the laboratory, one needs to ask under what conditions transfer appears. Findings from various sources suggest that transfer generally happens by way of two rather different

mechanisms (see Perkins and Salomon, 1994, for review). Reflexive transfer involves the recruitment of automatic, procedural learning by triggering well-practiced routines specific to those in the learning context, which is thought to rely more on sensory inputs and bottom-up information processing. Conversely, mindful transfer involves deliberate and effortful manipulation in search for a pattern, or relationship, to solving a problem (Langer, 2000), which is thought to rely upon the top-down attentional control network, comprised of prefrontal and related polymodal association cortices (Farb et al., 2007; Wass, Scerif, and Johnson, 2012).

Accordingly, this distinction in transfer may explain why training interventions designed to enhance function-specific abilities show limited transfer effects, presumably because of the intervention's inability to engage more domain-general cognitive and neural architectures that promote mindful transfer effects. In other words, interventions that promote and cultivate this attribute of "mindful transfer" target a domain-general, associative, and polymodal neural architecture, thereby bridging the necessary connection from near to far transfer gains.

Thus, an ideal training program would be one that targets broad transfer effects to domains of cognitive functioning that directly influence everyday functioning. One particularly advantageous feature of MBT is that it simultaneously enhances moment-to-moment attentional control and reduces distractions from internal and external disruptions, in addition to improving emotional well-being (see Prakash et al., 2014, for review), which can vary substantially from person to person. Furthermore, MBTs engage

the operations of large-scale functional brain networks involved in the modulation of cognitive control networks involved in everyday functioning (see Peterson and Posner, 2012; Tang et al., 2015 for reviews).

Cognitive control and mindfulness training

Experimental and neuropsychological traditions have both emphasized the role of the unitary and ubiquitous function of controlling and regulating attention (Engle & Kane, 2004; McCabe et al., 2010; Hofmann, Schmeichel, & Baddeley, 2012). Cognitive control is a fundamental aspect of human cognition (Miller & Cohen, 2001), which guides voluntary, complex behavior, specifically in the context of solving difficult (novel) problems, altering habitual responses, and correcting errors (Cohen, Aston-jones, & Gilzenrat, 2004). More specifically, this ability requires the provision of top-down support for task-relevant processes (MacDonald et al., 2000; Dosenbach et al., 2008). One component in particular is responsible for maintaining the ongoing representations of the attentional demands used to bias processing in favor of task-relevant stimuli and responses, e.g., implementing attentional control during working memory tasks.

Accordingly, cognitive control is a dynamic process implemented by a distributed brain network that involves closely interacting, but anatomically dissociable frontal brain regions. A seminal functional neuroimaging study by MacDonald et al. (2000) found that dorsal lateral prefrontal cortex (DLPFC) activity was more involved in the implementation of cognitive control by representing and actively maintaining the attentional demands of the task, which has been replicated by others (Vanderhasselt, De

Raedt, Baeken, 2009; Cieslik et al., 2013). This maintenance component of cognitive control is thought to engage similar neural pathways involved in the executive component of attention in working memory (Engle, 2003; McCabe et al., 2010). In contrast, anterior cingulate (ACC) activity was selectively activated during incongruent-type trials (MacDonald et al., 2000; Cieslik et al., 2013), which is consistent with the role of the ACC in error-related and conflict-related monitoring (Carter et al., 1998). The conclusion from these studies is that the lateral PFC and ACC appear to have distinct, yet complementary roles within a larger frontal network serving cognitive control, where the former serves the maintenance component and the latter serves the monitoring component of cognitive control.

What is important to the psychological conceptualization of mindfulness practice is the ongoing refinement of one's attentional control abilities (Malinoski, 2013; Brown & Ryan, 2003; Lutz, Slagter, Dunne, & Davidson, 2008), with substantial effects observed on how people process information, and how they regulate attention and emotion (see, Lippelt, Hommel, & Colzato, 2014, for a recent review). During mindfulness training, meditators cultivate a state of awareness that emerges through paying attention on purpose, as a nonjudgmental attention to experiences in the present moment (Kabat-Zinn, 1985). By training these self-monitoring processes, MBT's target the primary "focus" of one's own cognition, a mechanism similar, if not isomorphic, to the "central executive" of WM, but which is generated and regulated endogenously – within one's existing knowledge and problem-solving space.

Training cognitive control with MBTs can have a direct impact across a variety of real-world cognitions, extending out to resiliency and stress reduction in challenging and high-demanding environments. To this end, although meditation research is still in its infancy, a number of studies have demonstrated neuroplastic changes that are associated with better performance on a variety of different cognitive control metrics. For example, consistent MBT-related improvements have been observed in working memory (Jha et al., 2010; Zeidan et al., 2010; Mrazek et al., 2013), sustained attention (Valentine and Sweet, 1999; Moore and Malinoski, 2009; Semple, 2010; Morrison et al., 2014; Jha et al., 2015), and changes in mindfulness-related personality traits (Takahashi et al., 2005; Sahdra et al., 2011; de Vibe et al., 2015). The proposed study will examine each of these abilities and their neural correlates.

The potential for synergistic effects of mindfulness training and brain stimulation

With respect to pushing forward real-world applications of cognitive training techniques, it has been recently proposed that combining cognitive training with brain stimulation techniques can facilitate the neuroplastic changes that allow for an acceleration of learning within a cognitive training environment (Clark and Parasuraman, 2014; Martin et al., 2015). In particular, transcranial direct current stimulation (tDCS), a low-cost, portable, non-invasive brain stimulation technique has been recently employed to modulate the excitability of functional brain networks (Polanía et al., 2011; Keeser et

al., 2011; Peña-Gómez et al., 2012; Hunter et al., 2015)[1]. In particular, this device has been used to accelerate the neurophysiological mechanisms responsible for neuroplasticity during working memory training (see Brunoni and Vanderhasselt, 2014, for review), complex visual search training (Clark et al., 2012), and other various training techniques (see Coffman et al., 2014 for review).

However, despite research demonstrating the utility of concurrent tDCS with cognitive training, the author is not aware of a single published study that has combined tDCS with MBT. While mindfulness practice stimulates and pushes one's core (domain-general) cognitive control capacity limits, brain stimulation techniques, e.g., tDCS, can be used to facilitate the ongoing neural patterns of functional connectivity toward long-lasting neuroplastic changes. To this end, one possible execution of tDCS in the context of MBT is to target the cortical network hub involved in top-down cognitive control processes and sustained attention; namely, the right prefrontal areas of the frontal-parietal control network (see Corbetta and Shulman, 2002; Peterson and Posner, 2012). More specifically, the right inferior frontal gyrus (IFG) may be an optimal target for stimulation as it has been shown to play a critical role in attentional control processing (Hampshire et al., 2010).

[1] More specifically, single-session tDCS is generally thought to increase the threshold for spontaneous firing of cortical neurons near the anode electrode (with positive polarity) while decreasing it near the cathode (with negative polarity) (Nitsche and Paulus, 2000; Dieckhöfer et al.,2006).

Utilizing neuroimaging technologies to evaluate neuroplastic change and efficacy

An emerging idea advocates that cognitive constructs arise from a collection of brain areas functioning together as large-scale networks (Liang, He, and Yang, 2015). Thus, investigating the human brain as an integrative network of functionally interacting brain regions provides a platform for characterizing the neural substrates of higher-order cognitive processes. Functional brain imaging data have revealed topologically organized, domain-general, distributed brain networks (Damoiseaux et al. 2006; Power et al. 2011). The central technique for quantifying network dynamics is functional connectivity, which is defined as the synchronization of neuronal activity between anatomically separate brain regions; namely, the temporal dependency between spatially remote neurophysiological events (Friston et al., 1994; Biswall et al., 1995; Greicius et al., 2003), which can be assessed with functional neuroimaging techniques, such as EEG and fMRI.

The dynamic relationships among the default-mode network (DMN), cognitive control network (CCN), and the salience network (SN) have received much attention in recent literature (Cocchi et al. 2014), and are thought to be engaged during MBT (Malinowski, 2013; Doll et al., 2015). Neuroimaging studies have shown that MBT can alter the task-related connectivity during cognitive control tasks and the state-independent intrinsic connectivity patterns during rest (see Malinowski, 2013; Witkiewitz, Lustyk, and Bowen, 2013; and Tang, Hölzel and Posner, 2015 for reviews). With respect to the constituent anatomical regions that comprise each of these networks, fMRI studies have

shown consistent activations in right-lateralized prefrontal and parietal cortices related to sustained attention (Cabeza and Nyberg, 2000; Clark et al., 2000; Calhoun et al., 2006; Polich, 2007; Hampshire et al., 2010; Peterson and Posner, 2012) , in bilateral insulae and posterior cingulate related to self-awareness (Vanhaudenhuyse et al., 2010; Manna et al., 2010), and cognitive switching (Menon and Uddin, 2010; Liang et al., 2014), in the left hippocampus related to the modulation of cortical arousal and responsiveness – mediating some of the benefits of meditation (Hölzel et al., 2011), and trait mindfulness (Doll et al., 2015). To this end, the network properties of the DMN, CCN, and SN can be used to assess possible training-related reconfigurations in the intrinsic circuitry of these networks using resting-state functional connectivity analyses (Chapman et al., 2013; Hunter et al., 2015; Doll et al., 2015). In particular, dynamic functional network connectivity (dFNC) analysis provides a method for evaluating quasi-stable intrinsic brain organization by revealing information about functional connectivity states (i.e., dynamic pattern of functional connectivity among networks over time), how long a person resides in such states (i.e., state dwell time), and how flexible these states transitions from one to another (see Allen et al., 2012; Damaraju et al., 2014).

Furthermore, given the excellent temporal resolution provided by electrophysiological methods, namely EEG, which provide metrics for the dynamic processes that underlie cognitive control processes and their electrophysiological correlates. Neural assemblies have been proposed as a conceptual framework for the

integration of distributed neural activity, with oscillatory activity[2] providing a metric for how they are transiently linked by reciprocal dynamic connections (Thomson and Varela, 2001). Furthermore, the "bottom-up" and "top-down" heuristic can be further operationalized as a large-scale network that integrates both endogenous and "incoming" activity, where *power* and *phase* synchronization across cortical regions can be used as a metric to assess the mechanisms for large-scale integration and neuroplasticity.

Overall, in order to characterize the neuroplastic effects associated with the frequently observed cognitive control enhancements by MBTs, an examination of large-scale functional brain networks allows for a very promising system-level approach. To this end, frontal theta-band synchronization and parietal alpha-band de-synchronization have been considered plausible candidates for the assessment of cognitive control (Gevins and Smith, 2000; Sauseng et al., 2005; Klimesch, 2012; Roux & Uhlhaas, 2014).

The knowledge gab between cognitive control & mindfulness training

Although mindfulness training studies have shown very promising results, with general improvements observed in novice meditators on various tests that require some variant of cognitive control processing, the exact cognitive and neural mechanisms mediated within cognitive control have yet to be fully investigated, especially in terms of

[2] Brain oscillations measured by EEG reflect fluctuations in dendritic electrical activity of populations of neurons. Measurements are typically confined to the cortical surface as trans-sulcal and geometrically opposing populations can be difficult or impossible to measure with EEG. Synchronous activity from small populations of pyramidal cells are generated by radially-oriented dipoles located in gyral crowns (see Cohen, 2014, p.33, for review). It is important to note that different cognitive processes and neural functions seem to utilize different frequency ranges or conjunctions of frequency ranges, with which changes in frequency-specific rhythmic activity correlate with task demands, including perceptual, cognitive, motor, linguistic mnemonic, and other functional processes.

the maintenance and sustained attention processes involved in cognitive control, their interactions, and their corresponding neural signatures. Indeed, current mindfulness studies have only assessed either the maintenance component alone (Jha et al., 2010; Zeidan et al., 2010; Mrazek et al., 2013), or sustained attention alone (Moore and Malinoski, 2009; Semple. 2010; Morrison et al., 2014; Jha et al., 2015).

To this extent, the current knowledge gab within the mindfulness training field is that within each (independent) study showing an improvement in a specific feature of cognitive control, there has yet to be a study that employs multiple representative metrics of attentional control processing and sustained attention, which is the primary objective for the present study. Not only will the inclusion of separate cognitive control tasks allow for a more precise investigation of the specific effects of mindfulness training, but it will also permit researchers to accurately evaluate the unique and independent contributions of each subcomponent, both at the levels of performance and neural network activation patterns, that constitute cognitive control.

Primary objectives and significance

Owing to the recent developments in neuroimaging and related analytic techniques, there has been progress made in regard to understanding some of the more basic mechanisms underlying the efficacy of mindfulness meditation (Tang, Hölzel and Posner, 2015). However, there is still a lot we do not understand, specifically in regard to tracking the specific cognitive control processing involved, and the underlying neural plastic changes associated with mindfulness training in a standardized, methodological fashion,

which is only now becoming consistent within the larger cognitive training literature (see Klingberg et al., 2010; Shipstead et al., 2012; Enriquez-Geppert, Huster, & Herrmann, 2013, for reviews). Furthermore, while there are neuroimaging studies investigating the training-induced alterations produced by mindfulness training, they are scarce; moreover, there has yet to be a study that combines multiple neuroimaging modalities to better understand the overall effects of MBT with tDCS. Indeed, the inclusion of information obtained from multiple imaging modalities will provide a more accurate representation of the neuroplastic changes with increased spatial-temporal precision.

In line with establishing innovative and novel neuroplasticity-based interventions in a systematic and methodological fashion, the overarching objective of this dissertation project is to compare important metrics of neuroplastic change in order to evaluate the combined effects of mindfulness training with tDCS. The assessment of cognitive control abilities and their corresponding brain patterns of activation using electroencephalography (EEG) and functional magnetic resonance imaging (fMRI) will be the primary metrics to evaluate change in this study. Furthermore, the present study aims to investigate the relation between training-induced alterations in performance, and the resting-state functional patterns of activation, while incorporating the individual differences on various personality traits and intrinsic connectivity.

Together, this dissertation study will provide important contributions to the development of methods for conducting experiments on neural and cognitive plasticity. Advancements in this particular domain of research will ultimately guide future studies

with the goal of tailoring a neuroplasticity-based interventions that maximize an individual's cognitive capacity, specifically by expanding his or her skill sets and abilities that can be transferred to various aspects of real-world cognition. Furthermore, with respect to MBTs in particular, this dissertation project will be able to disassociate the specific and overlapping effects of meditation training and their underlying brain functional alterations, which can also be used to tailor future MBTs and brain stimulation protocols.

Literature Review

Maintenance of cognitive control assessed by the attentional focus of working memory

Research over the past decade have suggested that individual differences in working memory capacity (WMC) reflect basic differences in cognitive control (Engle, 2003). In particular, the executive-attention theory of WMC proposes that high-, compared to low-WMC individuals are better at controlling attention, resulting in more stable representations of stimulus-response mappings and less interference from task-irrelevant information (Kane and Engle, 2002; Engle, 2003; Unsworth et al., 2014)[3]. Thus, efficient WM performance requires the simultaneous maintenance of relevant information over a short time period (i.e., target accuracy) and inhibition of distracting,

[3] This executive control aspect of WM is distinct from the "scope" components of WM, which refers to the amount of information that can be actively maintained at a given time (Cowan et al., 2005). Relatedly, the so-called contralateral delay activity has previously been shown to increase in amplitude as the number of memory items increases, up to the individual's working memory capacity limit, from 300 – 900 ms after target stimulus onset (Ikkai, McCollough, and Vogel, 2010).

non-task relevant information from entering the attentional processing stream (Gazzaley et al., 2005; Vogel et al., 2005).

There are a number of different tasks designed to assess WM capacity, but the n-back and complex WM tasks are thought to specifically engage the attentional control aspect within WM. The n-back task in particular has been well-studied and has been widely used across studies as a WM assessment of updating (Owen et al., 2005), which requires attentional control to maintain relevant information (e.g., task goals) in the face of interference, and ignore this information when it becomes irrelevant, and replace it with new information (Miyake and Friedman, 2012). Relatedly, in terms of the importance of using an n-back task, performance gains on adaptive n-back training transfer to tasks that are heavily reliant on attentional control abilities, such as the flanker and Simon tasks (Colom et al., 2013), and measures of fluid intelligence (Jaeggi et al., 2008).

Biomarkers for the maintenance subcomponent of cognitive control

Frequency-domain metrics

Synchronous oscillations between neuronal ensembles are proposed as a mechanism for inter-regional communication (Thompson and Varela, 2001; Buzsaki and Draguhn, 2004), and can be measured with EEG data using time-frequency analysis techniques. Depending on the task and frequency-band of interest, power-based (overall sum of activity) and phase-based (timing, or re-setting of activity) metrics are primary candidates to assess neuroplastic changes.

While power-based measures of oscillatory activity estimate the amount of energy in a specific frequency band at some interval of time (i.e., the squared length of the complex vector before or after stimulus onsets), phase-based metrics estimate the timing of population-level activity to some task-relevant features (e.g., targets and distractors), which has been conceptualized as a measure of "functional configuration", "neuronal entrainment", or "functional states" (Cohen, 2014). In particular, inter-trial phase clustering (ITPC)[4] estimates the phase clustering, or "neural entrainment", of band-specific timing over all trials of interest. For instance, if a particular event in a task elicits ITPC, the neural networks contributing to that ITPC returns the same, or similar, functional configuration for that particular event. This consistency is driven by the timing of afferent signals that reset the ongoing oscillations to the appropriate functional brain dynamics in order to maximize information processing or to facilitate interregional coupling. Of particular interest is that ITPC relates to detecting the event-related timing of functional activation patterns that lead to neuroplastic changes (Cohen, 2014).

Frontal theta rhythms as an indicator of cognitive control

Cognitive control in the healthy brain is thought to partly depend on medial and DLPFC theta oscillations (4–8 Hz) by serving as the temporal code that coordinates neuronal populations involved in implementing control (Berka et al., 2007; Reinhart et

[4] ITPC measures the extent to which a distribution of phase angels at each time-frequency-electrode point across trials is non-uniformly distributed in polar space. ITPC is bound between zero and one, with zero indicating complete uniformly distributed phase angles and one indicates completely identical phase angles (Cohan, 2014).

al., 2015). More specifically, medial-frontal theta oscillations appear to signal the need for adaptive control in stimulus novelty, response conflict, negative feedback, and behavioral errors (see Cavanagh and Frank, 2014 for review). Moreover, increased frontal midline theta power was observed after an intensive integrative body-mind training, suggesting an enhancement of cognitive control processing (Tang et al., 2009).

Accordingly, both fontal theta power and phase synchrony play an important role in the maintenance subcomponent of cognitive control (Sarnthein et al., 1998; Uhlhaas et al., 2008). In particular, for higher working memory load trials during n-back performance, theta power has been shown to increase in the initial phases of WM encoding, with later sustained oscillatory activity (Missonnier et al., 2012). Thus, during efficient WM performance, the later sustained power can be used as a metric of active maintenance (of WM items) and general continual cognitive engagement and WM updating (Massonnier et al., 2012).

Near transfer tasks to assess cognitive control: complex WM-span tasks

One primary goal of cognitive training is to improve general cognitive abilities useful in everyday life, beyond performance specific to a trained task. It is likely that performance of the trained task would be improved by the training, but its effects could be limited to the particular trained task (Jaeggi et al., 2008)[5]. Studies examining the

[5] In fact, according to Lövdén et al., 2010, the problem is the misattribution of improvements due to the treatment, but were actually due to practice-related and task-specific skills or strategies attributed to knowledge acquisition, e.g., task-specific strategies, memorizing response mappings, perceptual expertise, etc.

efficacy of cognitive training techniques will benefit by assessing the transferability of training-related performance gains to other similar tasks (Lustig et al., 2009). Therefore, it is of great importance to succeed in reproducing the improved performance gained from training in one task, on another, different task with no prior training on the second. Thus, a transfer task must be employed in order to test the commonality with the trained task, a commonality that is the target and primary variable of manipulation within the intervention. The classical complex working memory span tasks, such as the operation and spatial span tasks, were initially developed to also measure the executive attentional component of working memory and have been shown to correlate with performance on tasks that require the top-down guidance of attention (see Chow and Conway, 2015).

Far transfer tasks for the maintenance subcomponent of cognitive control

The importance of evaluating working memory and "fluid" abilities together is because they share common variance due to this general ability to solve novel and complex tasks, all of which require one to *effectively control attention* (Hofman, Schmeichel, and Baddeley, 2012; Unsworth et al., 2014). Broad cognitive abilities, such as fluid intelligence and self-regulation, are thought to moderate beneficial facets of professional and intellectual accomplishments, such as academic achievement (Gold et al., 1995; Di Fabio et al., 2009) and psychosocial adaptation (Huepe and Salas, 2013). It has also been proposed as having a bidirectional relationship with perspective changing (Huepe and Salas, 2013) and the accomplishment of competences regardless of significant socioeconomic adversity (Cicchetti and Blender, 2006).

Thus, fluid intelligence is effectively known as the "fluid" quality of being able to direct the process of analyzing novel problems and identifying patterns and relationships that underpin these problems (Cattell, 1963). To this extent, it is this "fluid" ability that is also thought to be involved in the attentional processing involved in mindfulness training (Mrazek et al., 2012). For this study, this "fluid" ability was assessed by the Ravens Progressive Matrices (Ravens, 1990) and the abbreviated Shipley-2 IQ score (Shipley et al., 2009).

Tonic alertness and sustained attention measures

Mindfulness training has also consistently produced enhancements in core cognitive processes in addition to working memory, namely in sustained attention. Indeed, the ability to focus one's attention over an extended period of time while resisting distraction is a necessary condition for adaptive, goal-directed behavior, which captures the central involvement of sustained attention and general tonic levels of arousal during mindfulness training (Malinoski, 2013). More specifically, as the mediator focuses, monitors, and sustains attention on the relevant object of meditation, the alerting and salience networks—among others, are engaged, which involves the tonic effects of vigilance to that object and phasic effects of attentional modulation to other distractor objects.

The disassociation between tonic and phasic activity is important as it pertains to the operationalization of the training-induced changes expected on patterns of brain activity during sustained attention tasks. The activation states of cerebral cortex for tonic

arousal states are thought to impact the ability to process information where the activation itself contains no specific information (see Oken, 2006, for review). These activation states are tonic in that they are relatively global, i.e., the endogenously generated background arousal when unmodulated by task events. Furthermore, this global background activity may reflect the general properties of one's intrinsic functional architecture, which can be acquired during resting-state sessions or during the baseline intervals during a sustained attention task, whereas, the activation states that are phasic are typically more localized, i.e., exogenously generated by task events. Phase-locked activity across trials within a task may serve as the bases to measure functional configuration over time at different frequency bands.

Biomarkers for sustained attention: P3 as neurophysiological marker of attentional allocation

Event-related potentials (ERPs) are averaged time-locked responses to an event and have provided useful information regarding cognitive control processing using EEG (see Drew et al., 2006 for review). For instance, the canonical, attention-driven ERP component, P3[6], is a nonspecific marker for attentional processing of any stimulus. More specifically, this marker is thought to index stimulus evaluation and the intensity of cognitive control processes, such as, updating in working memory, inhibiting a dominant response, and integrating information into existing networks (Kok, 2001; Polich, 2007).

[6] Also known as the "late positive component" (LPC), or simply P300, which indicates that the voltage deflection of this component is positive and reaches a peak around 300 milliseconds after the stimulus onset.

However, the P3 also has specific and distinct functional roles depending on the type of manipulations within tasks that require different levels of attentional demands. Indeed, the generation of the P3 has been dissociated into two different component parts, the P3a and P3b, each composed by distinct spatial topographies that serve different cognitive functions. The P3a is generated in frontal brain regions involved in maintaining stimulus information and processing in-frequent stimuli, and the P3b is generated in temporal-parietal areas involved in memory-related storage processes (Polich, 2007). Furthermore, the attention-driven, P3a, is thought to temporally precede the P3b and elicit a stronger (higher amplitude) response in order to transmit contextually relevant information to memory-related processes. Accordingly, latency and amplitude measures of the P3a are candidate metrics to examine the need to enhance focal attention during stimulus detection relative to the contents of working memory and sustained attention (Soltani and Knight, 2000).

The three-stimulus oddball task – in which a target is detected among frequent non-changing standard stimuli and infrequent distractor stimuli – produces reliable neural signatures of the sustained attention brain circuit (Polich and Criado, 2006). Of particular interest is that this task was originally designed to elicit, and effectively distinguish, the constituent components of the canonical P3, namely the P3a and P3b.

Furthermore, event-related fMRI have been employed to examine the specific anatomic locations of brain regions involved for both the P3a and P3b during the three-stimulus oddball (Clark et al., 2000; Bledowski et al., 2004). In particular, target stimuli

have been shown to evoke fMRI signal increases in multiple brain regions including the thalamus, occipital-temporal cortex, bilateral superior, medial, and inferior frontal cortices, as well as, inferior parietal, superior temporal, and insular cortices. Distractor stimuli have been shown to evoke an fMRI signal change bilaterally in inferior anterior cingulate, medial frontal, inferior frontal, and right superior frontal gyri (Clark et al., 2000).

In addition, another study, which also employed the three-stimulus oddball task, combined information from both EEG and fMRI and found similar results. That is, the EEG-derived P3b was produced by parietal and inferior temporal areas, whereas frontal areas and the insula contributed mainly to the attention-related P3a (Bledowski et al., 2004). This particular finding of the contributions of the insula to distractor processing (i.e., the generation of the P3a) converges on a crucial role for the right insula in particular as producing an early cognitive control signal that disengages the DMN and activates task-specific, executive control networks (Ham et al., 2013).

Overall, these results point to the involvement of distinct attentional subsystems in target and distractor processing (Clark et al., 2000; Bledowski et al., 2004), which involve brain regions that are relevant for attentional processing during mindfulness practice. Moreover, given the robust responses elicited by this task and the brain regions involved, it has also been used to assess the neuroplastic effects of MBTs (Lutz et al., 2009; Slagter et al., 2009; Cahn and Polich, 2009; Cahn, Delorme, Polich, 2013). Indeed, recent studies that employed the three-stimulus oddball task before and after meditation

practice found some very consistent training-related findings across studies (Lutz et al., 2009; Slagter et al., 2009; Cahn and Polich, 2009; Cahn, Delorme, Polich, 2013). For instance, within MBT protocols, a consistent finding is a reduced (overall) P3 amplitude during attention-related task performance compared to control groups; that is, MBT subjects typically exhibit a reduction in P3 amplitude in response to rare stimuli, which is thought to co-vary with self-reported gains in trait mindfulness (Cahn & Polich, 2009). This pattern of results was interpreted as the MBT group exhibiting greater resource allocation and more efficient processing during tasks requiring attentional control (Cahn & Polich, 2009; Slagter et al., 2007).

Alpha and theta contributions to sustained attention

Furthermore, the neuroelectric architecture of the P3a phenomenon is also thought to reflect transient event-related changes in power of the theta and alpha frequency bands, contributing more broadly to the distinction between phasic and tonic activity. In particular, the P3a is thought to stem from the initial inhibitory activation elicited by focal attention to a distracting stimulus, indexed by an increase in theta frequency modulations, and thereby increasing the inhibitory control of these processes. Alpha power is also thought to play a crucial role in inhibitory and arousal processes.

Alpha oscillations (usually defined in the range of about 8–14 Hz) have been studied rigorously ever since they were first discovered by Hans Berger in 1924, particularly as they relate to cortical anticipatory arousal states during baseline assessments of cortical activations (i.e., cortical idling hypothesis; Pfurtscheller, Stancak,

Neuper, 1996), and to active cortical inhibition during task engagement (i.e., inhibition timing hypothesis; Klimesch, 1999; Klimesch, Sauseng, Hanslmayr, 2007). Although the exact role of alpha has yet to be fully characterized, alpha is considered a robust measure of the temporal structure of information processing in the brain (Klimesch, 2012). In regard to cognitive control processing in particular, alpha is dynamically involved in maintaining an optimal balance between excitatory and inhibitory phases that are relevant for neural communication during rest and task-related demands (Klimesch et al., 2007; Crespo-Garcia et al., 2013; Roux & Uhlhaas, 2014)[7].

In healthy humans, high alpha power amplitudes dominate the EEG during baseline, resting-state conditions, especially when subjects' eyes are closed, which is called alpha synchronization. Alpha synchronization is thought to reflect a tonic psychophysiological state for "internalized" and "anticipatory" attention during baseline conditions. Furthermore, alpha synchronization can also be time-locked to events, which is termed event-related synchronization (ERS). In particular, during the inter-stimulus "baseline" interval preceding each task event, tonic arousal states are reflected by alpha ERS over posterior EEG sites as the participant anticipates the presentation of the next stimulus (Klimesch, 1999). To this end, Klimesch and colleagues (2007) hypothesized that alpha ERS may also reflect top-down control of attention, observed as a "readiness" to process the next event, or perform a new task. However, during the target response, the

[7] Inhibitory inter-neurons have been proposed as the generators of alpha activity (Buzsáki and Draguhn, 2004).

high alpha amplitudes diminish (i.e., decreased ERS), which is termed alpha blocking, alpha suppression, or alpha desynchronization (ERD; Klimesch, 1999). Alpha ERD has been associated with more efficient brain functioning across tasks that distinguish between expertise levels (Grabner, Neubauer, Stern, 2006).

Altogether, alpha oscillations seem to support attentional processes by: (1) allowing for sufficient baseline arousal states (pre-stim ERS) to implement cognitive demands, (2) suppressing inhibition during target stimuli (ERD), and (3) actively filtering out distractor stimuli (ERS), which prevents interference from conflicting stimuli (Klimesch, Sauseng, Hanslmayr, 2007; Tuladhar et al., 2007). Therefore, if attentional control and vigilance are strong prior to task responding, EEG-alpha ERS will be high, and ERD during task performance will be subsequently high as well.

To this end, there have been several biomarkers proposed for evaluating the attention-related effects produced by MBTs (Cahn and Polich, 2006), such as: (1) increased alpha phase consistency during standard processing (i.e., enhanced stimulus representation of the habituated standard stimuli); (2) decreased alpha during distractor processing (i.e., decreased automated attentional engagement, or the bottom-up orienting response); and (3) increased theta phase synchrony to target responses (i.e., increased attentional engagement).

Altogether, given the robust responses obtained from the oddball task and their association with meditation practice, both EEG (in the time-domain and time-frequency domain) and event-related fMRI methods will be employed in the present study to assess

the effects of MBT and tDCS. Furthermore, given that right-lateralized fronto-parietal network plays a role in exerting top-down attentional control over lower sensory regions as a reorienting response (Corbetta and Shulman, 2002), which is thought to be enhanced with MBTs (Malinoskwi, 2012; Tang, Hölzel an Posner, 2015), analyses will focus primarily on right-hemispheric activity, which is also of interest given the placement of the anode tDCS electrode. In addition, analyses on oddball performance during the final block of oddball performance have been used to compare sustained attention decrements between MBT group and a control group (Cahn, Delorme, Polich, 2013).

Outcomes variables to assess trait transfer: self-reports on personality metrics

With respect to the interaction between cognitive training outcome and personality traits, there have been several studies that highlight the need to include personality trait measures as moderators of transfer gains due to cognitive training. For example, one study examining the influence of neuroticism and consciousness (from the Big five inventory) on WMT outcome found that dual n-back training was more effective for participants low in neuroticism (Studer-Luethi et al., 2012). This particular finding highlighted the role of the famous inverted U-shaped curve where a moderate level of activation facilitates the best performance, whereas under- or over-activation impairs performance (Yerkes & Dodson, 1908). Thus, according to this recent study, anxiety-like (i.e., neuroticism) interferes with efficient processing and limits storage resources of the WM system. Furthermore, conscientiousness was associated with better gain scores in the single n-back and improvement in near transfer measures, but lower far transfer

performance, suggesting that subjects scoring high in this trait developed task-specific skills preventing generalizing effects.

Given that mindfulness practice has been shown to involve and enhance attentional control processes (Lutz et al., 2008; Tang and Posner, 2009; Hölzel et al., 2011; Slagter et al., 2011), baseline dispositional-traits of focused attention are hypothesized to predict individual differences in treatment-related outcomes. Furthermore, tDCS has also been shown to interact with personality traits (Peña-Gómez et al., 2011), tonic dopamine levels (Plewnia et al., 2013), and resting-state functional connectivity (Peña-Gómez et al., 2012). Thus, this proposed study will also include metrics that fully capture trait-related moderators of one's cognitive control abilities, such as trait mindfulness, attention, and intrinsic functional connectivity.

Although personality traits have been shown to explain a significant amount of variability in cognitive control and executive attention abilities (Schaie et al., 2004; Johnson et al., 2010; Hale et al., 2011; Mõttus et al., 2015), they have yet to be fully examined within the context of a combined MBT and tDCS training paradigm. Furthermore, there is no consensus on the personality inventories to assess dispositional variations in a cognitive control ability (Feldman et al., 2006; Anicha et al., 2012). Nonetheless, variations in trait mindfulness (or lack thereof) are thought to reflect cognitive abilities related to executive control (Baer et al., 2004). Thus, for this study, in the context of executive attention, the mind-wondering scale (MWS; Mrazek et al., 2013) and sub-scores from the Big-five Inventory (BFI; Rammstedt & John, 2007) and Barrett's

Impulsivity Scale (BIS; Patton, Stanford, and Barratt, 1995) will be used. The MWS is particularly relevant as it was developed to measure trait levels of task-unrelated thought, i.e., mind-wandering, which is thought to constitute a psychological baseline that emerges when the mind is otherwise unoccupied, and therefore inversely related to focused attention. The 'attention' and 'self-control' subscales within the BIS are also important for executive attention, with higher scores indicating endorsements of "concentration" and "planning", respectively. The consciousness subscale within the BFI is applicable to executive attention as it specifically asks questions regarding "distraction", "efficiency" and "organization". To this end, it is hypothesized that these self-report measures will evaluate a "focused attention", or executive attention trait measure that may interact with the proposed MBT and tDCS intervention.

Furthermore, in order to specifically measure trait mindfulness, self-perceived attentional impairments, and motivational (or self-regulation) sensitivities, the following tasks were used to measure each trait, respectively: the mindful attention awareness scale (MAAS; Brown and Ryan, 2003) and the attention related cognitive errors scale (ACRES; Cheyne et al., 2006. The MAAS was particularly useful for this study as it focuses exclusively on the cognitive, or attentional aspects of trait mindfulness, whereas many other scales incorporate emphasize the emotional aspects. The ACRES assesses the frequency of everyday mistakes that are likely to be caused by failures of attention (i.e., this scale is thought to measure lapses of attention).

Altogether, the trait characteristics of the individual, and the nature of the training and the brain networks involved can either facilitate or inhibit each other's response to that signal. It is proposed that although personality traits and motivation may pose as difficult moderators to assess intervention improvements, they are powerful conceptual tools to better understand and foster successful training (Hertzog and Dunlosky 2012; Redick et al. 2013; Bürki et al., 2014; Jaeggi et al., 2014). Indeed, trait-related changes are also valuable in order to capture possible training-related effects that transfer to contexts outside the laboratory.

Possible biomarkers for trait-related attributes: resting-state functional connectivity

Evaluating resting-state network connectivity before and after a neuroplasticity-based intervention has proven useful in the evaluation of network adaptation and integration (see Taya, 2015 for review). The central idea is that if a large-scale functional brain network (e.g., frontal parietal control network) is continuously engaged in MBT, then the intrinsic connectivity of brain regions that comprise that network may be strengthened following Hebbian learning principles, and consequently may result in near and far transfer gains. Given the importance of evaluating any training-related modifications to the intrinsic connectivity of functionally-relevant large-scale networks, fMRI-based metrics of resting-state functional connectivity will be employed, which have been shown to be robust and last for relatively long durations (days or weeks) (Lewis et al., 2009).

The intrinsic connectivity assessed with fMRI are observed as slow (<0.1 Hz) spontaneous fluctuations in the blood oxygen level dependent (BOLD) signal that show high correlations across functionally related brain regions (Biswal et al., 1995). The organization of intrinsic functional connectivity has been suggested to depend upon the structural connection across local and distant brain regions and upon synaptic plasticity (van Den Heuvel et al., 2009; Honey et al., 2009). The functional role of intrinsic functional connectivity was asserted on of the substantial energy demand associated with the "resting" state of the brain, which is thought to entail a finely tuned balance between metabolic demands and regionally regulated blood supply (Raichle, et al., 2001). Fox et al., 2006 proposed that since the brain is active even in the absence of a task, there must be an internal dynamic modulating the ongoing functional connectivity, reflecting specific functional roles[8], and it this coordinated activity that has formed the basis of the DMN and other intrinsic networks.

The DMN, in particular, links precuneus and posterior cingulate cortex with medial frontal regions and bilateral inferior parietal regions (Raichle, 2001; Greicius et al., 2003; Fox et al., 2006). Unlike other intrinsic networks, the regions of the DMN show increased functional connectivity during rest and a deactivation during engagement of

[8] Propose that intrinsic networks: (1) represent a record, or memorization of a temporally coherent network that modulates in a task-dependent manner, providing a priori hypothesis from INs about aptitude in a variety of task conditions (e.g., attention tasks), intelligence and even personality traits; (2) organize and coordinate neuronal activity, particularly among regions that commonly work in concert, which is in accordance with the temporal binding hypothesis; and (3) represent a prediction regarding expected use (i.e., the brain develops and maintains an intrinsic probabilistic model of anticipated events (Fox et al., 2006).

goal-directed cognitive tasks. Thus, the DMN is unique in that it reflects an intrinsic 'idling' of the brain that may be tightly coupled with attentional processes (Gusnard et al., 2001). The "coupling" between the dynamics of the DMN and attentional networks (e.g., frontal-parietal networks) can be described as the so-called anti-correlation between the two networks, which suggests distinct attentional processes (Fransson, 2005). Indeed, it's hypothesized that the interplay between the DMN and task-related networks can significantly impact behavioral performance (Uddin et al., 2008). For example, a failure to suppress activity in the posterior node of the DMN is associated with attentional lapses (Weissman et al., 2005). Furthermore, Hampson et al. (2006) reported that greater connectivity between the posterior cingulate and medial prefrontal nodes of the DMN correlated with better performance on a working memory task, suggesting that deactivation of a brain area may require increased (rather than decreased) connectivity with the DMN. In addition to the possible influence of DMN dynamics on attentional networks, the DMN has been linked to other core processes of human cognition, including the integration of cognitive and emotional processing (Raichle, 2001; Greicius et al., 2003), monitoring the external world (Gusnard et al., 2001) and mind-wandering (Mason et al., 2007).

The application of independent component analysis (ICA) to resting-state fMRI data has proven very useful because it discovers functionally related "groups" of voxels that characterize a brain network (McKeown et al., 1997; Calhoun et al., 2001). ICA is a data-driven method that works by decomposing a set of signals into maximally

independent components by minimizing the mutual information between the components (Calhoun et al., 2001); that is, the ICA model identifies sources whose voxels have the same time course and thus each component can be considered a temporally coherent network[9]. Thus, ICA can reveal inter-subject and inter-event differences in the temporal dynamics: its major strength being the ability to reveal the dynamics of spontaneous fluctuations in resting-state scans, for which a temporal model is not available.

Brain dynamics are prominent during resting-states since mental activity is unconstrained, thereby requiring more sophisticated and novel analytical techniques that assume that spatio-temporal brain patterns of functional connectivity are non-stationary. Dynamic functional network connectivity (dFNC) is a very useful measure of the quasi-stable temporal dependency among ICA components over time. This dynamic dependency is computed by using short time windowed correlations computed on time courses of spatial independent components and then clustering these dynamic connectivity patterns using *k*-means clustering approach (Allen et al., 2012). This analysis results in centroids of dynamic connectivity patterns in resting state networks, called "states", which can further quantify individual differences in the amount of time a subject resides in one particular state throughout the duration of a scan (i.e., state dwell times) and the flexibility that a subject may exhibit as the number of transition from one state to another.

[9] Unlike PCA, which finds the direction of maximal variance, using second-moment statistics; ICA finds directions which maximize independence, using higher-moment statistics (McKeown et al., 1997; Calhoun et al., 2001)

Altogether, the stability of intrinsic networks across conditions suggests that the strength of these brain connections may be related to some stable subject trait such as a cognitive ability, intelligence or a personality dimension (see Vaidya and Gordon, 2013 for review). Indeed, a recent study found an association between higher levels of dispositional mindfulness and connectivity of the DMN (Prakash et al., 2014). Higher levels of mindfulness disposition were associated with network integrity of the dorsal posterior cingulate cortex (PCC), indicating the possible overlap between trait mindfulness and a "cognitive switch" brain area that interfaces with cognitive control brain networks (Leech et al., 2011). The authors suggested that mindfulness traits may reflect the flexible modulation of neuronal regions (Prakash et al., 2014).

Furthermore, within the context of evaluating the effects of an MBT, a more recent experiment compared the inter-network interactions between the DMN, SN, CCN, which are thought to subserve cognitive control functions that overlap with mindfulness (Doll et al., 2015). This study found that increased mindfulness was negatively associated with the network correlations between the anterior (ACC) and posterior (PCC) nodes of the DMN, and between the SN and posterior node of the DMN. The decoupling of the DMN within itself and with the SN indicate an enhancement of focused-related processes, and an improved sensitivity to mind wandering. Critically, however, a few major limitations of this study include no pre/post comparisons and no evaluation of the behavioral implications of these findings, which will be addressed in the current study.

The proposed objective for the current study is to include the information obtained from neurocognitive intrinsic networks to assess the neuroplastic changes associated with MBT and tDCS. These changes will also be assessed to the extent that they translate to performance gains in near and far transfer tasks, as well in the personality trait measures.

Hypotheses within the neural efficiency & individual-differences framework

With respect to evaluating the training-related effects on brain activations, hypotheses will be formed within the neural efficiency framework. The neural efficiency hypothesis postulates that a higher cognitive capacity level is associated with more efficient brain functioning (Neubauer and Fink, 2009). For instance, individuals who score high on difficult tasks (e.g., working memory or progressive matrices tasks) tend to rely on frontal cortex less as they gain mastery of a cognitive skill (Gevins and Smith, 2000), whereas the inefficient use of frontal circuits—observed as high levels of activity during less demanding tasks, is associated with worse performance. To this end, the proposed hypotheses for the current study will rely upon the assumption that efficiency affords capacity. Thus, an altered functional engagement of the frontal cortices after training will be hypothesized (Neubauer and Fink, 2009).

Furthermore, another general assumption within the current study is that any changes observed at the level of functional network integration (i.e., oscillatory behavior) can be interpreted as evidence for far transfer gains if these training-related gains are associated with gains in other related tasks. This assumption is based on the nature of

observing changes in functional brain states; that is, changes at the level of functional network integration reflect gross information transfer alterations of the functional network involved, which are engaged during a variety of other untrained tasks. Thus, far transfer may be achieved by establishing relationships between these functional network integration metrics and enhancements in more general cognitive workloads using different tasks at a separate testing session.

Given the influence that cognitive control can have on cognitive plasticity is clearly suggested by changes in prefrontal regions, analysis for the proposed study will focus on the examination of training-related alterations to these prefrontal network dynamics. However, there are theories and empirical evidence that also heavily emphasize the global efficiency of the cerebral cortex (see Deary and Caryl, 1997). That is, the functional connectivity between the frontal and parietal cortices is thought to operate efficiency more rapidly during more demanding aspect of a task (particularly for working memory). Thus, by utilizing the n-back task with increasing levels of difficulty as a function of experimental groups over time, rapid changes in activation patterns in prefrontal regions, and its functional connectivity with more posterior regions can account for functional brain state changes related to training.

Hypotheses

$H_0$1: Training will produce transfer effects on cognitive control and efficient use of P3 processing.

The following hypotheses were made in comparing the mindfulness training + active tDCS (MBT+tDCS) group to a control training + sham tDCS (Cont+Sham) group to ensure training-related gains are specific to the intervention:

1. Changes in brain networks with MBT+tDCS will lead to increased cognitive capacity.
    1.1. Improved cognitive capacity will be associated with improved accuracy and faster response times during the n-back task, particularly as the working memory load increases, when compared to Cont+Sham.
    1.2. Improved cognitive capacity will also be associated with decreased P3 amplitude as the WM load increases, indicating more efficient neural processing, consistent with previous MBT studies showing decreased P3 amplitude, which has been interpreted as resulting from greater resource allocation during tasks requiring attentional control.
    1.3. Improved cognitive capacity will also be associated with changes in theta oscillations:
        1.3.1. Efficient WM processing (i.e., periods of increased accuracy) will be associated with increased sustained frontal theta power in the 300-900 ms range.

2. Improvements observed in the n-back EEG correlates will also transfer to complex WM span tasks on a separate assessment date.
    2.1. It is hypothesized that training-related gains observed in the n-back and their EEG correlates will positively correlate with S-span and O-span performance (near transfer), the Ravens and IQ score from the Shipley, and mindfulness trait measures (far transfer). Positive correlations are expected, such that increases in neural efficiency will transfer to performance gains in these near and far transfer measures.
3. It also hypothesized that individual differences in personality measures, e.g., MAAS, ACRES and MWS, will contribute to any observed training-related gains in both the performance measures and the EEG metrics.

$H_0$2: Training-related effects on sustained attention

The following hypotheses are made in comparing the MBT+tDCS group to Cont+Sham group:

1. Quicker RTs and less FA will be observed.
2. fMRI will reveal gross BOLD changes in anatomical regions involved in MBT+tDCS, e.g., ACC, insula, DLPFC, hippocampus, and rIFG:
    2.1. In particular, decreased activations in the frontal regions that are elicited by the distractor stimuli, which may reflect a decrease in the automated attentional engagement of irrelevant stimuli.

2.2. Increased activations in the parietal regions that are elicited by the target stimuli, which may indicate an enhancement of the neural circuitry involved in efficient attentional engagement.

2.3. Lastly, increased activations in visual and extrastriate cortices elicited by standard stimuli, which may reflect enhanced stimulus representation.

3. For the EEG time-domain analyses,

3.1. Decreased amplitude for the P3a will be associated with distractor stimulus presentation, which may indicate more efficient processing.

4. Phasic activity of sustained attention will be reflected by:

4.1. Increased alpha phase consistency will be associated with standard stimulus presentation, which may indicate an enhancement of stimulus representation of the habituated standard stimuli.

4.2. Decreased alpha phase consistency will be associated with distractor stimulus presentation, which may indicate a decrease automated attentional engagement.

4.3. Increased theta phase synchrony will be associated with target stimulus presentation, which may indicate effective attentional allocation (within the P3 latency range)

5. Individual differences in personality traits will further enhance any treatment-related outcomes.

$H_0$3: Training-related transfer effects on intrinsic connectivity

1. The dynamic functional network connectivity patterns (i.e., dFNC) among the DMN, SAL, and the CCNs will be significantly different in comparison to baseline and the Cont+Sham group.
    1.1. In particular, increases in the amount of dwell time in states that are distinguished by inter-network interactions (i.e., dFNC) between the DMN, CCN and SAL may reflect a stable change in states that correspond to a "readiness" for decoupling of the DMN during cognitive demands and an improvement in focus-related processing.
    1.2. Decreases in the amount of dwell time in states that are distinguished by increased dFNC within the DMN and decreased dFNC between the SAL network and the CCN may indicate an enhancement of attentional control circuitry.
    1.3. Increased number of state transitions occurrences, which may indicate an enhancement in cognitive flexibility.
    1.4. dFNC metrics of interests will be correlated with baseline and/or post-raining measures of WM and/or personality trait measures.

CHAPTER 2: MATERIALS AND METHODS

The proposed methods for assessing neuroplastic change in the present study are displayed in Figure 2, including the procedures used to assess the neuroplastic changes associated with the proposed mindfulness-based training with tDCS protocol

(MBT+tDCS) compared to an active control training with sham stimulation group (Cont+Sham).

Figure 2: A generalized and study-specific framework for assessing neuroplastic change.

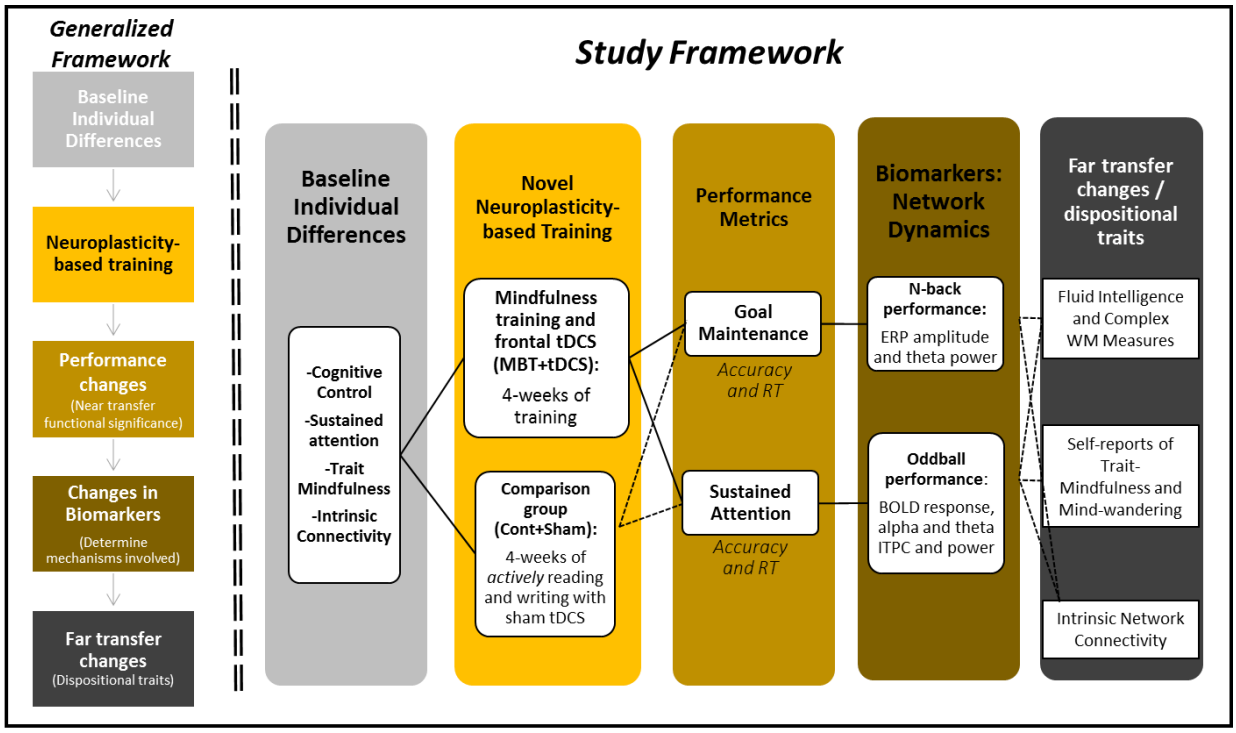

By including performance and neuroimaging metrics within a single construct, this framework allows for the examination of neuroplastic changes, which span multiple measurement scales that can be compared relative to baseline and an active control group. Markers include measures of neural entrainment (inter-trial phase clustering; ITPC), tonic alpha and theta-band power, and blood-oxygenation-level dependent (BOLD) signals. Far transfer measures may consist of self-reports, performance, and intrinsic network connectivity.

Participants and screening

For all EEG-related hypotheses, a total of 34 healthy adults were recruited from a larger pool of subjects who enrolled into the MIRACLE study located at UNM[10]. These participants were recruited from the larger Albuquerque area by advertisements posted throughout the community via paper fliers, website listings (e.g., Craigslist or others), newspapers, television and radio ads, and other forms of media, including email listservs at UNM, and other local Albuquerque employers (e.g., Sandia Labs and VA Hospital). All demographic information are provided in Table 1.

For all the fMRI-related hypotheses, a total of 30 healthy participants were recruited from the larger pool of subjects who enrolled into the MIRACLE study located at UNM and at Georgia Institute of Technology (GIT). There were 16 recruited from UNM and 14 recruited from GIT. The participants from GIT were recruited using similar methods used to recruit the UNM sample, namely by advertisements posted throughout the community via paper fliers, website listings, etc. See Table 2 for all demographic information pertaining to the fMRI group.

Inclusion Criteria

Individuals who were interested in participating in the study contacted a staff member staff to determine eligibility. Individuals were eligible if they meet the following

[10] Multifaceted Intervention for Robust Adaptive Reasoning and Problem Solving Focused Customized Learning and Enhancement – Phase 1a, which examined the effects of various types of cognitive training. This research was supported by the Intelligence Advanced Research Projects Activity (IARPA) via contract #2014-131270006.

conditions:

1. Between the ages of 18-50,
2. Right handed,
3. Received a degree from a four year college or were enrolled in a four-year degree program and completed at least two years of coursework,
4. A native English speaker,
5. Access to a personal computer with reliable internet access and Google Chrome functionality.

Exclusion criteria:

Participants were excluded from the study if they meet any of the following conditions:

1. More than 1 hour per week of commercial brain training game use over the last month.
2. More than 1 hour per week of mindfulness meditation training or practice over the last month, or a prior history of a sustained mindfulness meditation practice.
3. History of head injury with loss of consciousness for more than 5 minutes.
4. Uncorrected hearing or vision impairment, including color blindness.
5. An allergy to latex (used in brain stimulation electrodes).
6. Prior experience with receiving electrical brain stimulation.
7. Taking medications that produce significant effects on the central nervous system.
8. Diagnosis of major neurological disorder.
9. Indications of possible personality or psychiatric disorder including substance use disorders (with the exception of nicotine dependence).
10. Intelligence quotient (IQ) scores on the Shipley-2 IQ test of less than 90.
11. Participants were also excluded if they are pregnant or were unsure if they may be pregnant or have any contraindications for MRI, including: severe claustrophobia, non-MRI compatible cardiac pacemakers; implantable defibrillators; aneurysm clips; neural stimulators; artificial heart valves; ear implants; insulin pumps; drug infusion devices; IUDs; magnetic dental appliances; metal fragments or foreign objects in the eyes, skin or body; metal plates, screws and prosthetics; non-removable metal piercings; tattoos on the head and neck, other certain older tattoos or permanent makeup (eyeliner) using metal containing inks, some medicated patches, or any other condition, metal implant or other injury or device that is contraindicated for MRI.

Experimental Procedure

Participants who were eligible and gave their consent to participate were then asked to complete a baseline assessment of neuropsychological functioning, which was completed again after training, 4-weeks later. The entire assessment lasted up to 180 minutes, and included established measures of attention, working memory, and fluid intelligence, such as operation span, symmetry span, Raven's progressive matrices, and Shipley IQ. The operation complex span task requires participants to remember words presented interleaved with judgements of the veracity of math equations (see Unsworth et al., 2005). The S-span requires participants to determine if designs are symmetrical along a vertical axis interleaved with highlighted locations of a sequence of boxes that appear in a 4x4 grid. At the end of a trial, participants are asked to reproduce the locations of the highlighted boxes. The Raven's progressive matrices requires participants to solve a matrix by identifying the missing item that completes the pattern. Patterns are presented with a 2x2, 3x3, or 4x4 square matrix with items presented in black on a white background (see Raven and Court, 1998).

Tests were randomized differently for each subject, but the order of tasks was preserved at the post-training assessment for each subject. Within the baseline/post-training assessments, trait-related measures were also obtained, including the mind wandering scale, mindful attention and awareness scale (MAAS), attention related and cognitive errors scale (ACRES), Barratt impulsivity scale (BIS), the big five inventrory-10 (BFI), and the mind-wandering scale (MWS). (Note: due to time constraints in the

larger study, only the EEG sample completed the MAAS and ACRES; both samples completed the BFI, BIS, and MWS).

On a separate day (usually 1-2 days) after the baseline/post-training neuropsychological assessments, EEG or fMRI were acquired. For the UNM subjects who underwent both EEG and fMRI, the two visits were separated by 1-3 days. For the subjects who underwent EEG, the tasks were the 1-, 2-, and 3-back tasks, and a visual three-stimulus oddball task, among others, which took ~100 mins to complete (including EEG prep time). The tasks included for the subjects who underwent fMRI were a resting-state scans (cross-hair fixation for 5 mins), and the same three-stimulus oddball task used during the EEG session, among other tasks, which took ~70 mins total to complete. Lastly, for the final visit, the participants were also asked to complete the study-specific Exit Questionnaire (see Appendix A), which asked about the participants' experience with the training, as well as his or her experience with tDCS, specifically whether he or she thought it was effective. The questionnaire also asked participants to provide specific examples where he or she noticed improvement or decline in any aspect of daily life, or work/school settings.

Training and Randomization

Participants recruited for this dissertation project were assigned to either the mindfulness meditation training with active tDCS (2.0 mA) group or an active control training condition with sham tDCS (0.1 mA). Participants were randomly assigned to groups based on age, gender, and IQ.

Mindfulness-based training with active tDCS (MBT+tDCS)

Participants assigned to the meditation intervention group received access (over the internet) to podcasts that provided guided mindfulness meditation sessions. Participants were asked to listen to these podcasts for 30 minutes per day, five days per week, for 4 weeks of training. The recording consisted of a guided mediation from experienced mindfulness training practitioners and therapists from The University of New Mexico. There were 2 types of meditation techniques that the participants could choose from, either a focused attention (FA) or open monitoring (OM) meditation technique. In general, both FA and OM meditation methods represent the main techniques of Buddhist meditation practices (Lutz et al., 2008).

In FA meditation, the meditator is instructed to simultaneously focuses on a particular item, thought, or object and to actively ignore everything else that might tend to distract attention, e.g., bodily sensations, environmental noise, or intrusive thoughts, by redirecting attention constantly back on the same focus point. Breath-awareness was the primary object of focus in our MBT technique, which was designed to help cultivate concentration, mental clarity, and general mindfulness.

For the OM technique, the meditator is open to perceive and observe any sensation or thought thereby allowing attention to be flexible and unrestricted. Body scan and general open awareness were the primary targets of attention within our OM technique. In particular, our OM sessions were designed to enhance awareness and clarity by moving attention and awareness to different parts of the body and the environment,

just as they are without any judgment or pretense. Appendix D provides a list of responses to frequency asked questions regarding MBT, which was printed and handed out to participants randomized into this group at the beginning of the study.

There was also one 50-minute mindfulness webinar, which allowed participants to ask questions and provide feedback about their meditation experiences. These podcast were accessible to participants via websites that were created and maintained by Charles River Analytics (CRA). Of the 5 training sessions per week, 2 took place in the laboratory with concurrent active tDCS (see tDCS protocol below).

Active control group with sham tDCS

An "active" control task with sham stimulation (see tDCS protocol below) was used to control for test-retest (practice-related) effects on the outcome measures, to ensure the control subjects were engaged in the experiment and interacted with study personnel similar to the intervention group (see Shipstead, Redick and Engle, 2012), and to control for placebo-like effects that may result from one "assuming" that one is receiving active tDCS.

Participants assigned to the control training group also received access (over the internet) to podcasts that provided various images and passages of text by which the participants were asked to write about as if they were a journalist or other related profession. The Cont+Sham subjects viewed pictures and wrote about them for 30 minutes per day, five days per week, for 4 weeks of training. Like the MBT group,

of the 5 control training sessions per week, 2 were also completed in the lab with concurrent sham tDCS.

TDCS protocols: Right frontal stimulation

Given that the objective of using tDCS was to enhance MBT by targeting the cortical networks involved in top-down cognitive control processes and sustained attention, the right prefrontal areas of the frontal-parietal control network (see Corbetta and Shulman, 2002; Peterson and Posner, 2012) was our primary target for anodal stimulation. In particular, given that the right IFG has been shown to play a critical role in attentional control (Hampshire et al., 2010), we placed the anode electrode over F10 (or rIFG) and the cathode electrode over contralateral upper-arm for both groups. With this placement, we intended to preferentially modulate excitatory signaling in large-scale functional connectivity of the right-lateralized attention network (Hunter et al., 2015). Furthermore, by removing the direct influence of the cathode on cortical activity, this montage allows for a more precise evaluation of anodal tDCS on rIFG cortical excitability. The placement of the tDCS electrodes was the same for the Cont+Sham group.

Figure 3 displays the current distribution of the active stimulation tDCS montage (see Bikson et al., 2012 for more details), which highlights the excitability of the right IFG, right insula and other regions thought to be involved in mediation practice.

Figure 3: Modeled current distribution of right frontal tDCS montage used during mindfulness-based training.

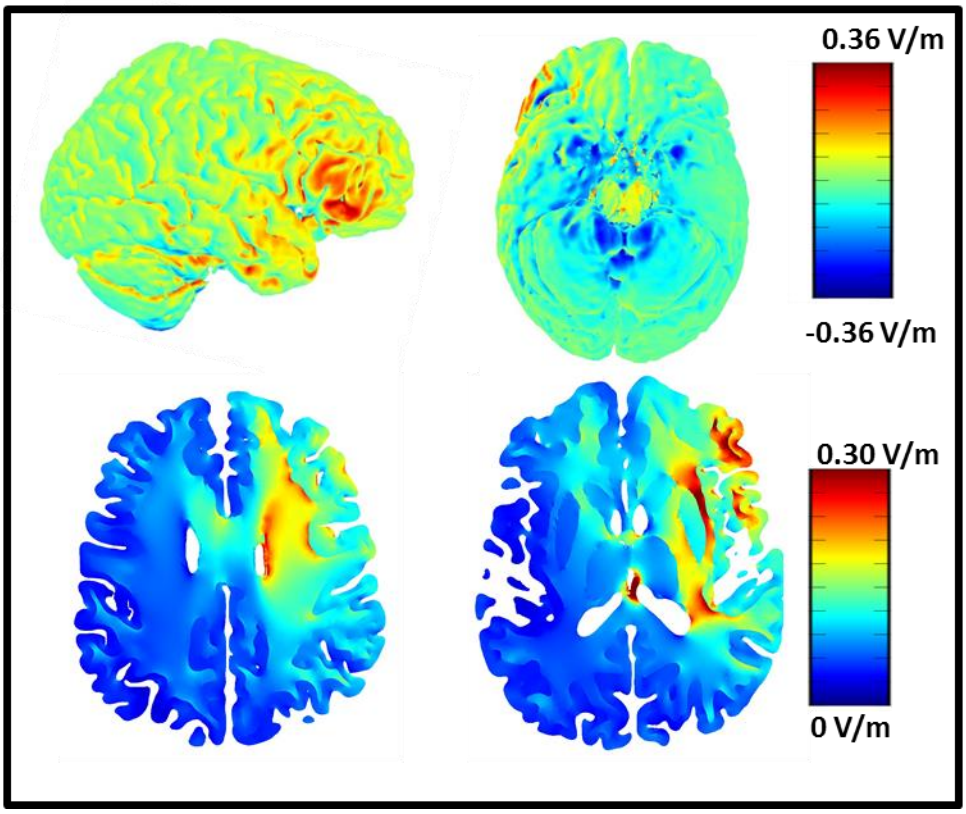

Modeled current distribution for F10 (anode) and contralateral upper bicep (cathode) placement based on forward head model using finite element modeling (Bikson et al., 2012 for more details). This model highlights the excitability of right inferior frontal gyrus, right insula, and other subcortical regions. [Courtesy of Alexander David and Marom Bikson, CCNY]

An ActivaDose II Iontophoresis Delivery Unit (Activatek , Salt Lake City, UT) was used to deliver current for this study. Additional equipment for "double blinding" the tDCS session was also used, which was designed and built by a biomedical engineer

located at the MIND Research Network on UNM's campus. In particular, a coded switch box with 4 inputs for two current generators so that one current generator was set to 0.1 mA and the other to 2.0 mA. The coded switch box had only two outputs for the anode and cathode to be placed on the participant. Depending on 1 of 6 code setting, the current from one of the input leads was diverted and the other was passed through the two output leads connected to the participant. The experimenter was not aware of which codes corresponded to which bypass leads, thereby ensuring that the experimenter was blinded to stimulation type. However, because there was no MBT+Sham group assigned to this study, experimenters (but not the participants) could infer that the participant was receiving active stimulation. This double-blinding procedure was implemented effectively in the Cont+Sham group since there was a Cont+tDCS group assigned within the larger study.

For tDCS preparation, slightly moistened, thin sponges were placed on the participant's right sphenoid bone corresponding to 10-20 EEG location F10 (anode) and the left lateral upper bicep muscle (cathode). The square-shaped saline water-soaked sponges were connected to electrodes ($11cm^2$) that delivered a very weak electrical current. The MBT+tDCS group received a full dose of current (2.0 mA) for 30 minutes, while the Cont+Sham group received a sham dose (0.1 mA) for 30 minutes.

Prior to training, participants were asked to complete a baseline mood assessment, and a sensation questionnaire, which was administered periodically during tDCS. In particular, participants were asked to describe their physical sensations at approximately

1, 5, and 30 minutes after the start of tDCS to monitor participant ratings for itching, tingling, and heat/burning on a 10-point Likert scale (see Appendix B). The tDCS session was stopped if participants reported a 7 or higher on any scale (N=1). In this instance, the tDCS was stopped, but the cognitive training was continued. When the training session was over, participants were given the opportunity to ask questions regarding their mood and mental state to make sure that they have no lingering effects. Results comparing sensation ratings are reported in Appendix B.

For both groups, it is important to note that in addition to the subjects being scheduled for 2 tDCS sessions per week, they were separated by at least one day between tDCS sessions. This was done to ensure there were no lingering effects of tDCS from the previous tDCS session. However, some adjustments were made to accommodate subjects' schedules, e.g., 1 tDCS session on one week and 3 tDCS sessions on the following week. Also, there was one participant enrolled into this study that reported scabbing on the skin which required healing before another tDCS session. This person missed 2 consecutive tDCS sessions as a result and reported no other issues.

Neuroimaging

EEG n-back task procedure, stimuli and timing parameters.

In the n-back task, participants were presented with a sequence of letters one at time and asked to match the current letter to one presented *n* letters prior in the sequence. For this study, there were three experimental blocks, where each block increased in working memory load, starting with 1-back, 2-back and then the 3-back. This ordering of

experimental blocks was the same for all subjects at baseline and post-training for a total of 17 mins to complete all three blocks.

For each block, stimuli were classified as a target "hit" (or match) one-third of trials (or 35 possible targets) with non-targets, or "non-match" letters, two-thirds of all trials (or 70 possible non-targets), resulting in a total of 105 trials per block. Participants used their right thumb to respond whether a letter in the sequences was a target, or "match".

The first 10 letters of the alphabet (black Tahoma font) were selected as the possible letter stimuli. The letters were presented on the center of screen (visual angle in height = 1.5°) on a light gray background (RGB triplet dimensions: 192, 192, 192), which allowed for the most optimal identification of letters while minimizing afterimages. The duration of each letter was 500 ms with 1400 ms inter-stimulus interval (ISI). Responses that were 100 ms or less from stimulus onset were ignored from subsequent analyses. The n-back task was administered using Presentation 14.0 (Neurobehavioral System Inc., Berkeley, C.A.) and behavioral data was extracted using Excel VBA programming.

EEG visual oddball task procedure, stimuli and timing parameters.

The three-stimulus visual oddball task used for this study has been described in detail in previous studies (Clark et al., 2000; 2015). In short, participants were asked to recognize and respond to a single target letter while non-target letters were presented in a series. There were four experimental blocks, where each block consisted of 90 total stimuli and last approximately 3 minutes in length, with interspersed rest periods. The

ordering of stimuli was the same for all subjects at baseline and post-training for a total of ~14 mins to complete all four blocks.

For each block, stimuli were classified as an infrequent target "hit" 9% of trials ("X", or 32 possible targets), an infrequent distractor non-target 9% of all trials ("C", or 32 possible distractor letters), and a frequent standard non-target 82% of trials ("T", or 296 possible standard letters), with a total of 360 trials. Participants were to respond with a single speeded button press with the right thumb for every instance the target letter was presented.

The letters were presented on the center of screen (visual angle in height = 1.5°) on a light gray background (RGB triplet dimensions: 192, 192, 192), which allowed for the most optimal identification of letters while minimizing afterimages. The duration of each letter was 200 ms with an ISI that varied from 550 ms to 2250 ms across trials. The oddball task was administered using E-prime (Psychology Software Tools, Inc., Pittsburgh, PA) and behavioral data was extracted using Excel VBA programming.

All statistical analysis were performed using SPSSv22 (SPSS Inc., Chicago, IL.)

fMRI visual oddball task procedure, stimuli and timing parameters.

The three-stimulus visual oddball task used in the fMRI portion of this study was the same task used in the EEG portion of this study, which is described in detail in the previous section.

EEG acquisition

EEG data were acquired using a BioSemi 128-channel ActiveTwo system. BioSemi Active-electrodes offer a solution for the common problems associated with high electrode impedance and cable shielding. This system replaces the conventional "ground" electrodes with an active (Common Mode Sense; CMS) and passive (Driven Right Leg; DRL) electrodes to form a feedback loop, which drives the average electrical potential at the scalp (from CMS) as close as possible to the analog-to-digital (AD) converter reference voltage in the AD-box (BioSemi: www.biosemi.com/faq/cms&drl.htm). Bipolar electro-oculogram (EOG) recordings were acquired with BioSemi Flat-Type Active-electrodes, which were placed below the left eye and at the outer canthus of the eye. Bipolar electrocardiogram (ECG) recordings were also obtained with BioSemi Flat-Type Active-electrodes, which were placed symmetrically approximately 1 cm lateral and inferior to the clavicle bone. All signals were recorded using ActiView software and digitized at 1,024 Hz with 24-bit AD conversion.

Subject-specific EEG locations were obtained by creating a 3D-digitization of electrode locations relative to each subject's anatomical landmark locations (i.e., nasion, inion, and both preauricular points) using the Polhemous FastTrak system. One out of the four (Small, medium, large and extra large) BioSemi EEG head caps was fitted based on the subject's head circumference and was then centered on the head of each subject,

ensuring that electrode site Cz was equidistant between the inion and nasion, and between both preauricular points. This procedure was completed at baseline and post-training.

EEG Preprocessing

Figure 4 displays the general EEG pre-processing analysis steps, from artifact rejection to averaged responses used for subsequent within- and between-subject comparisons. In particular, EEG data were pre-processed using the MATLAB toolboxes EEGLAB (http://sccn.ucsd.edu/eeglab/) and ERPLAB (http://erpinfo.org/erplab), all of which require MATLAB Signal Processing toolbox. After the removal of any DC offset, channel locations were then linked to each participant's dataset. Bad channels were then visually detected and removed from each dataset, and Independent Components Analysis (ICA) was used to remove blinks, cardiac signal, and 60 Hz line noise artifacts from the data.

The EEG scalp distribution was re-referenced to the average of all scalp electrodes. However, given that EEG data depends on the reference electrode, which changes voltages, power amplitudes and phase angels (Yuval-Greenburg et al., 2008; Michel, 2009), the average-referenced EEG n-back data was compared to scalp distributions using a mastoid reference (the average between left and right electrodes over each mastoid bone). The results are presented in Appendix D. In short, although there were mean differences between P3 amplitudes and power amplitude in the theta range, these differences were not statistically insignificant (*p's* > 0.14). Furthermore, it is important to note that although the potential values, phase, and power amplitudes at the

electrodes change based on the selected re-referencing procedure, the potential differences *between electrodes* are not affected because this mathematical transformation is linear across electrodes (Michel, 2009; Cohen, 2014). Accordingly, the same (average) re-referencing procedure was implemented on both time- and frequency-domain data.

Figure 4: EEG pre-processing and analysis steps used on all tasks for this study

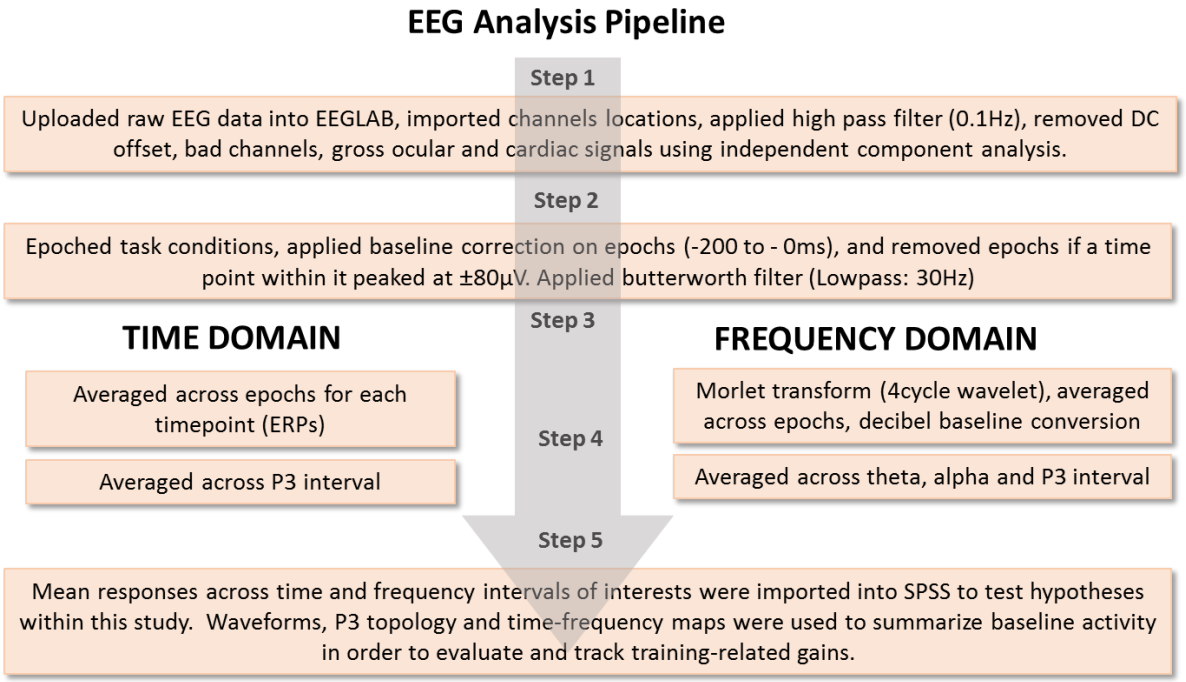

Time frequency analysis

Time-frequency decomposition was performed by convolving stimulus-locked single-trial data from all electrodes with complex Morlet wavelets,

$$e^{i2\pi ft}e^{-t^2/(2\sigma^2)}$$

where *t* is time, *f* is frequency, which ranged from 1 to 40 Hz in 40 logarithmically spaced steps, and σ is the width of each frequency band (4 cycles) to obtain comparable frequency precision at low and high frequencies. Instantaneous power was estimated as the square of the complex convolution signal $Z(\text{power} = \text{real}[z(t)]^2 + \text{imag}[z(t)]^2)$ and averaged across trials. Power values at each time-frequency point were normalized by converting to the decibel (dB) scale to account for power-law scaling of oscillations in different frequency bands (amplitude increases when frequency decreases) by using the formula:

$$dB_{tf} = 10 \log_{10} (\text{power}_{tf} / \text{mean baseline}_{f})$$

For this analysis, the decibel is a ratio between the strength of power activity after stimulus onset and the mean strength of power activity 200 ms prior to stimulus onset (i.e., baseline level of power). Thus, dB-converted power represents the change in power relative to baseline power.

All time-frequency analyses were conducted using modified MATLAB scripts (requiring MATLAB Signal Processing Toolbox) obtained from Cohen, 2014.

Phase-based coherence analysis

Inter-trial phase clustering (ITPC; also known as phase-locking value/factor, phase coherence, and several other terms; ITPC is preferred here because it is a description of the analysis rather than an interpretation of the result; see Cohen, 2014), which refers to the average of complex phase angles between trials over time (Varela et al., 2001; Cohen, 2014). Below is the equation used to derive ITPC:

$$\mathrm{ITPC_{tf}} = \left| n^{-1} \sum_{r=1}^{n} e^{ik_{tfr}} \right|$$

Within the ITPC formula, *r* refers to trials, *n* refers to the number of trials, and *tf* corresponds to a time-frequency point within each trial. This measure allows for the assessment of task-related phase-based synchrony. One main advantage of using this method is that it provides stronger evidence for task-related modulations, or neural entrainment (Cohen, 2014).

fMRI acquisition and data processing:

There were a total of 30 subjects (both groups combined) who also underwent the fMRI portion of the study. For each subject, the rest scan was acquired first, followed by 1 of 3 tasks presented in random order, including the visual oddball task. High-resolution T2*-weighted functional images were acquired using a gradient-echo EPI sequence with TE = 30 ms, TR = 2 s, flip angle = 90°, 3 mm^3 isotropic voxels. A structural T1-weighted MPRAGE scan was also acquired at the beginning of the scan session (TR = 2250 ms, TE = 3.98 ms, flip angle= 9°, 1 mm^3 isotropic voxels).

Preprocessing was completed using statistical parametric mapping (SPM; Wellcome Department of Imaging Neuroscience, London, UK. http//www.fil.ion.ucl.ac.uk/spm), within MATLAB (Mathworks Inc., Sherbon MA). The first three EPI volumes were discarded to remove T1 equilibration effects. Realignment was then completed using INRIalign and slice-timing correction was applied, with the

middle slice used as the reference frame. Data were then spatially normalized into the standard Montreal Neurological Institute (MNI) space, resliced to 3 mm × 3 mm × 3 mm voxels, and smoothed using a Gaussian kernel with a full-width at half-maximum of 10 mm. No subjects were excluded due to excessive head motion, defined as more than 3.0 mm of translation in any plane or more than 5 degrees of rotation in any plane. The six parameters for head movement were included as covariates in the level-one analysis.

Resting-state scans were 5 mins in duration (150 volumes). Participants were instructed to keep their eyes open during the scan and fixate on a foveally presented white cross hair against a black background. A relatively high-dimensional model-order (c=75) independent component analysis (ICA) was performed on the pre-processed resting-state data using Group ICA fMRI Toolbox (GIFTv3.0a; http://mialab.mrn.org/software/gift/). Prior to group ICA, voxel time series were z-scored to normalize variance across space, minimizing possible bias in subsequent variance-based data reduction steps. Thereafter, there were two principle component analyses (PCA) data reduction steps along directions of maximal group variability, first at c=100 and again at c=75. The infomax ICA algorithm, which incorporates nonlinearities in the transfer function to capture higher-order moments in the BOLD resting-state fluctuations, was implemented to detect the independent source components in the data. To ensure stability of estimation, the ICA algorithm was repeated 20 times in ICASSO. Back-reconstruction of each individual-subject's resting-state data was run using GICA3 (as implemented in GIFTv3).

One sample t-test maps were computed for each components' spatial map across all subjects and thresholded, $q < 0.05$, FDR-corrected, to obtain regions of peak activation clusters within each component. Networks were then identified using the aggregate spatial maps that overlapped with anatomical regions of interest, specifically those RSNs that comprise DMN (including ACC, PCC, middle frontal gyrus and precuneus), cognitive control networks (CCN; frontal and frontal-parietal networks), and the "salience" and visual oddball networks (SAL; bilateral insulae and dorsal cingulate, right-lateralized IFG, and a bilateral inferior parietal and premotor cortex network). Spatial correlations were computed to help identify the resting-state networks (RSNs) that overplayed the most with the visual oddball activations. All three of the selected SAL networks showed the highest correlations ($R^2 > 0.32$) compared to the other 72 component maps. As described in more detail in the Results section, ten components were identified that met this criteria and were used in all subsequent analyses.

Dynamic functional network connectivity (dFNC) analysis was conducted using the dFNC toolbox in GIFTv3.0a, which is described in detail in Allen et al., 2012. In summary, to explore certain quasi-stable connectivity patterns, functional network connectivity dynamics underwent sliding time-window correlations and k-means clustering of windowed correlation matrices. In particular, a tapered window was created, which was computed as a convolution of a rectangle (width = 22 TRs; 44 s) with a Gaussian distribution ($\sigma = 3$ TRs). This time window slid in steps of 1 TR, resulting in W= 113 windows. Then, the k-means clustering algorithm was used to construct the

structure of reoccurring functional connectivity patterns to windowed covariance matrices (using the L1 Manhattan distance function). Only covariance between the 10 pre-selected RSNs were used in the clustering analysis, maximizing the dynamic connectivity patterns (variance) within and between cluster centroids unique to the intrinsic organization of networks that comprise the DMN, CCN and SAL, resulting in $(10 \times (10 - 1))/2 = 45$ features. The resulting centroids were then used to set a clustering of all data (29 subjects × 113 windows = 3277 instances).

Based on these subject state vectors, average dwell times for each centroid (or "state") and each subject were computed as the amount of variance accounted for within each state of all time windows; that is, the proportion of subject time windows assigned to each state. Also, for each subject at baseline and post-training, the number of transitions from one state to another was obtained, which was computed by considering functional connectivity time windows as a Markov chain that transitions between a discrete number of states, resulting in an averaged transition matrix (see Allen et al., 2012 for details). Between-group and within-group (time) differences in dwell times in each state as well as the number of transitions between states were evaluated using repeated measures ANOVA.

Statistical comparisons

Unless noted otherwise, all statistical comparisons were evaluated in this study using repeated measures ANOVAs. The assumptions of normality, homogeneity of variances, and equality of the covariance matrices were evaluated using the Shapiro-Wilk

and Kolmogorov-Smirnov tests, Levene's test of equality, and Box's test, respectively. There was 1 outlier (in the Cont+Sham group) that positively skewed the shape of the distribution on several variables. For this reason, this subject was omitted from all subsequent statistical analyses. Thereafter, all tests to evaluate the assumptions of the factorial ANOVAs were non-significant (*p's* > 0.01).

CHAPTER 3: EEG RESULTS

Participant demographics

There was a total of 4 participants who were dropped from the study, leaving a total of 29 subjects remaining for subsequent data screening. More specifically, there were 3 subjects from the Cont+Sham group who were dropped from the study due to non-compliance issues (i.e., missed more than 2 scheduled appointments and did not responds to e-mails or phone calls). There was also 1 subject from the MBT+tDCS group who notified study personnel that they could no longer participate due to the time commitment in the study. Table 1 displays all demographic information for all subjects who were included in subsequent analyses. One-way ANOVAs and χ^2 tests were computed to test if there were any baseline differences in demographic information and pre-defined personality metrics. There were no statistically significant differences between groups on any of the baseline demographic and personality trait measures (*p's* > 0.19).

Table 1: Mean (SD) and corresponding statistics on sample demographic information (n = 29).

	Control+sham (n=13)	**MBT+tDCS (n=16)**	**Comparisons[a]**
Age (yrs)	26.6 (4.2)	28.4 (6.7)	*F=0.57, p = 0.45*
College Education (yrs)*	5.2 (1.5)	6.1 (1.8)	*F=1.57, p = 21*
Estimated IQ*****	111.2 (6.6)	112.0 (8.8)	*F=0.07, p = 0.79*
Sex (F)	8|5	10|6	χ^2 *=0.54, p=0.45*
Number of training sessions	15.8 (2.8)	16.2 (3.8)	*F=0.11, p = 0.74*
Number of tDCS sessions	7.2 (1.2)	7.1 (0.8)	*F=0.01, p = 0.91*
MWS	17.1 (5.2)	18.3 (4.6)	*F=0.41, p = 0.52*
BFI Conscientiousness	8.4 (1.5)	7.1 (1.7)	*F=3.65, p = 0.14*
BIS Attention	9.5 (3.0)	10.4 (2.7)	*F=0.64, p = 0.43*

[a.] One-way ANOVAs and chi-square test were computed to test any differences across each of the groups displayed. No baseline differences observed. MWS=Mind Wandering Scale; BFI=Big Five Inventory; BIS=Barrett's Impulsivity Scale. Note: all participants enrolled in this study were right handed.

Statistical analyses on n-back performance

In order to test within-subject (baseline vs post-training and WM load) and between-subject (Cont+Sham vs MBT+tDCS) comparisons on both performance and EEG data, 2x2x3 repeated measures ANOVAs were obtained, with group designation as the between-subjects factor and time (baseline and post-training) and working memory load (1-back, 2-back, and 3-back) as the within-subject factors. The group means and standard errors (SE) for each of the WM load conditions are displayed in Figure 5.

Figure 5: Mean, SE and statistical comparisons of accuracy and reaction times for all WM load conditions within each group at baseline and post-training.

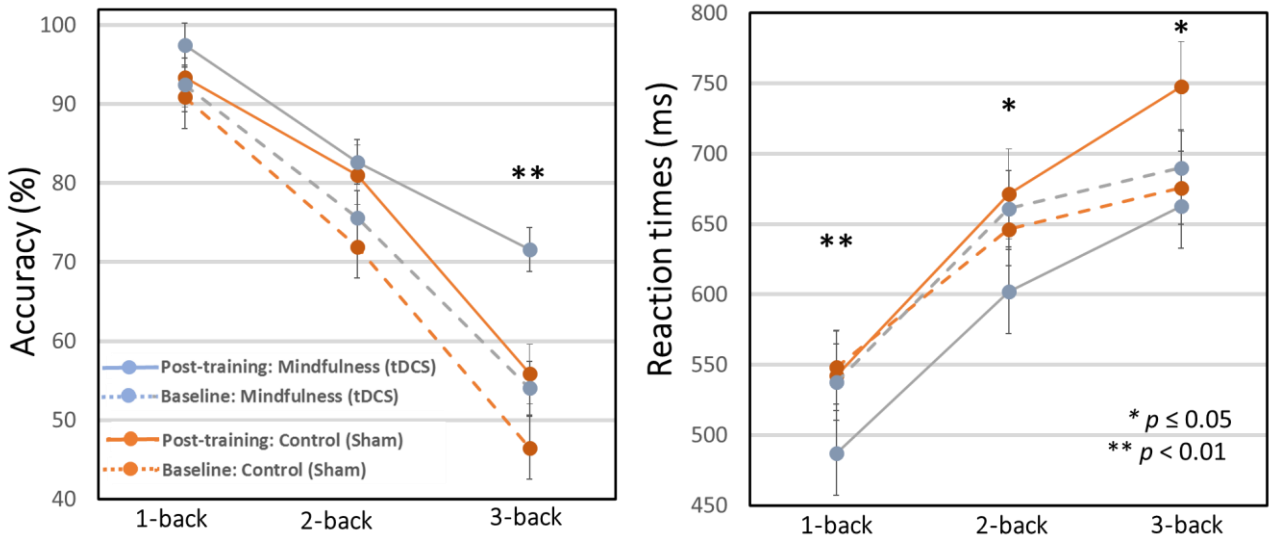

Baseline data are represented by dotted lines and post-training data by solid lines for both the MBT+tDCS (blue) and Cont+Sham (red) groups. After training, the MBT+tDCS group was more accurate during the 3-back condition and quicker to respond across all WM load conditions relative to baseline and post-training performance of the Cont+Sham group.

For the accuracy measures (i.e., hit rate), there was a main effect of time (post-training > baseline), $F(2, 26) = 28.36$, $p < 0.001$, $\eta_p^2 = 0.54$, and WM load (1-back > 2-back > 3-back), $F(2, 26) = 169.67$, $p < 0.001$, $\eta_p^2 = 0.88$. These results are consistent with practice-related effects and the increased difficulty of this task as a function of each WM load condition. Although there was not a statistically significant group×time×load

interaction ($\eta_p^2 = 0.04$), pair-wise t-tests were conducted to evaluate the proposed hypotheses, which showed a significant increase on post-training 3-back performance in the MBT+tDCS group compared to the Cont+Sham group ($t = 2.42$, $p < 0.01$). There were no differences between groups for the 1-back or 2-back (p's > 0.49). Furthermore, post-training 3-back accuracy was significantly increased relative to baseline within the MBT+tDCS ($t = 4.07$, $p < 0.001$). There were no differences between groups on baseline accuracy scores for any of the WM load conditions (p's > 0.26), nor between baseline and post-training accuracy within the Cont+Sham group for any of the WM load conditions (p's > 0.10).

For the n-back RT measures, there was a main effect of WM load (3-back > 2-back > 1-back), $F(2, 26) = 60.15$, $p < 0.001$, $\eta_p^2 = 0.72$, which is consistent with the accuracy results in that slower RTs were observed as a function of increased WM load. There was also a group × time interaction, $F(2, 26) = 9.27$, $p = 0.006$, $\eta_p^2 = 0.28$), where follow-up one-way ANOVAs showed that post-training RTs in the MBT+tDCS group were faster than the Cont+Sham group RTs when collapsing across WM load conditions ($p = 0.02$, $\eta_p^2 = 0.22$). Furthermore, collapsed across WM load conditions, within-subject comparisons showed that the MBT+tDCS group responded quicker after training relative to baseline ($p = 0.01$, $\eta_p^2 = 0.25$). It is worth noting that these differences were most pronounced for the 1-back ($p = 0.002$) and 2-back ($p = 0.03$) conditions. There were no differences in baseline RTs between groups ($p = 0.85$, $\eta_p^2 = 0.01$), nor between time points within the Cont+Sham group ($p = 0.12$, $\eta_p^2 = 0.09$).

Statistical analyses on n-back P3 amplitudes

The baseline group-level P3 waveforms are displayed in Figure 6 for Pz, Fz and F10 electrode sites. Interestingly, there was a negative deflection at P3 latency for the lateral frontal electrode sites.

Figure 6: Baseline group-level ERP waveforms for Pz, Fz, and F10 as a function of working memory load.

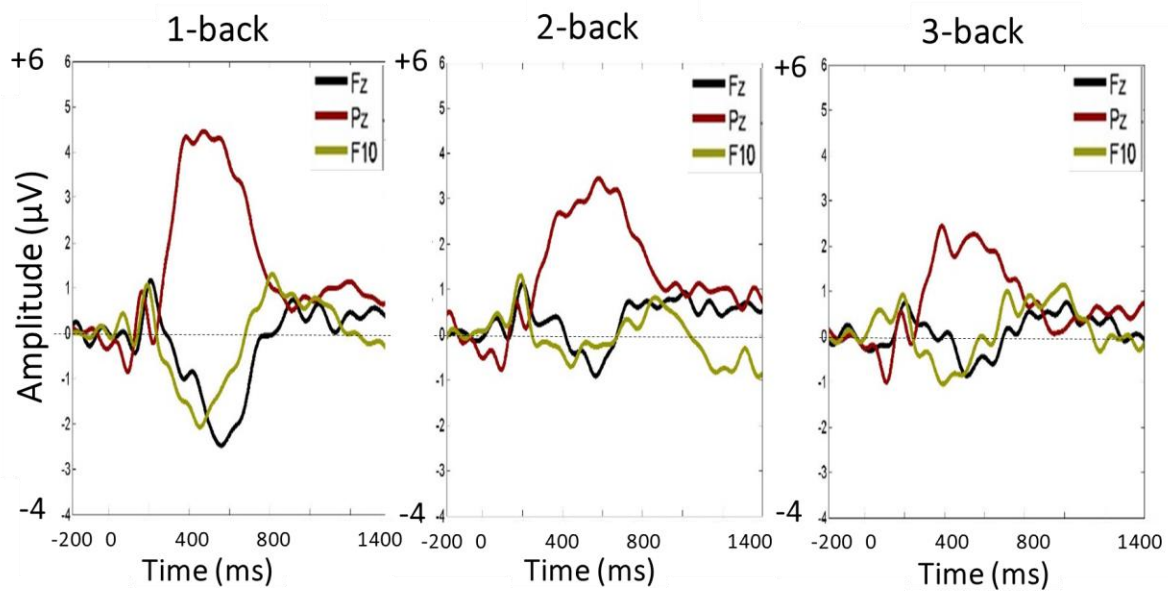

As expected, the P3 amplitude decreased as a function of WM load after a target hit. P3 activity was averaged between 350 – 650 ms for all subsequent analyses.

The baseline group mean P3 topologies for each of the WM load conditions are displayed in Figure 7. Results show the expected P3 topology, with activity centralized over posterior electrodes, with activity more dispersed to frontal sites (e.g., Fz and F10) as a function of WM load.

Figure 7: Baseline ERPs and mean P3 topology as a function of working memory load (target hits).

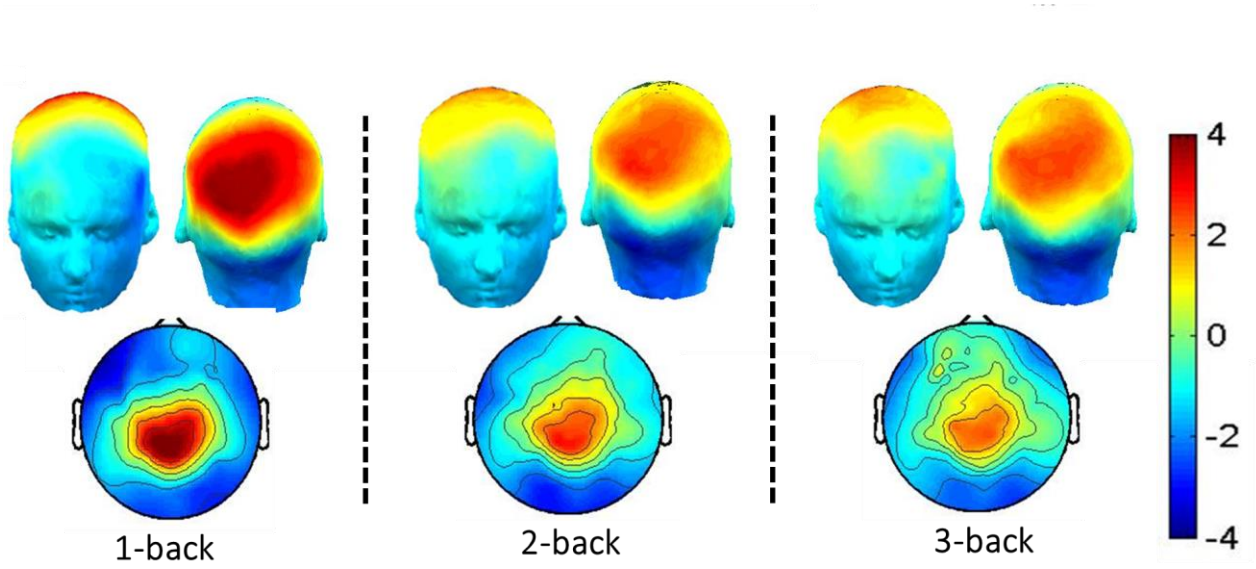

Group mean P3 activity (350-650 ms) across all subjects for each working memory load condition.

Finally, P3 group means, SEs, and statistical comparisons for each of the WM load conditions and each electrode site of interest are displayed in Figure 8.

Figure 8: Mean, SE and statistical comparisons of P3 amplitude for all WM load conditions and electrode sites of interest within each group at baseline and post-training.

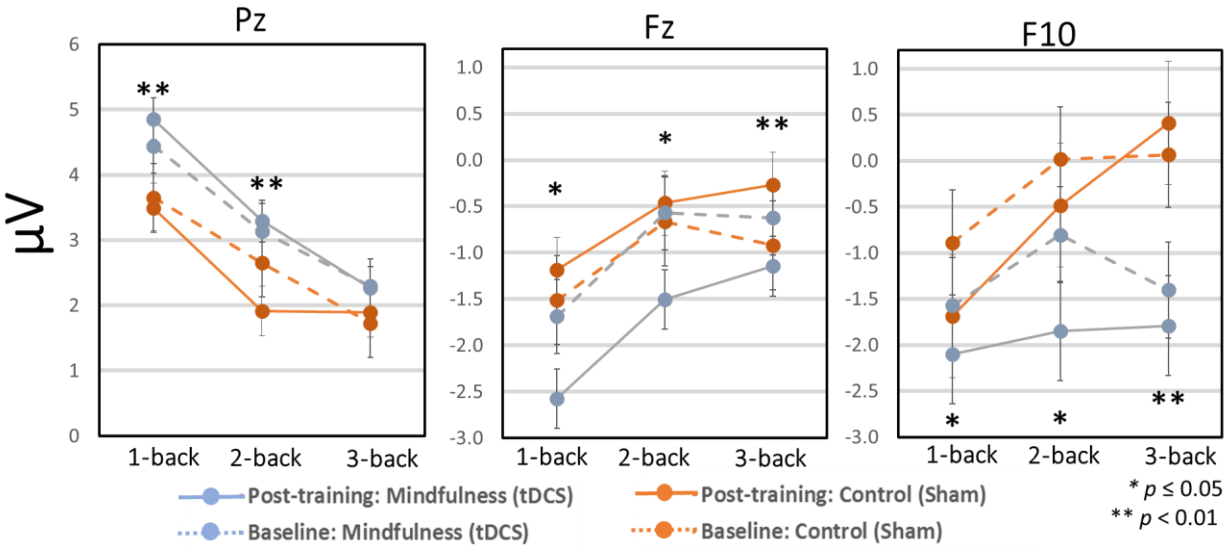

Baseline data are represented by dotted lines and post-training data by solid lines for both the MBT+tDCS (blue) and Cont+Sham (red) groups. P3 activity was computed as the average between 350 – 650 ms for all n-back conditions. Compared to the Cont+Sham group, results show positive increase in P3 amplitude across less demanding WM load conditions for electrode site Pz, and decreased positive amplitude across all WM load conditions for electrode sites Fz and F10 in the MBT+tDCS group.

At electrode Pz, there was a main effect of WM load on P3 amplitude (1-back > 2-back > 3-back; $F(2, 26) = 118.18$, $p < 0.001$, $\eta_p^2 = 0.84$), similar to the WM performance accuracy results, but with a larger effect size. Pair-wise t-tests were conducted to evaluate the hypothesized differences within and between subjects. There was a significant increase in post-training 1-back responses ($t = 3.07$, $p = 0.005$) and 2-

back responses (t = 2.57, p = 0.01) in the MBT+tDCS group compared to the Cont+Sham group. There were no differences between groups on baseline Pz responses in any of the WM load conditions (p's > 0.10), nor between baseline and post-training Pz responses within the Cont+Sham group in any of the WM load conditions (p's > 0.27).

At location Fz, there was a main effect of WM load, such that mean P3 amplitude (350 - 650 ms) approached a positive amplitude as a function of increased WM load, $F(2, 26) = 12.17$, $p = 0.002$, $\eta_p^2 = 0.34$. There was also a group × time interaction, $F(2, 26) = 4.41$, $p = 0.04$, $\eta_p^2 = 0.16$. Follow-up one-way ANOVAs showed that post-training P3 amplitude in the MBT+tDCS group was more negative in amplitude compared to the Cont+Sham group when collapsing across WM load conditions ($p = 0.003$, $\eta_p^2 = 0.32$). It is worth noting that these differences were most pronounced for the 3-back condition (t = 3.06, p = 0.006). Furthermore, collapsed across WM load conditions, the MBT+tDCS Fz responses were more negative in magnitude after training relative to baseline (p = 0.03, $\eta_p^2 = 0.18$). There were no differences in baseline Fz responses between groups (p = 0.88, $\eta_p^2 < 0.01$), nor between time points within the Cont+Sham group (p = 0.38, $\eta_p^2 = 0.03$).

At location F10, where anodal tDCS was applied, there was a main effect of WM load, similar to Fz in that the positive amplitude increased as a function of increased WM load, $F(2, 26) = 6.24$, $p = 0.02$, $\eta_p^2 = 0.21$. Pair-wise t-tests were conducted, which showed a significant decrease in positive amplitude on post-training 3-back responses (t=2.89, p=0.008) in the MBT+tDCS group compared to the Cont+Sham group. There were no differences between groups on baseline accuracy scores for any of the WM load

conditions (*p's* > 0.24), nor between baseline and post-training accuracy within the Cont+Sham group on any of the WM load conditions (*p's* > 0.21).

Comparisons on sustained theta P3 power

The baseline group mean sustained time-frequency maps for each WM load condition are displayed in Figure 9. The time range (300 - 900 ms) was selected based on the sustained duration of the P3 activity observed in the ERP waveforms (see Figure 7). Results show a consistent pattern of increased power as a function of WM load, specifically for Fz and Pz electrode sites. Interestingly, there was also a general pattern of decreased power (relative to baseline) for the 1-back condition in the Pz electrode.

Figure 9: Baseline group-level sustained theta power time-frequency windows for each n-back condition and electrode site of interest.

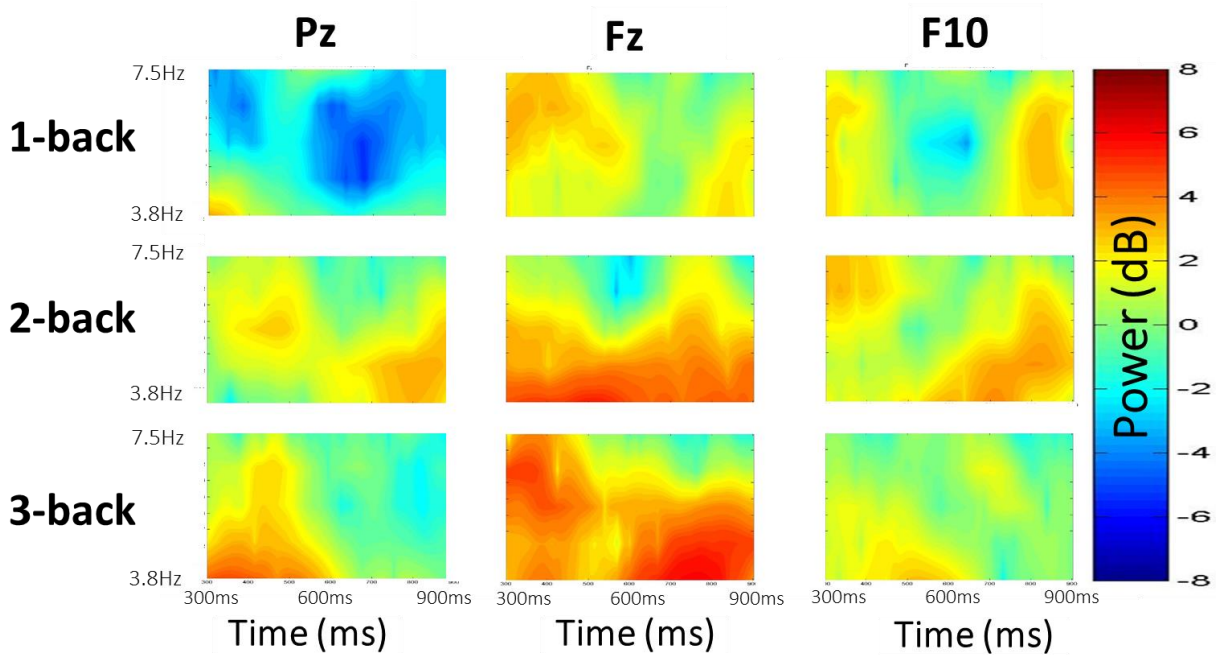

Theta power was decibel scaled and baseline corrected from -200 to 0 ms. Sustained theta power was averaged between 300 – 900 ms and from 3.8 – 7.5 Hz (log spaced), which was used in all subsequent comparisons. Results show a consistent pattern of increased power as a function of WM load, specifically for Fz and Pz electrode sites.

Time-frequency power group means, SEs, and statistical comparisons for each of the WM load conditions and each electrode site of interest are displayed in Figure 10. For location Pz, there was a group × time interaction, $F(2, 26) = 30.04$, $p < 0.001$, $\eta_p^2 = 0.57$, where follow-up one-way ANOVAs showed that post-training power in the MBT+tDCS group was increased compared to the Cont+Sham group when collapsing across WM load conditions ($p = 0.002$, $\eta_p^2 = 0.35$). It is worth noting that these differences were most pronounced for the 3-back condition ($t = 3.10$, $p = 0.005$). Furthermore, collapsed across WM load conditions, Pz theta power in the MBT+tDCS group was significantly increased after training relative to baseline ($p < 0.001$, $\eta_p^2 = 0.62$). It is important to note that for the 2-back condition only, there was an unexpected baseline difference between groups ($p = 0.02$). However, there were no differences within the Cont+Sham group between baseline and post-training Pz power for any of the WM load conditions (*p's* > 0.15), indicating that there were no training-specific changes within this group.

Figure 10: Mean, SE and statistical comparisons of theta power for all WM load conditions and electrode sites of interest within each group at baseline and post-training.

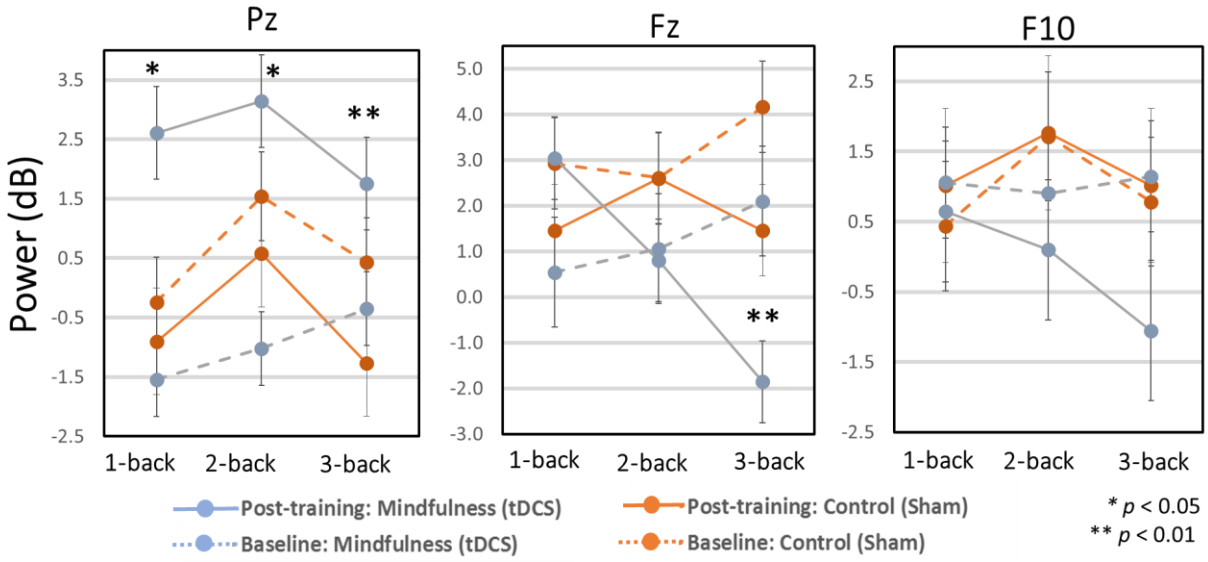

Baseline data are represented by dotted lines and post-training data by solid lines for both the MBT+tDCS (blue) and Cont+Sham (red) groups. Mean theta power was averaged between 300 – 900 ms and from 3.8 – 7.5 Hz (log spaced). General results show increased theta power across all WM load conditions for electrode site Pz, and a decrease in 3-back theta power for electrode site Fz in the MBT+tDCS group.

At electrode site Fz, there was a group × time × WM load interaction, $F(2, 26) = 7.77$, $p = 0.01$, $\eta_p^2 = 0.25$. Follow-up pair-wise t-tests showed that post-training power in the MBT+tDCS group was increased in the 3-back condition only compared to the Cont+Sham group ($t = 2.24$, $p = 0.03$). Also, this 3-way interaction was also driven by a pair-wise difference (baseline > post-training) that was specific to the 3-back condition only in the MBT+tDCS group ($t = 3.73$, $p = 0.001$). Lastly, to examine whether there

were pair-wise differences between WM load conditions within each group and time point, pair-wise t-tests showed a significant difference between 3-back power compared to the 1-back and 2-back, which was specific to the MBT+tDCS group at post-training only (p's < 0.001). There were no differences in baseline Fz power between groups (p's > 0.10), nor between time points within the Cont+Sham group (p's > 0.05).

For F10 power, there were no main effects, interactions or pair-wise difference between groups nor between time points (p's > 0.15).

Assessing possible near and far transfer gains in complex WM capacity, fluid IQ, and attention-related personality traits

Group means and SE of each transfer task and personality traits of interest are displayed in Figure 11. Between-subject comparisons showed a statistically significant increase in S-span scores only in the MBT+tDCS group compared to the Cont+Sham group (p = 0.02). There were no other statistically significant differences observed between groups in the other transfer measures (p > 0.21).

Figure 11: Mean, SE and statistical comparisons of near and far transfer relative change scores for each group.

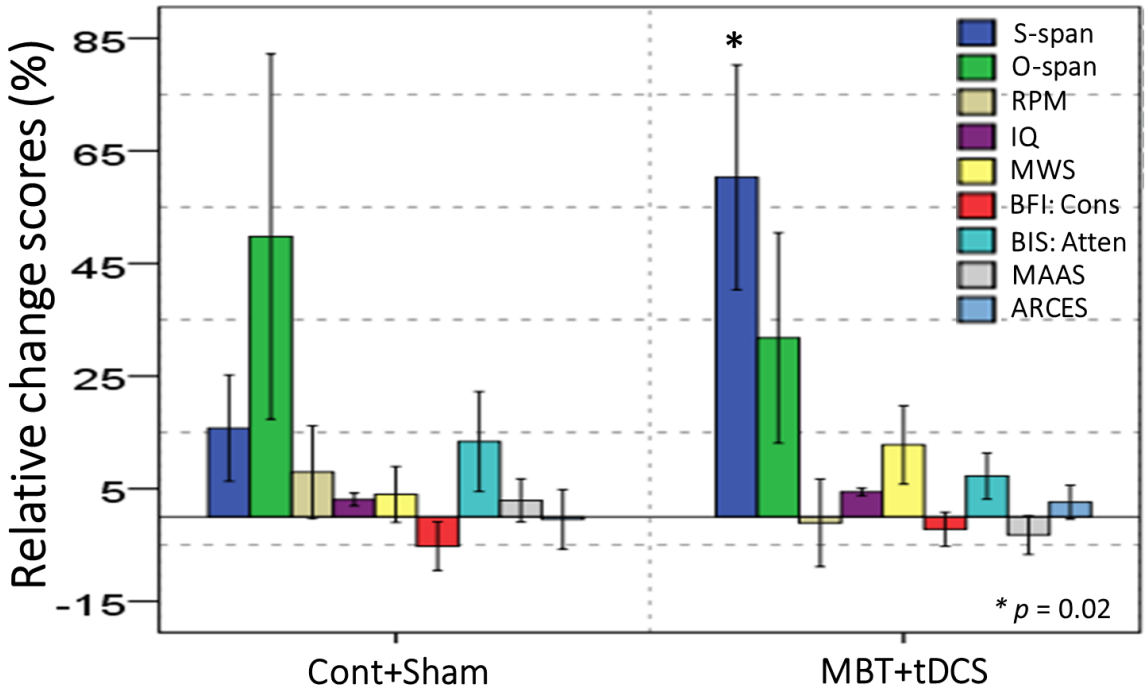

Relative change scores were computed as the difference between post-training and baseline scores divided by the baseline scores, which were then converted to percentage points. Bar graphs display mean and SE of the relative change scores for each variable. Results show a significant difference between groups for the s-span scores only. RPM=Ravens Progressive Matrices; MWS=Mind Wandering Scale; BFI=Big-five Inventory; Cons=conscientiousness sub-scale of BFI; BIS=Barratt Impulsivity Scale; Attn=Attention sub-scale of BIS; MAAS=Mindful Attention and Awareness Scale; ARCES=Attention-related Cognitive Errors Scale.

Examining whether gains in WM load "transferred" to complex WM capacity, fluid IQ, and attention-related personality traits

In order to examine whether the observed training-related gains observed on the n-back task were related to gains in WM tasks (S-span and O-span), fluid IQ tests (RPM and Shipley IQ), and attention-related personality traits, relative change scores (post-training – baseline / baseline) were computed for each variables that showed a significant difference in the previous analyses and the proposed transfer tasks. Pearson correlations were then computed to test if there were positive associations, such that an increase in a relative change score in one variable would correspond to an increase in a relative change score in the other transfer task. Similarly, the number of MBT sessions and the number of tDCS sessions were also correlated with these relative change scores in order to examine any possible training-related dose effects.

For the performance data, there was a significant association between the relative change in 3-back accuracy scores and S-span accuracy scores collapsed across both group, $r(29) = 0.49$, $p = 0.009$. However this correlation was primarily driven by the MBT+tDCS group, $r(15) = 0.58$, $p = 0.02$, indicating a transfer in WM ability that is specific to the MBT+tDCS group. There was no association observed within the Cont+Sham group, $r(14) = 0.07$, $p = 0.84$. There were also no statistically significant correlations observed between the n-back and O-span, nor between the RPM and IQ relative change scores collapsed across groups, nor within either group ($p's > 0.66$).

For the ERP data, there was a MBT+tDCS group-specific relationship between S-span relative change scores and relative changes in P3 amplitude during 3-back performance in the F10 electrode site, $r(15) = -0.55$, $p=0.04$. This finding suggests that those in the MBT+tDCS group who showed the largest training-related gains within the S-span also exhibited the largest relative decrease in change in P3 amplitude during high working memory load in the F10 electrode. This measure may be a prime candidate to assess transfer in other metrics. There were no other correlations observed between the EEG measures and the transfer relative change scores.

Furthermore, it is important to note that the only variable that correlated with relative change scores in the 3-back condition was theta power at the Pz electrode site, collapsed across groups, $r(29) = 0.46$, $p = 0.02$. Again, this correlation was primarily driven by the MBT+tDCS group, $r(15) = 0.61$, $p = 0.01$. There was no association observed within the Cont+Sham group, $r(14) = 0.07$, $p = 0.84$. This result suggest that those who showed the largest training-related gains in 3-back performance in the MBT+tDCS group also exhibited the largest relative change in power in the Pz electrode.

In order to examine whether individual differences in personality measures, e.g., MAAS, ACRES, BIS, BFI, and MWS were related to any of the observed training-related gains in performance measures (including transfer tasks) and the EEG metrics, Pearson correlations were also computed on the relative change scores for each variable. There were no associations observed when collapsed across both groups, nor within the Cont+Sham group alone ($p's > 0.08$). However, the MBT+tDCS group showed an

interesting relationship. There was a significant correlations between relative change scores for the O-span and relative change scores in the MWS, $r(15) = -0.60$, $p = 0.01$. Thus, the less a participant endorsed mind wandering attributes relative to baseline, the better they scored on average on the O-span task relative to baseline.

Lastly, for the EEG relationships between personality traits, only the relative change scores in the attention sub-scale within the BIS was significantly related to relative change scores in the P3 amplitude during the 3-back amplitude in the F10 electrode, $r(15) = 0.70$, $p = 0.004$. This finding suggests that the relative change in P3 amplitude during the most demanding condition of the n-back task in this study may transfer to other WM performance measures (i.e., S-span accuracy) and to attention-related personality traits. In addition, this attention sub-score of the BIS was also correlated with relative change scores in Pz 1-back power, $r(15) = -0.52$, $p = 0.04$, suggesting that a relative decrease in one's endorsements of attention-related problems, the higher the Pz power relative to baseline, further suggesting that increased theta power in Pz may be beneficial for engaging attention-related processes. There were no other correlations observed between the EEG measures and the transfer relative change scores.

Training dose-related effects on relative changes scores in WM performance, EEG correlates and personality traits

In order to examine the number of MBT sessions and the number of tDCS sessions was related to gains in n-back performance, n-back EEG correlates, transfer tasks, and personality traits, Pearson correlations were also computed on the relative

change scores for each variable. Although there were only 4 MBT+tDCS participants who attended the live web MBT seminars within the 4-week training interval, these subjects showed the highest increase in 3-back performance relative to baseline, $r(15) = 0.57$, $p = 0.02$. Moreover, relative change scores in S-span performance was positively correlated with the number of tDCS sessions, $r(15) = 0.63$, $p < 0.01$.

Testing training-related effects on sustained attention using visual oddball task

In order to test within-subject (baseline vs post-training) and between-subject (Cont+Sham vs MBT+tDCS) comparisons on sustained attention performance data, 2x2 repeated measures ANOVAs were obtained, with group designation as the between-subjects factor and time (baseline and post-training) as the within-subject factors. The group means and SDs for target accuracy and RTs as well as the average number of false alarms to distractor and standard stimuli are displayed in Table 2.

Table 2: Mean (SD) of visual oddball performance data at baseline and post-training within each group.

	Cont+Sham		**MBT+tDCS**	
	Baseline	*Post-training*	*Baseline*	*Post-training*
Target Accuracy	94% (4%)	93% (7%)	95%(8%)	96% (8%)
Target RTs (ms)	447 (37)	439 (31)	**451 (32)**	**428 (30)***
Distractor FA (count)	0.44 (0.9)	0.33 (0.5)	0.1 (0.3)	0.3 (0.8)
Standard FA (count)	1.5 (2.0)	1.1 (1.3)	1.0 (1.3)	1.2 (1.2)

*Within-subject comparison, $p < 0.05$; FA= false alarm.

For the RT measures, there was a main effect of time (post-training < baseline), $F(2, 26) = 9.52$, $p = 0.005$, $\eta_p^2 = 0.28$, suggesting a general practice effect across both

groups. Although the group×time interaction was not statistically significant ($\eta_p^2 = 0.10$, p=0.12), pair-wise t-tests were conducted and showed that the MBT+tDCS group responded quicker after training relative to baseline ($t = 3.61$, $p = 0.001$), while there was no difference in post-training RTs relative to baseline for the Cont+Sham group (p = 0.33). However, MBT+tDCS post-training RTs were not statistically different from the post-training Cont+Sham group ($p = 0.35$). There were also no baseline RTs differences between groups (p*'s* = 0.77).

Furthermore, for target accuracy, as well as the number of false alarms, there was no main effect of time nor a group×time interaction (p*'s* > 0.24). Pair-wise comparisons also showed no differences between groups at either time point, nor between time points within each group (p*'s* > 0.24).

Visual oddball time-domain comparisons of P3 amplitude

In order to test within-subject and between-subject comparisons on VOT EEG data, 2x2x3 repeated measures ANOVAs were obtained, with group designation as the between-subjects factor, and time (baseline and post-training) and stimulus-type (target, distractor, and standard) as the within-subject factors. The baseline group-level ERP waveforms for each group, stimulus-type, time point, and electrode site (Pz, Fz and F10) are displayed in Figure 12. The baseline group mean P3 topologies for each stimulus type are displayed in Figure 13.

Figure 12: Baseline group-level ERP waveforms for Pz, Fz, and F10 and each stimulus type in the oddball task.

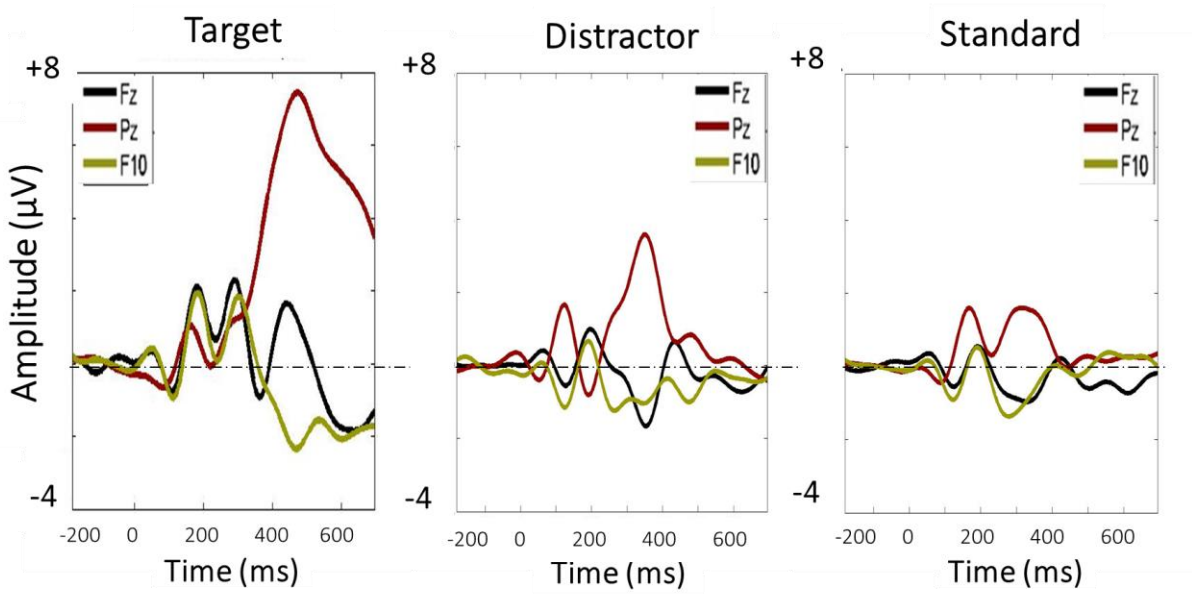

As expected, the that the posterior P3 peak amplitude for the target response was larger and ~100 ms later than the P3 peak amplitudes for the distractor and standard responses. Accordingly, for all subsequent statistical comparisons, P3 amplitude for target responses was averaged between 450 – 550 ms, and between 300 – 400 ms for the distractor and standard responses.

Figure 13: Baseline group-level P3 surface topology for each stimulus type in the visual oddball task.

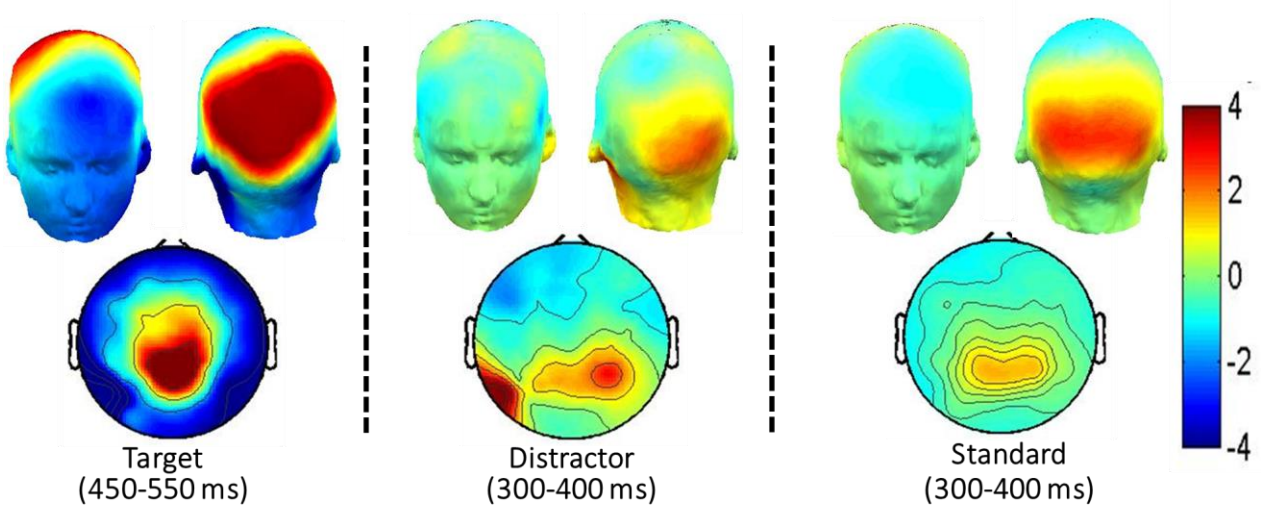

The P3 time intervals for each stimulus type was selected based on the baseline group-level waveforms. P3 amplitude for target responses was averaged between 450 – 550 ms, and between 300 – 400 ms for the distractor and standard responses.

Finally, P3 ERP group means, SEs, and statistical comparisons for each of the VOT stimulus types and each electrode site of interest are displayed in Figure 14.

Figure 14: Mean, SE and statistical comparisons of P3 amplitude for all conditions of the visual oddball task and electrode sites of interest within each group at baseline and post-training.

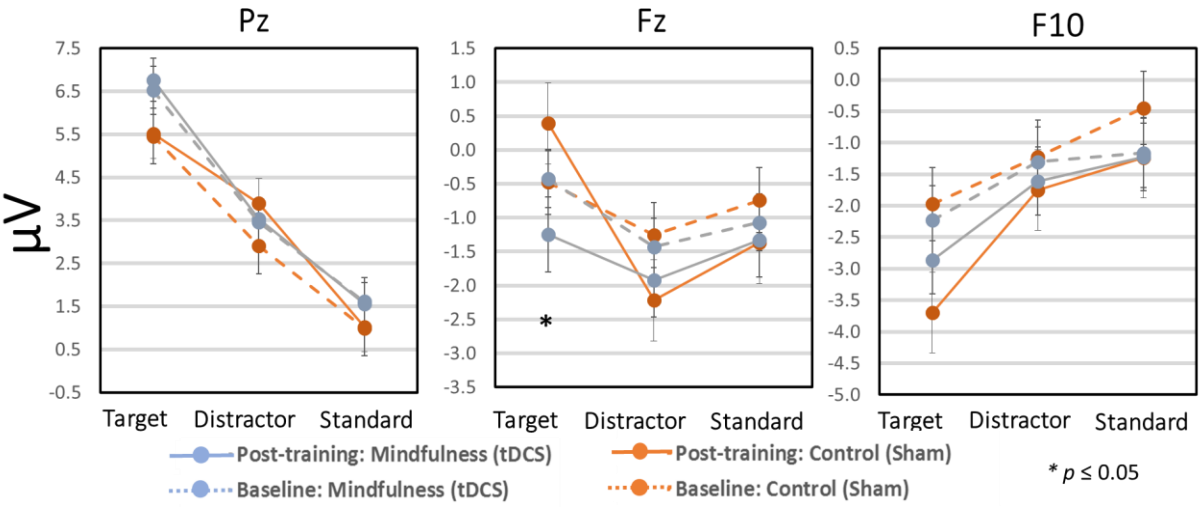

Baseline data are represented by dotted lines and post-training data by solid lines for both the MBT+tDCS (blue) and Cont+Sham (red) groups. P3 amplitude for target responses was averaged between 450 – 550 ms, and 300 – 400 ms for the distractor and standard responses. Results show increased negative amplitude for target responses at electrode site Fz only.

For electrode location Pz, there was a robust stimulus-type main effect (target > distractor > standard), $F(2, 26) = 94.98$, $p < 0.001$, $\eta_p^2 = 0.80$. Likewise for F10, there was also a stimulus-type main effect (but as a function of negative amplitude: target > distractor > standard), $F(2, 26) = 12.89$, $p < 0.001$, $\eta_p^2 = 0.35$. For both Pz and F10 electrode sites, there were no differences between groups nor between time points within either group (*p's* > 0.21).

For electrode location Fz, there was a group × time × stimulus-type interaction, $F(2, 26) = 7.49$, $p = 0.01$, $\eta_p^2 = 0.24$. Follow-up pair-wise t-tests showed that post-training P3 amplitude responses in the MBT+tDCS group were decreased in magnitude during target detection only when compared to the Cont+Sham group ($p = 0.05$). There were no differences in baseline Fz amplitude between groups (*p's* > 0.10), nor between time points within the MBT+tDCS group (*p's* > 0.05).

Phasic clustering of sustained attention

Figure 15 displays the time-frequency ITPC maps, which includes the selected time windows for early alpha and P3 theta synchronization for each stimulus type and electrode site.

Figure 15: Baseline group-level alpha and theta ITPC time-frequency windows for each visual oddball condition and electrode site of interest.

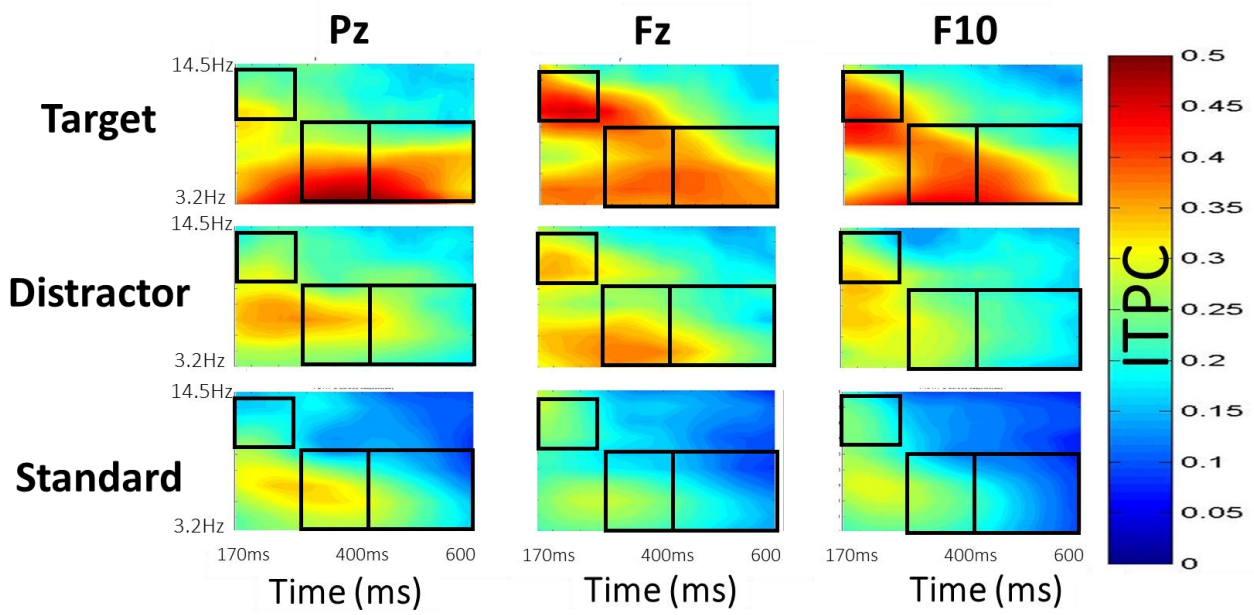

There were 3 time-frequency windows selected based on the peak level activity for each stimulus condition. For the alpha-band response: ITPC was averaged between 170 – 300 ms and 8.8 – 14.5 Hz (log spaced); for the early theta-band response (corresponding to distractor and standard responses): ITPC was averaged between 290 - 400ms and 3.2 – 7.45 Hz (log spaced); For the late theta-band response (corresponding to target response): ITPC was averaged between 400 - 600ms and 3.2 – 7.45 Hz (log spaced), which was used in all subsequent comparisons.

Figure 16 displays alpha-band ITPC group means, SEs, and statistical comparisons for each of the VOT stimulus types and electrode sites.

Figure 16: Mean, SE and statistical comparisons of alpha ITPC for each visual oddball condition and electrode sites of interest within each group at baseline and post-training.

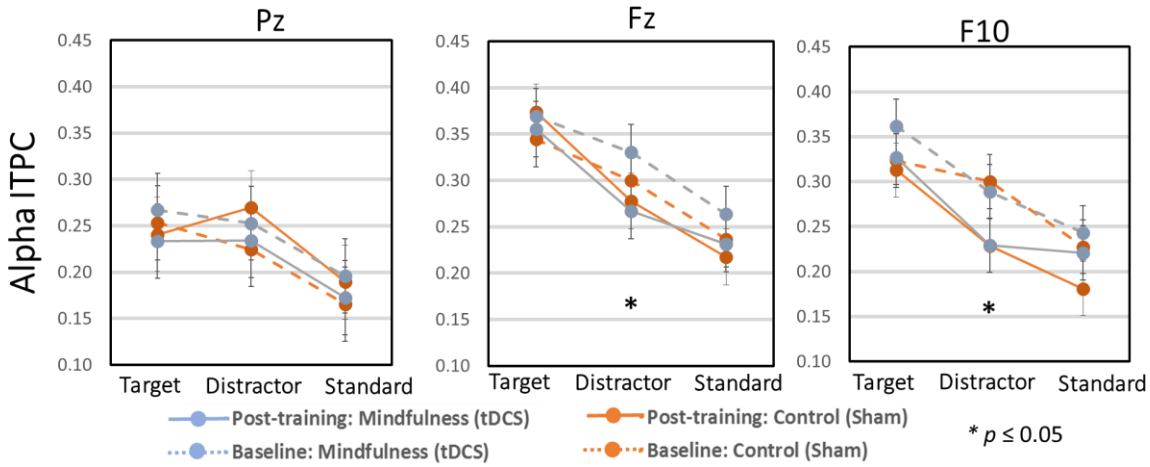

Baseline data are represented by dotted lines and post-training data by solid lines for both the MBT+tDCS (blue) and Cont+Sham (red) groups. Mean alpha ITPC was averaged between 170 – 300 ms and from 8.8 – 14.5 Hz. Results show decreased alpha ITPC for distractor responses at electrode sites Fz and F10 in the MBT+tDCS group.

For electrode location Pz, there was a stimulus-type main effect (target > distractor > standard), $F(2, 26) = 62.23$, $p < 0.001$, $\eta_p^2 = 0.72$; however, there were no differences between groups nor between time points within either group. For electrode location Fz, there was also a stimulus-type main effect (target > distractor > standard), $F(2, 26) = 101.35$, $p < 0.001$, $\eta_p^2 = 0.81$. Moreover, post-training alpha-band ITPC within the MBT+tDCS group was decreased relative to baseline ($t = 2.56$, $p = 0.01$). However, post-training alpha-band ITPC was not different between groups ($p > 0.82$). Similar findings were observed for electrode location F10. There was a robust stimulus-type main effect (target > distractor > standard), $F(2, 26) = 339.78$, $p < 0.001$, $\eta_p^2 = 0.93$. Likewise,

post-training alpha ITPC within the MBT+tDCS group was also decreased relative to baseline (t = 2.25, p = 0.04). However, post-training alpha-band ITPC was not different between groups (p > 0.98).

Theta-band phasic activity of sustained attention

Figure 17 displays theta-band ITPC group means, SEs, and statistical comparisons for each of the VOT stimulus types and electrode sites.

Figure 17: Mean, SE and statistical comparisons of theta ITPC for each visual oddball condition and electrode sites of interest within each group at baseline and post-training.

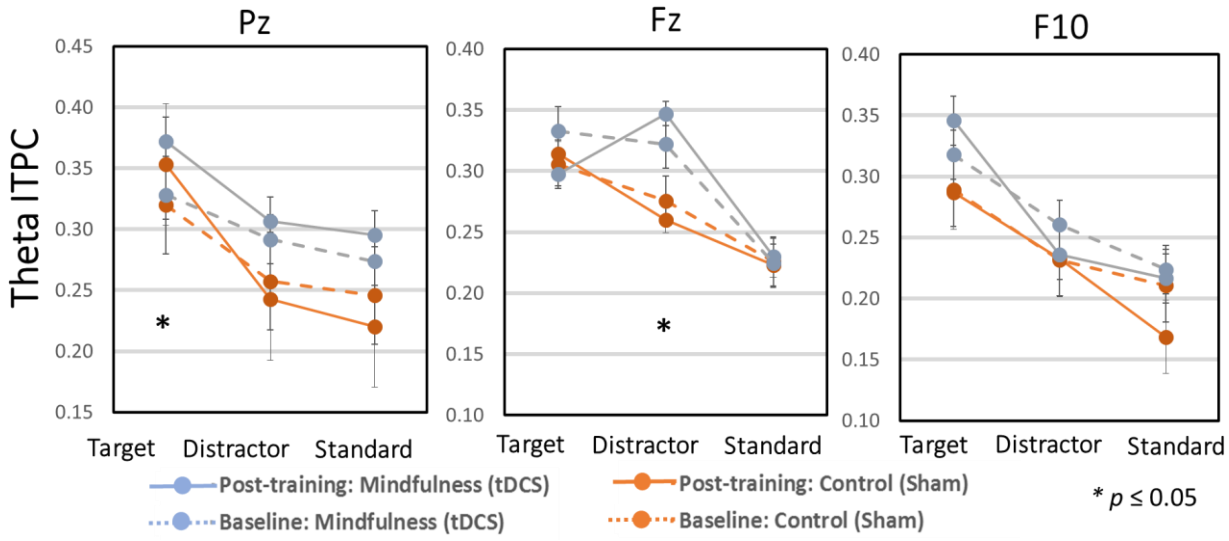

Baseline data are represented by dotted lines and post-training data by solid lines for both the MBT+tDCS (blue) and Cont+Sham (red) groups. Mean theta ITPC was averaged between 290 – 400 ms and 3.2 – 7.45 Hz for distractor and standard conditions, and between 400 - 600ms for the target condition. Results show increased theta ITPC for target responses at electrode site Pz and for distractor responses at Fz in the MBT+tDCS group.

For theta-band ITPC, there was only a main effect of stimulus-type across the three electrode sites (target > distractor > standard; *p's* < 0.005). For electrode location Pz, there was a pair-wise difference within the MBT+tDCS group, (p = 0.05). For electrode location Fz, post-training distractor ITPC in the MBT+tDCS group was higher compared to the Cont+Sham group (p = 0.02). There were no other group differences in theta ITPC nor differences between time points within either group (*p's* > 0.60).

Power activity of sustained attention

Figure 18 displays the time-frequency power maps, which includes the selected time windows for early alpha and P3 theta power for each stimulus type and electrode site.

Figure 18: Baseline group-level alpha and theta power time-frequency windows for each visual oddball condition and electrode site of interest.

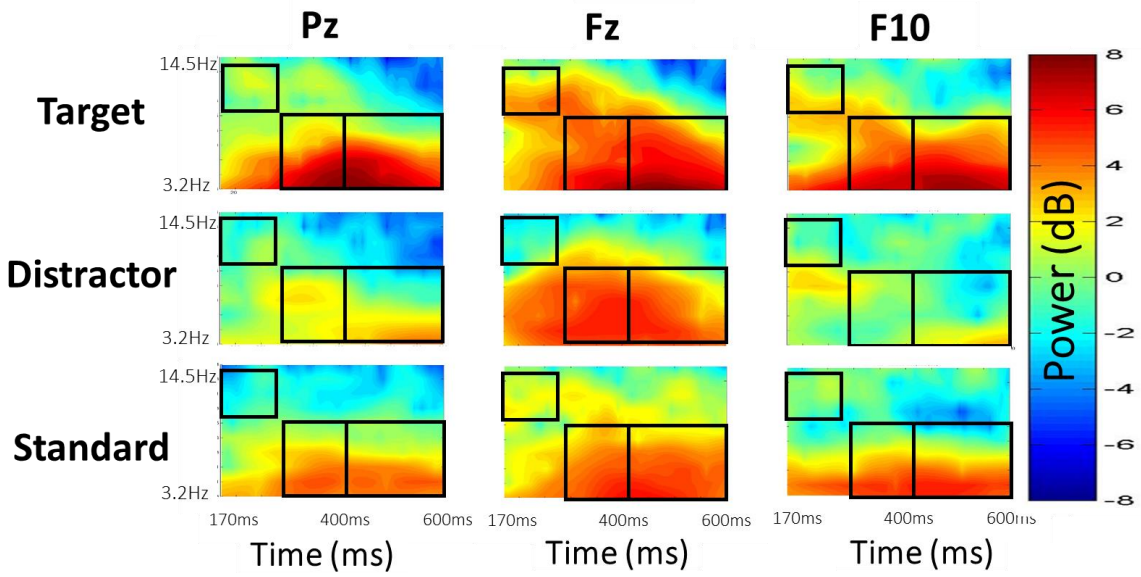

Alpha and theta-band power were decibel scaled and baseline corrected from -200 to 0 ms. Identical to the windows extracted for ITPC, alpha-band power was averaged between 170 – 300 ms and 8.8 – 14.5 Hz (log spaced); for the early theta-band response (corresponding to distractor and standard responses), power was averaged between 290 - 400ms and 3.2 – 7.45 Hz (log spaced). For the late theta-band response (corresponding to target response), power was averaged between 400 - 600ms and 3.2 – 7.45 Hz (log spaced), which was used in all subsequent comparisons.

Figure 19 displays the alpha-band power group means, SEs, and statistical comparisons for each of the VOT stimulus types and each electrode site.

Figure 19: Mean, SE and statistical comparisons of alpha-band power for each visual oddball condition and electrode sites of interest within each group at baseline and post-training.

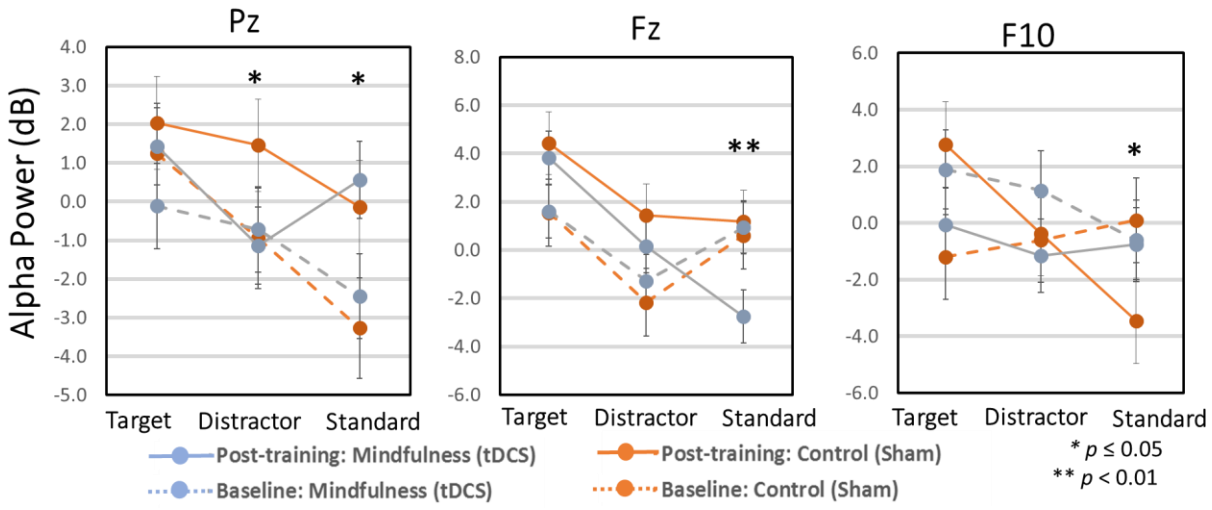

Baseline data are represented by dotted lines and post-training data by solid lines for both the MBT+tDCS (blue) and Cont+Sham (red) groups. Mean alpha-band power was averaged between 290 – 400 ms and 8.8 – 14.5 Hz for all conditions.

For electrode location Pz, there was a main effect of stimulus type, $F(2, 26) = 5.19$, $p = 0.03$, $\eta_p^2 = 0.18$. Also, post-training distractor alpha power was decreased in the MBT+tDCS group compared to the Cont+Sham group ($p = 0.05$). There was also a difference within the MBT+tDCS group when compared to baseline ($p = 0.04$) for the standard stimuli.

For electrode location Fz, there was a similar main effect of stimulus type, $F(2, 26) = 15.24$, $p = 0.001$, $\eta_p^2 = 0.39$. Post-training standard alpha power was decreased in the MBT+tDCS group compared to the Cont+Sham group ($p = 0.01$). Furthermore, within-subject comparisons also showed that post-training standard alpha-band power was decreased in the MBT+tDCS group when compared to baseline ($p = 0.02$).

For electrode location F10, there was a group × time × stimulus type interaction, $F(2, 26) = 7.69$, $p = 0.01$, $\eta_p^2 = 0.24$. Follow-up pair-wise t-tests showed a decrease in post-training alpha power in the MBT+tDCS group relative to baseline in the distractor condition only ($p = 0.04$). There were no other statistically significant differences observed.

Figure 20 displays the theta-band power group means, SEs, and statistical comparisons for each of the VOT stimulus types and each electrode site.

Figure 20: Mean, SE and statistical comparisons of theta-band power for each visual oddball condition and electrode sites of interest within each group at baseline and post-training.

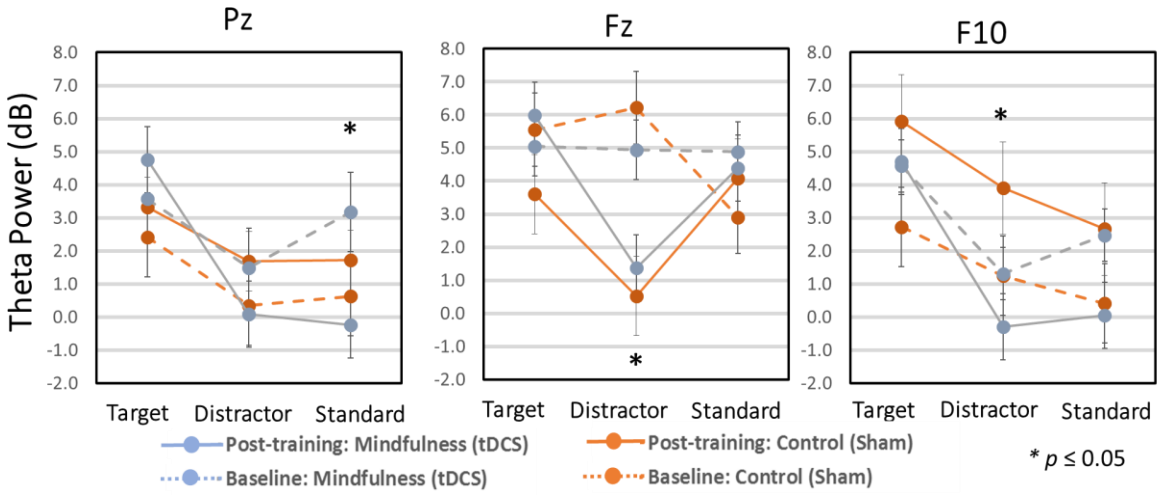

Baseline data are represented by dotted lines and post-training data by solid lines for both the MBT+tDCS (blue) and Cont+Sham (red) groups. Mean theta-band power was averaged between 290 – 400 ms and 3.2 – 7.45 Hz for distractor and standard conditions, and between 400 - 600ms for the target condition. Results show increased theta-band power for standard responses at electrode site Pz and for distractor responses at Fz and F10 in the MBT+tDCS group.

For electrode location Pz, there was a significant decrease in post-training standard theta power relative to baseline within the MBT+tDCS group only ($p = 0.02$). For electrode location Fz, there was a group × time × stimulus-type condition, $F(2, 26) = 6.69$, $p = 0.01$, $\eta_p^2 = 0.26$. Follow-up pair-wise t-tests showed a decrease in post-training distractor theta power within the MBT+tDCS group and the Cont+Sham group (p's < 0.008). For electrode location F10, there was a stimulus-type main effect (target >

distractor > standard), $F(2, 26) = 8.17$, $p = 0.009$, $\eta_p^2 = 0.25$. Pairwise comparisons also showed a decrease in the post-training distractor theta power between groups ($p = 0.03$), and a marginal difference in the same direction for the standard stimuli ($p = 0.08$). There were no other significant differences observed.

Examining whether EEG correlates of sustained attention transfer to performance and personality measures

In order to examine whether the observed training-related gains observed on the visual oddball task transferred to other performance gains and/or personality traits, relative change scores (post-training – baseline / baseline) were computed for each VOT variable that showed a significant difference in the previous analyses. Pearson correlations were then computed to test whether an increase/decrease in a relative change score in one variable would correspond to an increase/decrease in a relative change score in the other transfer task.

For the performance data and VOT EEG measures, there were significant associations between the relative change scores in S-span and alpha-band ITPC during the distractor trials for electrode sites Fz, $r(15) = -0.69$, $p = 0.004$, and F10, $r(15) = -0.60$, $p = 0.01$, within the MBT+tDCS group only. There was no association observed within the Cont+Sham group (p's > 0.16).

There were no statistically significant associations observed between the personality measures and the VOT EEG metrics.

CHAPTER 4: fMRI RESULTS

Participants

There were a total of 4 participants who were dropped from the study, leaving a total of 26 subjects remaining in the study. There were 3 subjects from the Cont+Sham group who were dropped from the study due to non-compliance issues (i.e., missed more than 2 scheduled appointments and did not responds to e-mails or phone calls). There was 1 subject from the MBT+tDCS group who notified study personnel that they could no longer participate due to the time commitment in the study. Table 3 displays all demographic information for all subjects who were included in subsequent fMRI analyses. One-way ANOVAs and χ^2 tests were computed to test if there were any baseline differences in demographic information and pre-defined personality metrics. Like the EEG sample, there were no statistically significant differences between groups on any of the baseline demographic and personality trait measures in the MRI sample (*p's* > 0.14).

Table 3: Mean (SD) and corresponding statistics on fMRI sample demographic information (n = 26).

	UNM		**GIT**		
	Control+sham (n=6)	**MBT+tDCS (n=8)**	**Control+sham (n=4)**	**MBT+tDCS (n=8)**	**Comparisons[a]**
Age (yrs)	26.7 (5.2)	27.6 (4.9)	22.8 (3.8)	25.7 (4.5)	*F=1.09, p=0.37*
College Education (yrs)*	2.0 (0.9)	2.6 (1.0)	2.0 (0.9)	1.8 (1.0)	*F=1.24, p=0.32*
Estimated IQ*	111.1 (15.7)	110.1 (12.2)	121.5 (7.8)	116.8 (7.9)	*F=1.14, p=0.35*
Sex (F)	4|2	5|3	2|2	6|2	χ^2 *=0.78, p=0.85*
Number of training sessions	16.7 (2.8)	17.8 (2.2)	18 (1.8)	17.5 (1.8)	*F=0.25, p=0.62*
Number of tDCS sessions	7.3 (0.5)	6.8 (1.5)	7 (0.8)	5.4 (1.7)	*F=4.0, p=0.07*
MWS	17.1 (5.2)	16.6 (4.9)	19.2 (5.3)	13.8 (5.8)	*F=0.69, p=0.56*
BFI Conscientiousness	8.3 (1.5)	8.4 (1.7)	6 (1.8)	7.5 (1.7)	*F=2.17, p=0.12*
BIS Attention	11.8 (3.5)	10.7 (2.4)	13.7 (3.5)	10.8 (3.3)	*F=0.80, p=0.51*

[a.] One-way ANOVAs and chi-square test were computed to test for any differences across each of the groups displayed. No baseline differences observed. MWS=Mind Wandering Scale; BFI=Big Five Inventory; BIS=Barrett's Impulsivity Scale.

Baseline BOLD response to all visual oddball stimuli.

Figure 21 displays baseline group-level BOLD responses to target stimuli and Table 4 displays the corresponding MNI coordinates and peak and cluster-level statistics. All results were corrected for multiple comparison using FDR adjusted p-values ($q < 0.05$). As expected, target stimuli produced a distributed network of brain regions involved in regulating attention, including bilateral insulae, dorsal anterior cingulate, right inferior and middle frontal gyri, left pre- and post-central gyri, occipital lobe, thalamus, and caudate (see Table 4 for peak-level and cluster-level SPM statistics).

Figure 21: Baseline group-level BOLD response to visual oddball target stimuli.

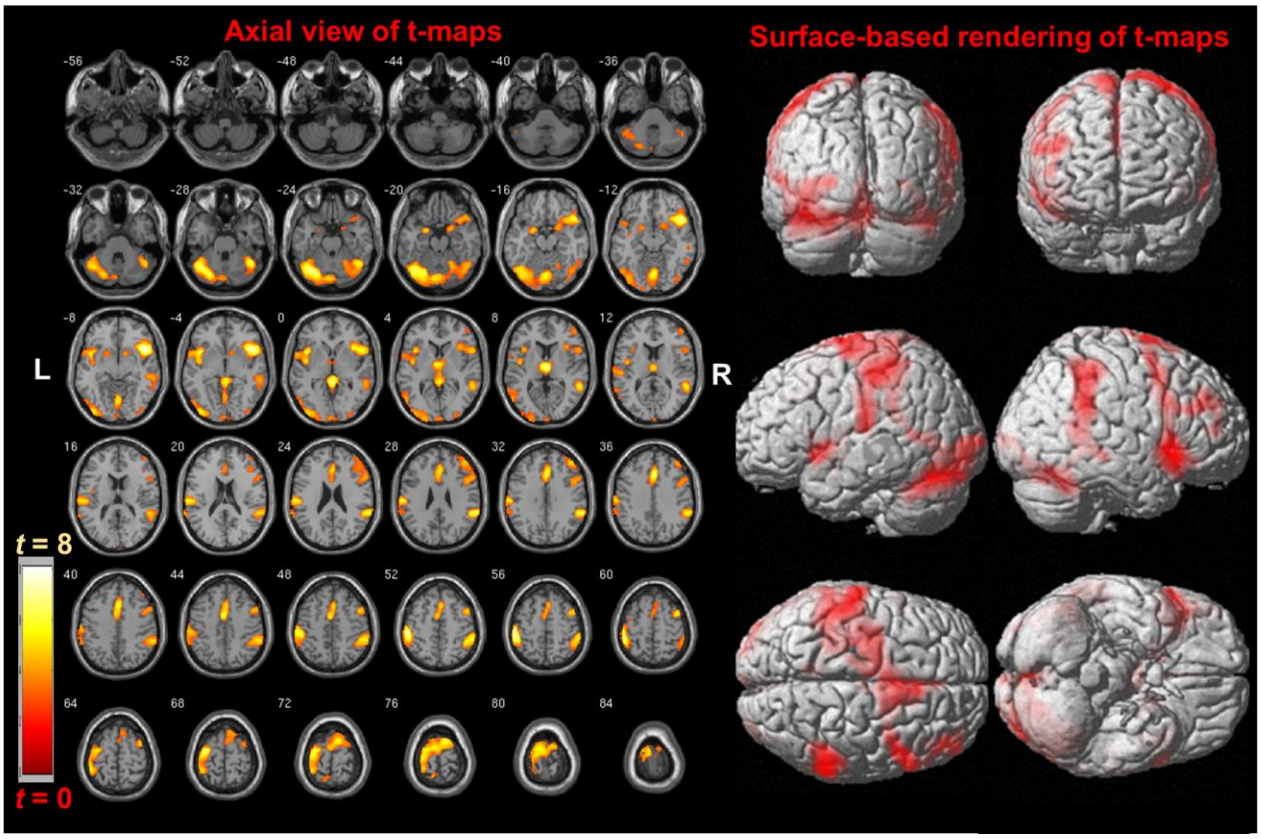

One-sample t-test was conducted using statistical parametric mapping (SPM 8) and was computed across all subjects (n=26) at baseline with a cluster extent threshold of 100 voxels and corrected for multiple comparisons using false discovery rate (FDR; $q < 0.05$). The MNI x-plane coordinate for each axial slice is displayed at the top left corner of each image. The visual oddball target stimuli elicited a distributed network of brain regions involved in attention, including bilateral insulae, dorsal anterior cingulate, right inferior and middle frontal gyri, left pre- and post-central gyri, occipital lobe, thalamus, and caudate. Table 4 includes all region-specific cluster-level t-scores.

Table 4: SPM statistics for baseline responses to visual oddball target stimuli.

Anatomical region	Cluster size (*k*)	Peak *q* (FDR-cor)	Peak *t-score*	MNI x, y, z (mm)
RH insula, inferior frontal and orbital gyrus	6520	<0.001	8.08	48 16 -6
LH postcentral gyrus and BA 2		0.001	7.41	-54 -24 56
LH inferior parietal cortex (BA 40)		0.001	7.27	-50 -36 56
LH cerebellum (declive) and extrastriate (BA 19)	3706	0.001	7.24	-36 -66 -26
Cerebellum (vermis 6)	774	0.002	7.02	2 -38 0
Thalamus and medial dorsal nucleus		0.002	6.76	4 -14 8
Middle and anterior cingulate and BA 24	1321	0.004	6.43	2 20 36
LH insula (BA 13), inferior and orbital frontal gyrus	832	0.004	6.43	-40 12 -2
LH STG		0.028	5.29	-42 -2 -2
RH inferior parietal lobule (BA 40)	1910	0.005	6.21	64 -44 30
RH STG		0.012	5.79	58 -46 8
RH cerebellum and extrastriate cortex (BA 37)	824	0.005	6.21	44 -54 -26
RH middle frontal gyrus	274	0.045	5.01	44 42 32

Contrast of target onsets was computed within a flexible factorial design in statistical parametric mapping (SPM 8), with a cluster extent threshold of 100 voxels. All listed regions were corrected for cluster-level multiple comparisons using false discovery rate (FDR; $q < 0.05$).

Figure 22 displays baseline group-level BOLD responses to distractor stimuli and Table 5 displays the corresponding MNI coordinates and peak and cluster-level statistics. All results were corrected for multiple comparison using FDR adjusted p-values ($q < 0.05$). As expected, distractor stimuli produced a distributed network of brain regions,

including bilateral extrastriate, left precentral gyrus, right insula, right IFG and inferior parietal cortex, as well as medial frontal gyrus (see Table 5 for peak-level and cluster-level SPM statistics).

Figure 22: Baseline group-level BOLD response to oddball distractor stimuli.

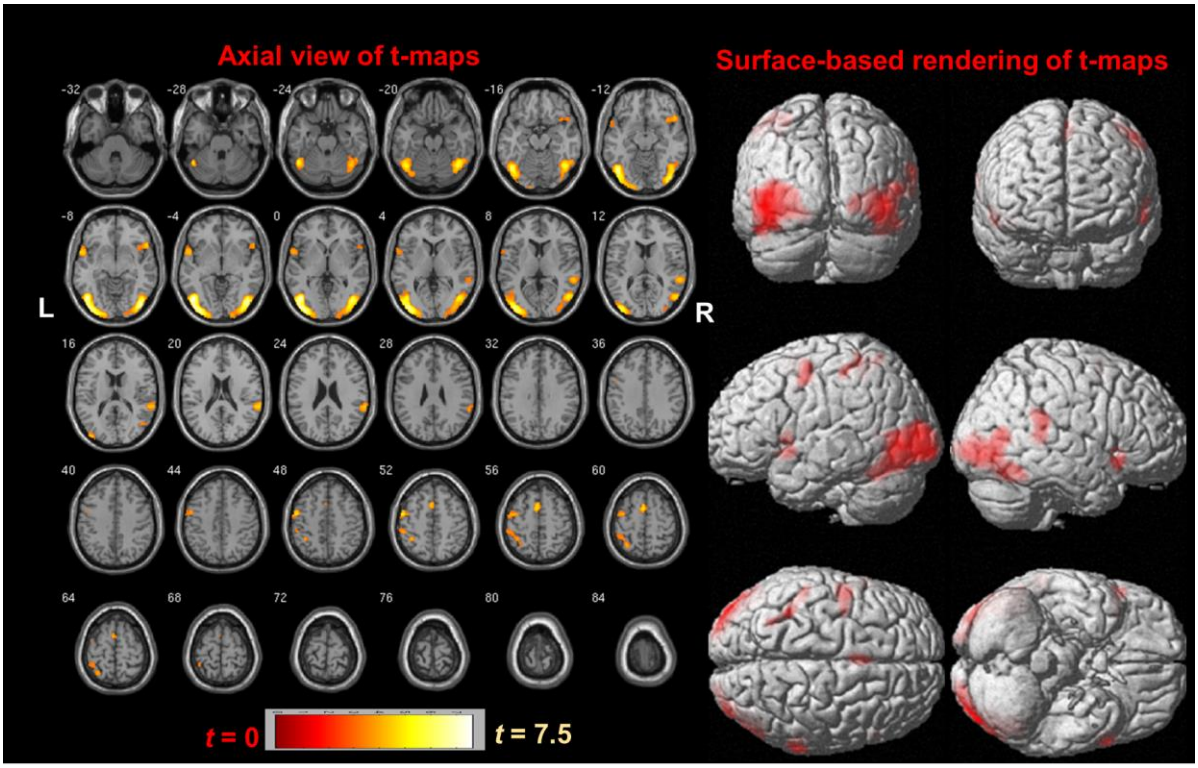

One-sample t-test was conducted using statistical parametric mapping (SPM 8) and was computed across all subjects (n = 26) at baseline with a cluster extent threshold of 100 voxels and corrected for multiple comparisons using false discovery rate (FDR; $q < 0.05$). The MNI x-plane coordinate for each axial slice is displayed at the top left corner of each image. The visual oddball distractor stimuli elicited a BOLD-response in lateral visual cortex, superior parietal lobule, bilateral insulae, superior frontal gyrus, left pre- and post-

central gyri, and right temporal-parietal junction. Table 5 includes all region-specific cluster-level t-scores.

Table 5: SPM statistics for baseline responses to visual oddball distractor stimuli.

Anatomical region	Cluster size (*k*)	Peak *q* (FDR-cor)	Peak *t-score*	MNI x, y, z (mm)
LH lateral occipitial (extrastriate)	2695	<0.001	7.61	-46 -72 -2
RH lateral occipitial (extrastriate)	1937	<0.001	7.42	44 -84 -8
LH precentral gyrus	235	0.047	5.11	-52 -4 52
RH insula and inferior frontal gyrus	194	0.049	5.02	56 20 -10
Medial frontal gyrus (BA 6)	188	0.057	4.98	-2 6 58
RH inferior parietal and RH superior temporal gyrus (STG)	384	0.101	4.72	66 -38 20
LH STG		0.114	4.69	-60 8 -8

Contrast of distractor onsets was computed within a flexible factorial design in statistical parametric mapping (SPM 8), with a cluster extent threshold of 100 voxels. All listed regions were corrected for cluster-level multiple comparisons using false discovery rate (FDR; $q < 0.05$).

Figure 23 displays baseline group-level BOLD responses to standard stimuli and Table 6 displays the corresponding MNI coordinates and peak and cluster-level statistics. All results were corrected for multiple comparison using FDR adjusted p-values ($q < 0.05$). As expected, standard stimuli produced a distributed network of brain regions, including bilateral visual cortex, left pre- and post-central gyrus, right insula, right IFG, as well as the right parahippocampal gyrus (see Table 6 for peak-level and cluster-level SPM statistics).

Figure 23: Baseline group-level BOLD response to standard stimuli.

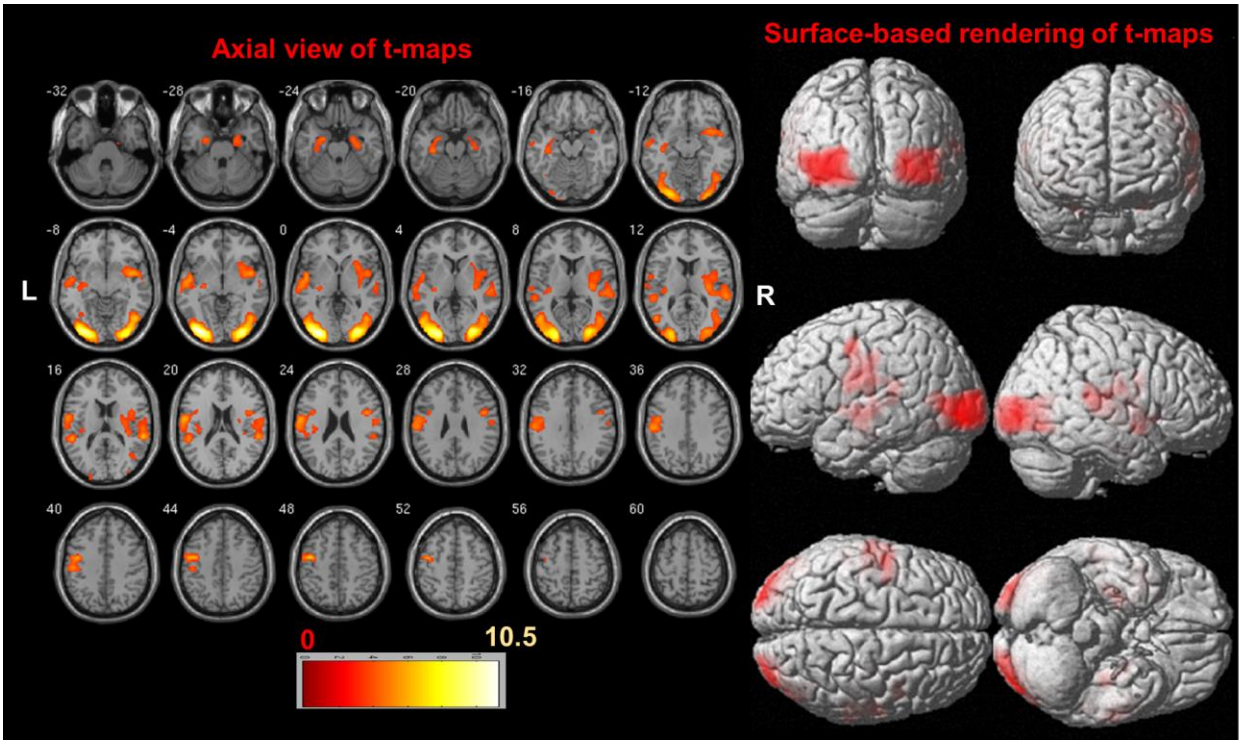

One-sample t-test was conducted using statistical parametric mapping (SPM 8) and was computed across all subjects (n = 26) at baseline with a cluster extent threshold of 100 voxels and corrected for multiple comparisons using false discovery rate (FDR; $q < 0.05$). The MNI x-plane coordinate for each axial slice is displayed at the top left corner of each image. The visual standard stimuli elicited a BOLD response in primary visual cortex, middle temporal gyrus, parahippocampal gyrus, right caudate, putamen, and right insula. Table 6 includes all region-specific cluster-level t-scores.

Table 6: SPM statistics for baseline responses to standard stimuli.

Anatomical region	Cluster size (*k*)	Peak *q* (FDR-cor)	Peak *t-score*	MNI x, y, z (mm)
LH visual cortex (extrastriate: BA 18)	3203	<0.001	11.26	-34 -88 -4
RH visual cortex (extrastriate: BA 18 and BA 19)	2800	<0.001	9.99	30 -88 2
LH precentral gyrus and BA 6	4251	0.004	6.66	-44 -4 48
LH postcentral gyrus and BA 43		0.022	5.79	-58 -8 22
LH STG		0.041	5.51	-50 -6 -2
RH postcentral gyrus, RH STG, and BA 40	3502	0.011	6.15	60 -36 16
RH insula and BA 13		0.026	5.71	46 2 -6
RH inferior frontal gyrus		0.046	5.24	46 2 26
RH parahippocampal gyrus	301	0.109	4.38	30 -16 -24

Contrast of standard onsets was computed within a flexible factorial design in statistical parametric mapping (SPM 8), with a cluster extent threshold of 100 voxels. All listed regions were corrected for cluster-level multiple comparisons using false discovery rate (FDR; $q < 0.05$).

Visual oddball BOLD changes in anatomical regions involved in MBT+tDCS

Factorial ANOVA conducted in SPM revealed gross BOLD changes in anatomical regions involved in mindfulness and anodal stimulation, e.g., ACC, insula, DLPFC, hippocampus, and rIFG. In particular, between- and within-subject statistical contrasts were obtained using a flexible factorial design, with a cluster extent threshold of 100 voxels and corrected for multiple comparisons at the cluster-level using FDR-correction ($q < 0.05$).

Figure 24 displays the statistical contrasts within and between groups on BOLD response to target stimuli. Between-subject comparisons showed that the post-training target BOLD responses in the MBT+tDCS group were increased in the left culmen of the cerebellum compared to post-training BOLD responses in the Cont+Sham group (peak-level: $t = 5.21$, $p < 0.001$). Furthermore, within-subject comparisons revealed a significant decrease in the post-training target BOLD response in BA9 (medial superior frontal gyrus) and left caudate relative to baseline in the MBT+tDCS group only (peak-level: $t's > 4.34$, $p's < 0.001$), which may indicate an increase in neural efficiency in target detection among these brain regions. However, there was no increased target BOLD signal in the hypothesized parietal cortex, nor were there any differences within the Cont+Sham group relative to baseline.

Figure 24: Statistical contrasts within and between groups in BOLD response to visual oddball target stimuli.

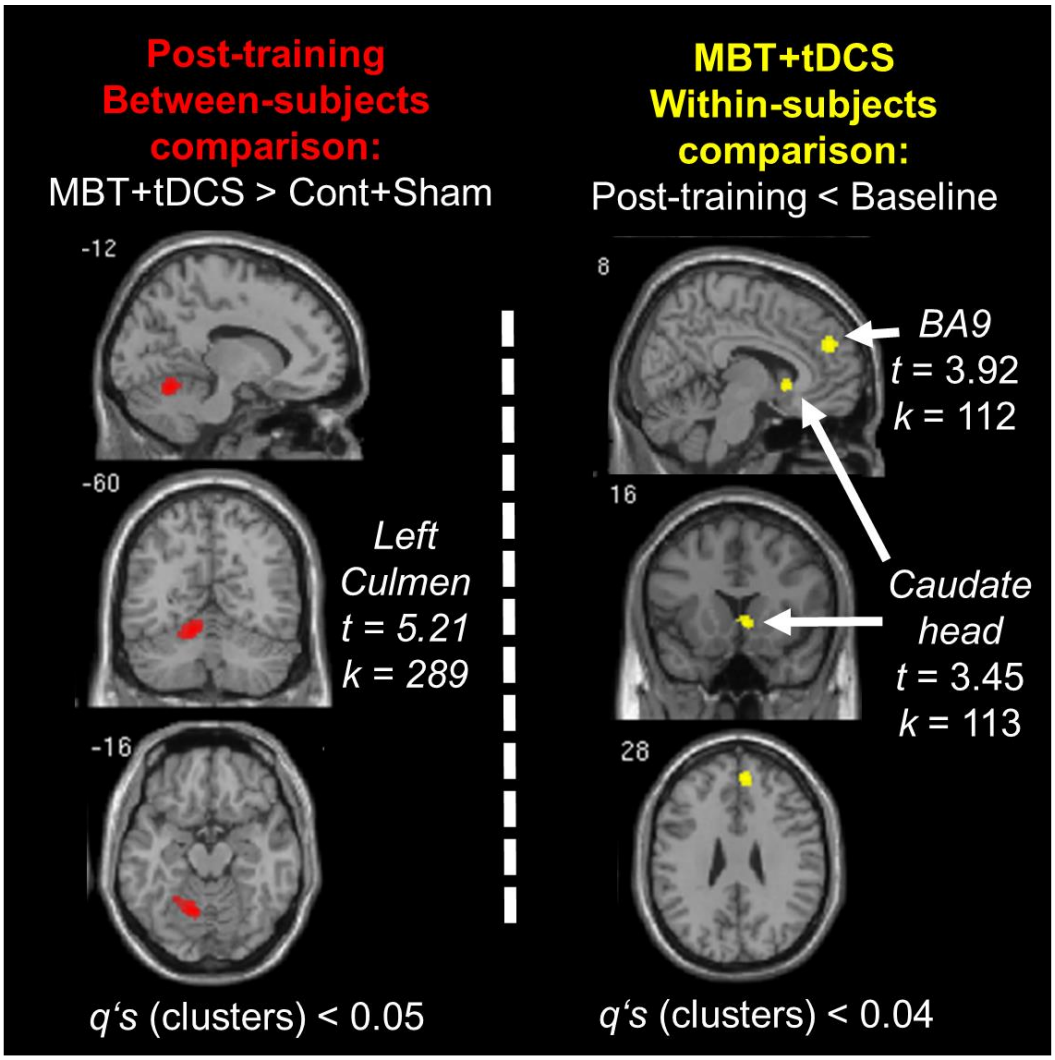

Pre-defined between and within-subject contrasts were computed using a flexible factorial design in statistical parametric mapping (SPM 8), with a cluster extent threshold of 100 voxels and corrected for multiple comparisons using false discovery rate (FDR; q < 0.05). The MNI x-plane coordinate for each axial slice is displayed at the top-left corner of each image. Post-training responses were increased in MBT+tDCS group

relative to the Cont+Sham group in the left culmen of the cerebellum. Also, post-training responses were decreased in the MBT+tDCS group relative to baseline in BA9 (medial superior frontal) and left caudate.

Figure 25 displays the pre-defined statistical contrasts within and between groups on the BOLD response to distractor stimuli. Between-subject comparisons showed that the post-training responses in the MBT+tDCS group were increased in parietal cortex (BA5)—extending to left hemisphere precuneus (peak-level: $t = 4.14$, $p < 0.001$), and bilateral insulae – with a larger effect, in terms of cluster size and peak-level difference, observed in the right hemisphere (peak-level: $p's < 0.001$; see Figure 25). Furthermore, within the MBT+tDCS group only, post-training distractor responses were significantly increased relative to baseline in left and right post-central gyri and left parahippocampal gyrus (peak-level: $p's < 0.001$). These results may indicate an overall increase in salience-related and general encoding processing after training in the MBT+tDCS group.

Figure 25: Statistical contrasts within and between groups in BOLD response to visual oddball distractor stimuli.

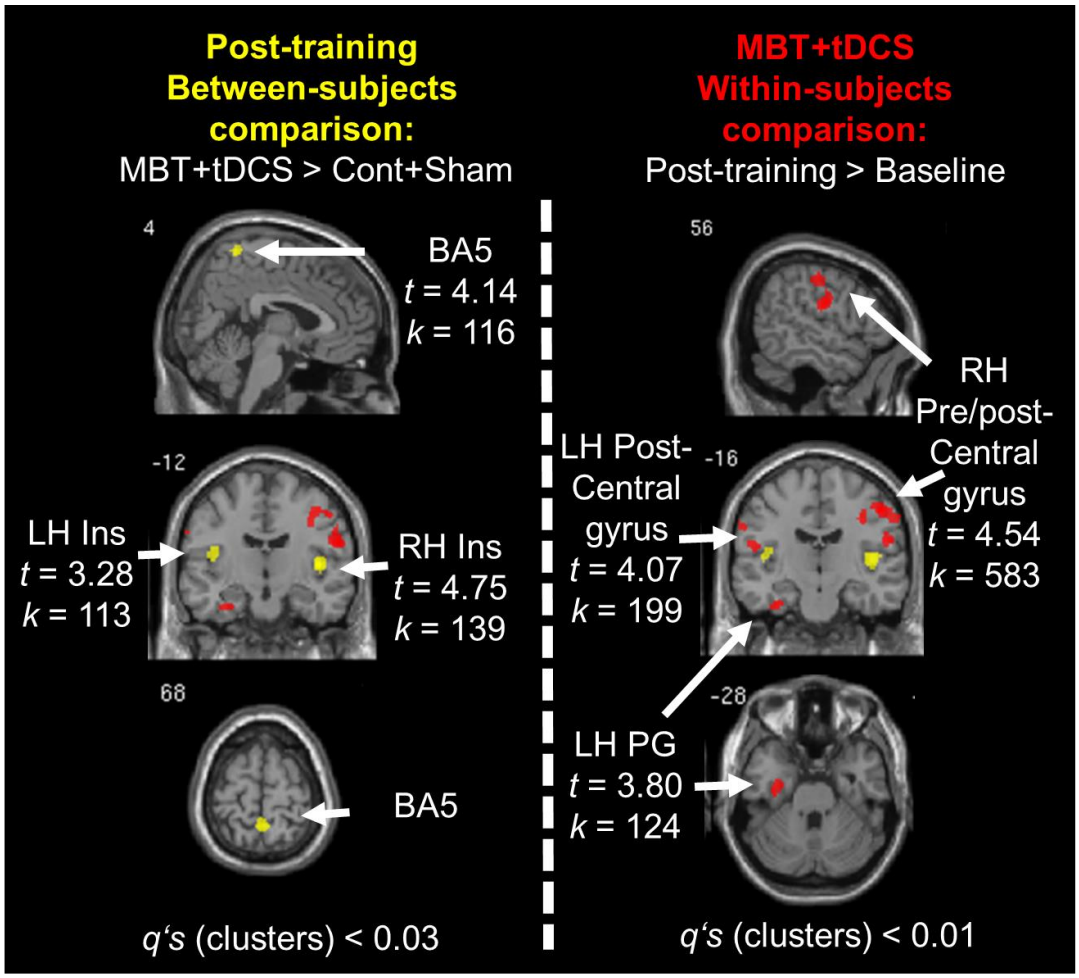

Pre-defined between and within-subject contrasts were computed using a flexible factorial design in statistical parametric mapping (SPM 8), with a cluster extent threshold of 100 voxels and corrected for multiple comparisons using false discovery rate (FDR; q < 0.05). The MNI x-plane coordinate for each axial slice is displayed at the top-left corner of each image. Post-training distractor responses were increased in MBT+tDCS compared to the Cont+Sham group in BA5 (extending Post-training responses were also

increased in left and right post-central gyri and left parahippocampal gyrus (PG) in the MBT+tDCS group relative to baseline.

Figure 26 displays the statistical contrasts within and between groups on BOLD response to standard stimuli. Post-training responses in the MBT+tDCS group were increased in posterior cingulate cortex compared to the Cont+Sham group (peak-level: $t = 4.84$, $p < 0.0005$), and relative to their own baseline (peak-level: $t = 4.13$, $p < 0.001$). These results suggest an enhanced response to frequent stimuli in the MBT+tDCS group. Furthermore, within the MBT+tDCS group only, post-training standard BOLD responses were significantly decreased relative to baseline in left putamen (PUT; (peak-level: $t = 5.25$, $p < 0.0005$) and right IFG (peak-level: $t = 4.30$, $p < 0.001$). This result may suggest enhanced neural efficiency to frequent standard response during a relatively easy task.

Figure 26: Statistical contrasts within and between subjects in BOLD response to standard stimuli.

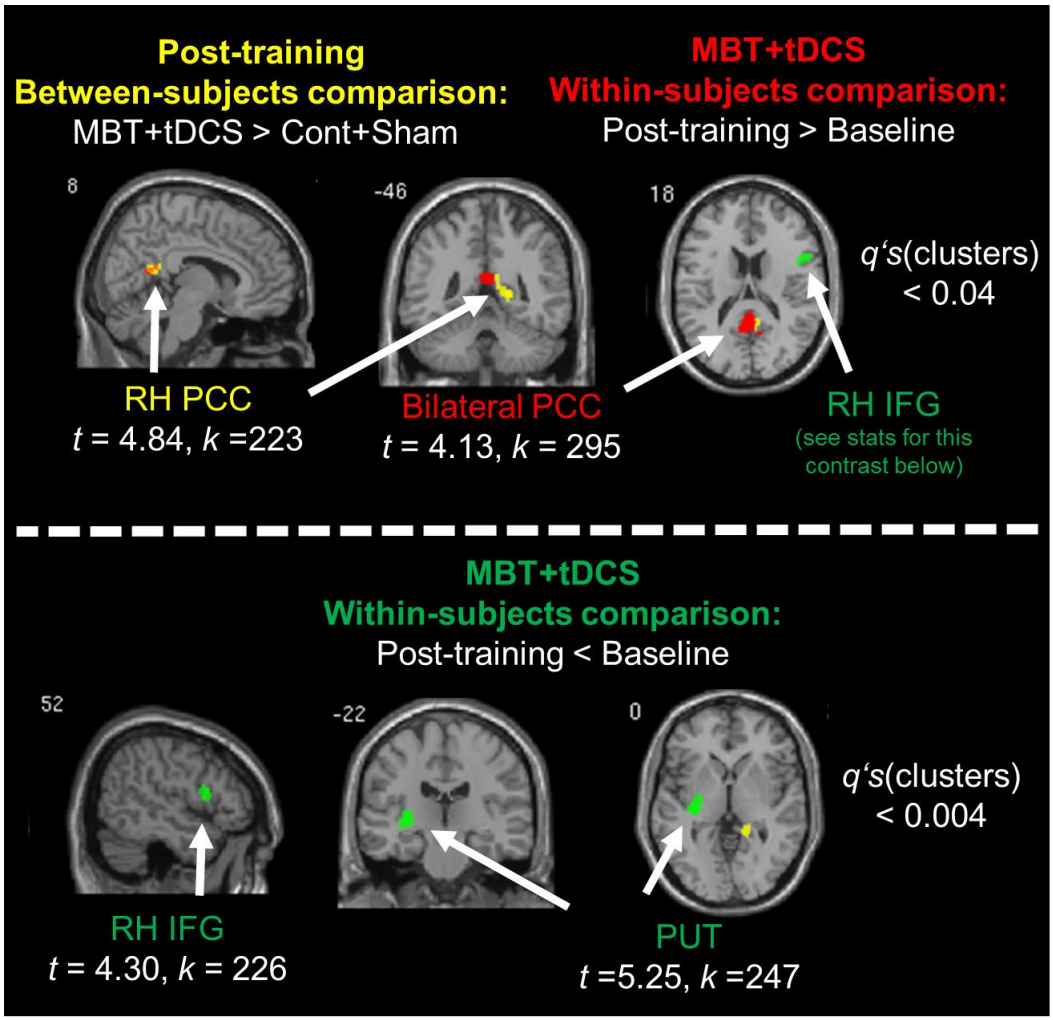

Pre-defined between and within-subject contrasts were computed using a flexible factorial design in statistical parametric mapping (SPM 8), with a cluster extent threshold of 100 voxels and corrected for multiple comparisons using false discovery rate (FDR; q < 0.05). The MNI x-plane coordinate for each axial slice is displayed at the top-left corner of each image. Post-training standard responses were increased in MBT+tDCS

compared to the Cont+Sham group in right posterior cingulate cortex (PCC). Post-training responses were decreased in left putamen (PUT) and right inferior frontal gyrus (IFG) in the MBT+tDCS group relative to baseline.

Spatial activations of pre-defined resting-state networks

Based on their anatomical and presumed functional properties, 10 RSNs were arranged into groups of sub-nodes that comprise the DMN (4 RSNs), the CCN (3 RSNs), and SAL (3 RSNs). Each group of RSNs are displayed in Figures 27-29 along with the respective Tables 7-9, which includes all region-specific cluster-level SPM *t*-scores.

Group-level RSNs that were assigned to the DMN are displayed in Figure 27 and the corresponding statistics are reported in Table 7. The precuneus sub-component of the DMN is displayed in red and also spans BA 7. An anterior cingulate cortex (ACC) RSN is displayed in blue and also includes BA 24 and 32. The posterior cingulate and bilateral angular gyrus network is displayed in green, which also includes a cluster in medial frontal gyrus (k = 108). A "frontal" sub-component of the DMN is displayed in magenta, which is comprised by one large cluster that spans bilaterally in middle frontal (MFG) and superior frontal gyri (SFG), and includes medial frontal gyrus.

Figure 27: Spatial maps of group-level ICA-generated resting-state networks (RSN) that comprise the default-mode network.

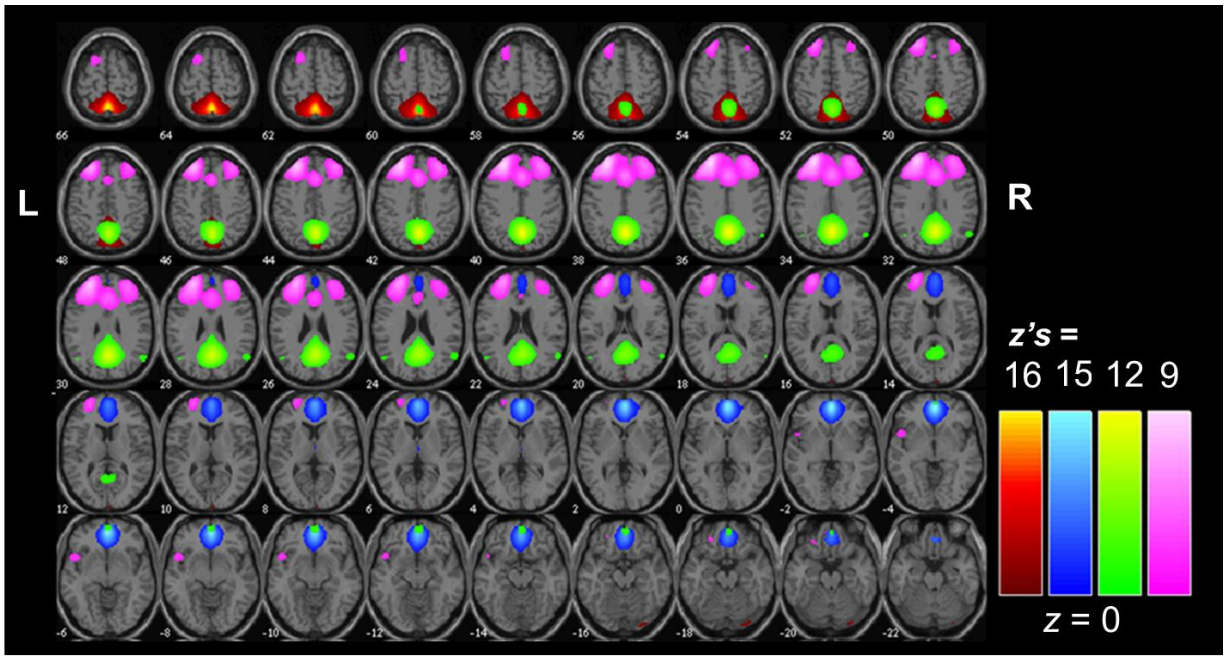

Spatial maps of baseline group (n = 26) ICA-generated RSNs are plotted as z-scores using GIFT, z > 3.0. The MNI x-plane coordinate for each axial slice is displayed at the bottom-left corner of each image. The "precuneus sub-component of the DMN" is displayed in red, an anterior cingulate cortex RSN is shown in blue, the posterior cingulate and bilateral angular gyrus network is displayed in green, and a "frontal DMN" RSN is shown in magenta. Table 7 includes all cluster-level statistics, which were computed in SPM 8.

Table 7: SPM statistics for baseline ICA-generated resting-state networks (RSN) that comprise the default-mode network.

Anatomical regions within each RSN	Cluster size (*k*)	Peak *q* (FDR-cor)	Peak *t-score*	MNI x, y, z (mm)
"Bilateral precuneus" RSN:				
Precuneus and BA 7	5342	<0.001	21.06	-8 -58 56
"Anterior cingulate cortex" RSN:				
Anterior cingulate, BA 24 and 32	4984	<0.001	25.86	2 36 2
Medial frontal gyrus		<0.001	22.83	-8 40 -12
"Posterior cingulate cortex" RSN:				
Posterior cingulate and precuneus	6886	<0.001	22.19	10 -58 32
BA 7		<0.001	20.18	-4 -68 36
LH angular gyrus	106	0.015	9.18	-44 -62 30
RH angular gyrus	153	0.037	8.53	52 -60 28
Medial frontal gyrus	108	0.171	7.49	-2 50 -14
"Frontal DMN" RSN:				
LH middle frontal and superior frontal gyrus	8402	<0.001	14.1	-26 38 38
RH middle frontal, RH superior frontal, and medial frontal gyrus		<0.001	12.9	24 40 44

One-sample t-tests were computed for each RSN within statistical parametric mapping (SPM 8), with a cluster extent threshold of 100 voxels. All listed regions were corrected for using family-wise error correction at the peak level (FWE; $p < 0.001$).

Group-level RSNs that were assigned to a CCN are displayed in Figure 28 and the corresponding statistics are reported in Table 8. A "bilateral frontal" RSN is displayed in red, which includes bilateral IFG and DLPFC, medial frontal gyrus, and a small cluster in BA 40 ($k = 141$). A left-lateralized frontal-parietal RSN is displayed in blue, which includes bilateral inferior parietal cortex, left MFG, BA 8, SFG, and middle temporal gyrus, with a cluster in BA 31 ($k = 201$). Lastly, a right-lateralized frontal-parietal RSN is

displayed in green, which includes right inferior parietal cortex, SFG, MFG and medial frontal gyrus.

Figure 28: Spatial maps of group-level ICA-generated resting-state networks (RSN) that overlap with task-related cognitive control networks.

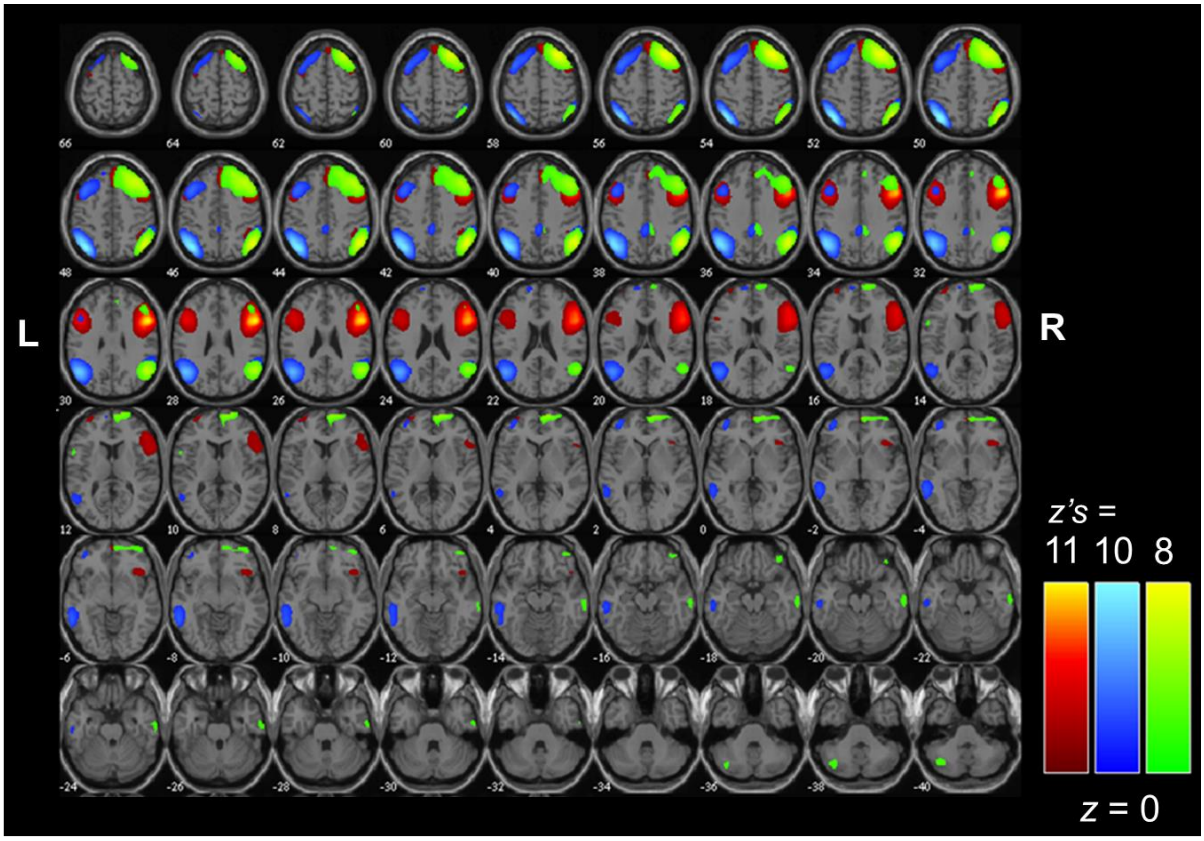

Spatial maps of baseline group (n = 26) ICA-generated RSNs are plotted as z-scores using GIFT, z > 3.0. The MNI x-plane coordinate for each axial slice is displayed at the bottom-left corner of each image. A bilateral frontal RSN is displayed in red, which also includes RH insula. A left lateralized frontal-parietal RSN is displayed in blue and a right lateralized frontal-parietal RSN is displayed in green, which also includes left cerebellum. Table 8 includes all cluster-level statistics, which were computed in SPM 8.

Table 8: SPM statistics for baseline ICA-generated resting-state networks (RSN) that overlap with task-related cognitive control networks.

Anatomical regions within each RSN	Cluster size (*k*)	Peak *q* (FDR-cor)	Peak *t-score*	MNI x, y, z (mm)
"Bilateral frontal" RSN:				
RH inferior frontal gyrus	5225	<0.001	24.47	42 8 32
RH middle frontal gyrus		<0.001	19.24	46 22 26
LH middle frontal gyrus	2012	<0.001	15.98	-42 16 22
LH inferior frontal gyrus		<0.001	12.43	-52 8 30
LH BA 6		0.001	10.28	-44 0 28
Superior frontal and medial gyrus	552	<0.001	15.08	2 38 50
RH BA 40	141	0.025	8.48	38 -48 48
"LH frontal-parietal" RSN:				
LH inferior parietal cortex (BA 40)	4428	<0.001	19.65	-56 -56 36
LH inferior parietal cortex (BA 39)		<0.001	19.58	-52 -66 28
LH angular gyrus		<0.001	17.49	-44 -66 36
RH inferior parietal cortex (BA 40)	2922	<0.001	17.76	52 -54 36
RH angular gyrus		<0.001	12.76	46 -70 46
LH middle frontal gyrus	2110	<0.001	15.45	-44 16 42
LH BA 8		<0.001	14.19	-34 14 54
LH superior frontal gyrus		0.001	10.2	-14 38 50
LH middle temporal gyrus	909	<0.001	11.3	-64 -42 -4
LH BA 20		0.002	9.91	-62 -20 -22
BA 31 and 7	201	0.015	8.64	-2 -34 40
"RH frontal-parietal" RSN:				
RH inferior parietal cortex (BA 40)	1800	0.024	10.14	40 -62 46
RH superior frontal gyrus	3247	0.024	9.56	18 18 50
RH middle frontal gyrus and BA 8		0.024	9.28	24 38 56
Medial frontal gyrus and BA 10	112	0.034	8.74	8 62 0

One-sample t-tests were computed for each RSN within statistical parametric mapping (SPM 8), with a cluster extent threshold of 100 voxels. All listed regions were corrected for using family-wise error correction at the peak level (FWE; $p < 0.001$).

Group-level RSNs that overlap with sub-components of the "salience" network (SAL) and also overlap with activations during the visual oddball task are displayed in Figure 29 and the corresponding statistics are reported in Table 9. A bilateral inferior parietal RSN is displayed in red, which includes bilateral inferior parietal cortex, with smaller clusters in left MFG, IFG and precentral gyrus. A right-lateralized frontal RSN is displayed in blue, which includes right DLPFC, IFG, and left MFG. A distributed RSN that includes brain regions that overlap with the canonical "salience network" is displayed in green, which includes bilateral insulae, medial frontal gyrus, right IFG, MFG, inferior parietal lobule, left precentral gyrus, and visual cortex.

Figure 29: Spatial maps of group-level ICA-generated resting-state networks (RSN) that overlap with the salience and visual oddball task network.

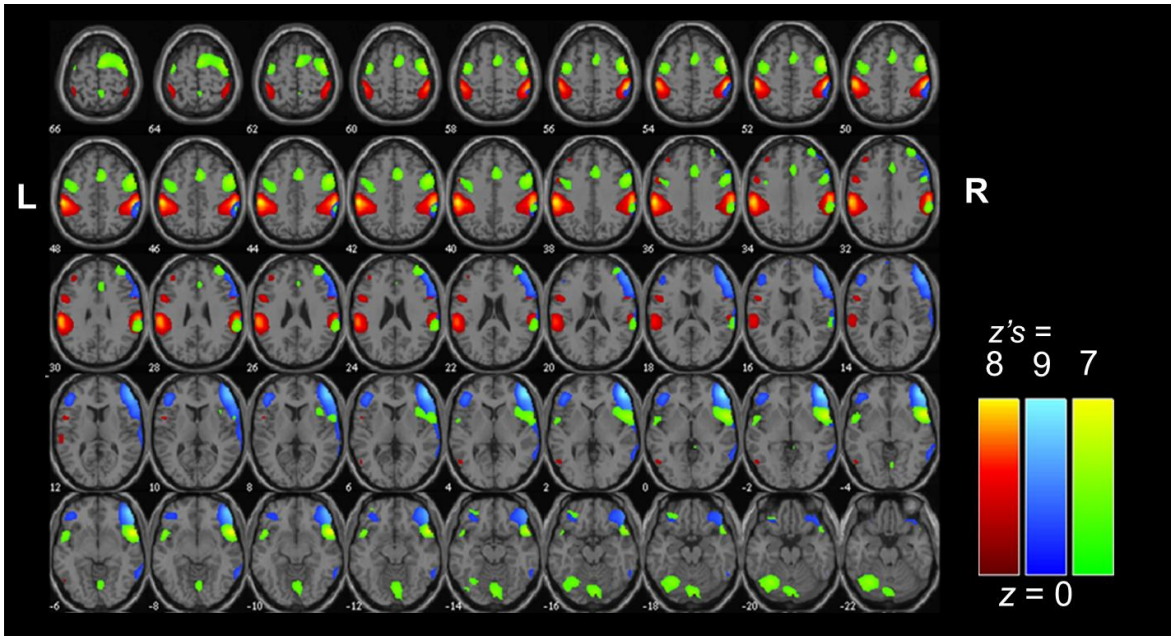

Spatial maps of baseline group (n = 26) ICA-generated RSNs are plotted as z-scores using GIFT, z > 3.0. The MNI x-plane coordinate for each axial slice is displayed at the

bottom-left corner of each image. A “bilateral inferior parietal” RSN is displayed in red, a “right-lateralized frontal” RSN is displayed in blue, and a bilateral insulae and dorsal cingulate RSN network is displayed in green, which overlaps with the task-related “salience” network. Table 9 includes all cluster-level statistics, which were computed in SPM 8.

Table 9: SPM statistics for baseline ICA-generated resting-state networks (RSN) that overlap with salience and visual oddball networks.

Anatomical regions within each RSN	Cluster size (*k*)	Peak *q* (FDR-cor)	Peak *t-score*	MNI x, y, z (mm)
"Bilateral parietal" RSN:				
LH inferior parietal cortex (BA 40)	3426	<0.001	16.32	-56 -44 26
RH inferior parietal cortex (BA 40)	3735	<0.001	16.13	52 -42 36
LH middle frontal gyrus	151	0.003	9.64	-42 40 34
LH inferior frontal gyrus	223	0.003	9.51	-52 8 16
LH precentral gyrus and BA 9		0.042	8.14	-54 6 8
BA 9		0.051	7.97	-50 4 32
"RH frontal" RSN:				
RH middle frontal gyrus and	5667	0.002	12.08	38 44 -12
RH BA 10 and 46		0.003	11.26	42 46 4
RH inferior frontal gyrus		0.006	10.6	40 44 12
LH middle frontal gyrus	617	0.029	9.28	-44 44 -2
"Saliance" RSN:				
LH insula	286	<0.001	13.72	-52 8 -4
Medial frontal cortex (BA 6)	3064	<0.001	13.35	4 4 60
Middle frontal gyrus		<0.001	12.55	26 4 68
RH BA 6		<0.001	12.1	60 2 40
RH insula (BA 13)	1333	<0.001	13.18	50 8 -8
RH inferior frontal gyrus		<0.001	11.86	46 16 -10
RH superior temporal gyrus		0.002	10.27	56 2 0
LH BA 19 (visual cortex)	1702	0.003	10.08	-40 -66 -20
LH cerebellum (declive)		0.004	9.8	-38 -58 -28
LH precentral gyrus (BA 6)	406	0.004	9.84	-42 -10 50
RH middle frontal gyrus and	217	0.01	9.06	32 48 24
RH inferior parietal lobule (BA 40)	392	0.016	8.74	64 -40 26

One-sample t-tests were computed for each RSN within statistical parametric mapping (SPM 8), with a cluster extent threshold of 100 voxels. All listed regions were corrected for using family-wise error correction at the peak level (FWE; $p < 0.001$).

Distinctive features among dynamic functional connectivity "states"

Figure 30 displays the baseline-specific cluster centroids that represent each state across the ten networks that comprise the DMN, CCN and SAL. There are two pertinent features that distinguish the functional connectivity state patterns. First, states 1, 4, and 6 are differentiated by a general positive dynamic connectivity pattern within the DMN network and between the LH frontal parietal network, with a simultaneous antagonistic ("anti-correlation") between the DMN and the networks grouped within the SAL category, which is most apparent, in magnitude, in state 1. Second, states 2 and 5 are characterized by less dynamic connectivity patterns within the DMN and more inter-grouping dynamic connectivity patterns; in particular, both states exhibited a mixture of positive and antagonistic connectivity patterns between the DMN and the SAL networks. State 3 is solely distinguished by a dispersion of solely positive connectivity patterns within and between network groups.

Figure 30: Statistically significant baseline cluster centroids (states) for the ten resting-state networks of interest, grouped as the default-mode network (DMN), cognitive control networks (CCN), and salience and visual oddball networks (SAL).

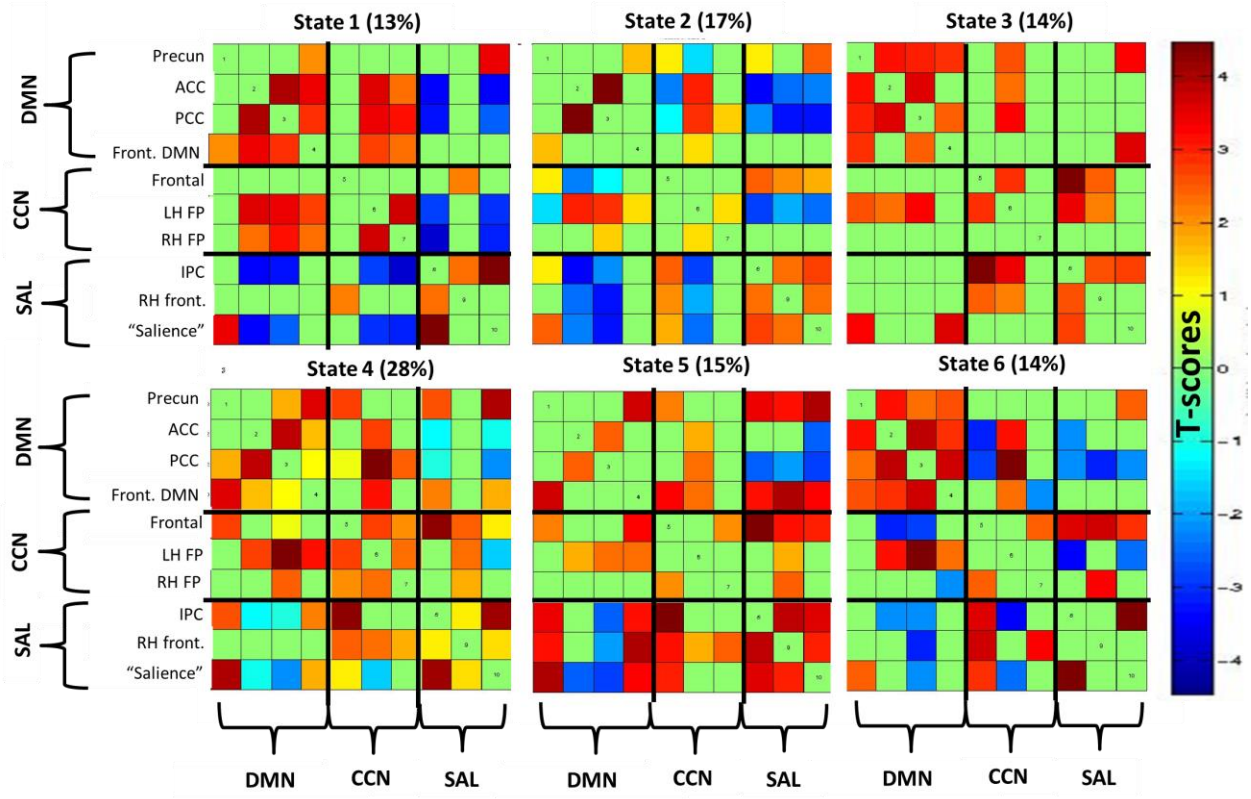

Each matrix represents the centroid of a cluster (for k = 6) and thresholded by computing a one-sample t-test on each connectivity pattern ($p<0.05$). Red cells indicate a positive connectivity pattern between two networks, while a blue cell indicates an anti-correlation between two networks. The percentage of occurrences is listed above each centroid.

Group comparisons on dFNC state dwell times

In order to test within-subject (baseline vs post-training for states 1-6) and between-subject (Cont+Sham vs MBT+tDCS) comparisons, 2x2x6 repeated measures

ANOVAs were obtained, with group designation as the between-subjects factor and time (baseline and post-training) and number of states (1-6) as the within-subject factors. Figure 31 displays the mean, SE and statistical comparisons on mean dwell time (i.e., proportion of subject time windows assigned to each state). Although there was not a group × time × state interaction ($p = 0.33$, $\eta_p^2 = 0.04$), pre-defined pair-wise comparisons showed that the MBT+tDCS group simultaneously spent more time in state 1 and less time in state 5 after training compared to the Cont+Sham group (p's < 0.05). It is important to note that there were near-zero differences at baseline between groups for these two states (p's > 0.96). There were no other differences observed between groups, nor within groups across time points in any of the other states (p's > 0.51).

Figure 31: Mean, SE and statistical comparisons on mean dwell time across each state.

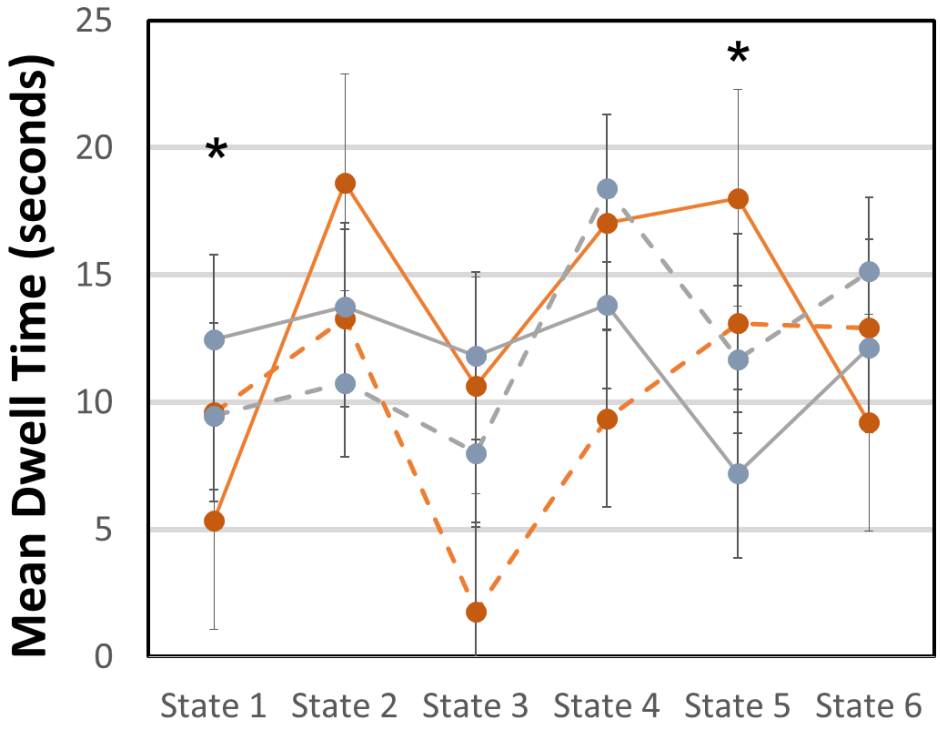

Each matrix represents the centroid of a cluster (for k = 6) and thresholded by computing a one-sample t-test on each connectivity pattern ($p<0.05$). Red cells indicate a positive connectivity pattern between two networks, while a blue cell indicates an anti-correlation between two networks. The percentage of occurrences is listed above each centroid.

Post-hoc group comparisons on dFNC "state" correlations

Based on the group differences observed in dwell times (see Figure 31), follow-up two-sample t-tests were computed to evaluate whether there were specific statistical differences in post-training dynamic connectivity matrices for states 1 and 5. Figure 32 displays the matrix of *t*-scores for states 1 and 5.

Figure 32: Two-sample t-tests between groups after training on patterns of dynamic connectivity for states 1 and 5.

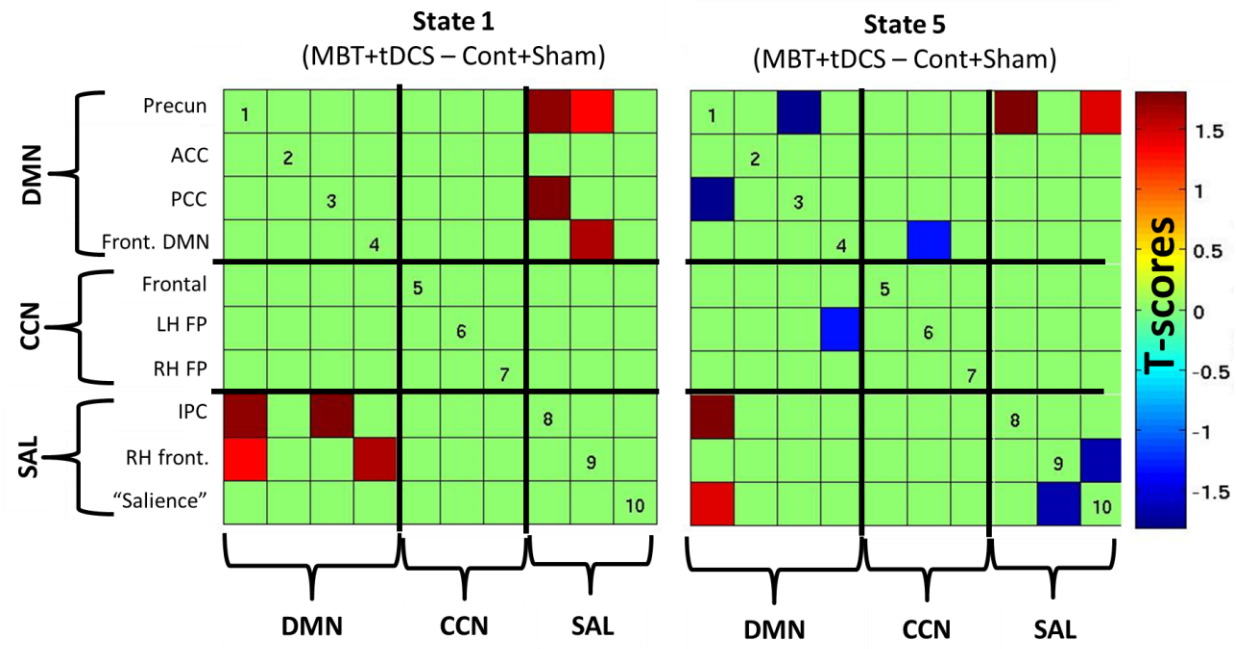

Each matrix represents the two-sample t-score associated with the group comparison on each dynamic connectivity pattern within states 1 and 5. Note: states 1 and 5 were the only centroids that showed a post-training group difference in mean dwell time (see Figure 31). For state 1, see Results section for interpretation of t-scores as the sign of the t-score changes based on the direction of the dFNC pattern. For state 5, red cells indicate a significant difference in dFNC such that MBT+tDCS > Cont+Sham and blue cells indicate MBT+tDCS < Cont+Sham.

For state 1, the MBT+tDCS group showed increased *positive* dynamic connectivity between the precuneus RSN (grouped as DMN) and bilateral inferior parietal RSN (grouped as SAL) ($p < 0.01$), and also between the "frontal" DMN and the right-lateralized frontal RSN (grouped as SAL) ($p < 0.05$). Furthermore, the MBT+tDCS group showed *less antagonism* (i.e., decreased anti-correlation) between the precuneus RSN and the right-lateralized frontal RSN (grouped as SAL) ($p < 0.05$), and between the posterior cingulate RSN (grouped as DMN) and the bilateral inferior parietal RSN (grouped as SAL) ($p < 0.01$).

For state 5, the MBT+tDCS group showed increased positive dynamic connectivity between the precuneus RSN and the canonical "salience" RSN ($p < 0.05$), and also between the precuneus RSN and the bilateral inferior parietal RSN ($p < 0.01$). Furthermore, the MBT+tDCS group also displayed a decrease in positive dynamic connectivity between: the precuneus RSN and the posterior cingulate RSN (both grouped as DMN) ($p < 0.01$), the "frontal" DMN and the LH frontal–parietal network (grouped as

CCN) ($p < 0.05$), and between the "salience" RSN and the right-lateralized frontal RSN (grouped as SAL) ($p < 0.01$).

Group comparisons on the number of dFNC state "transitions"

Figure 33 displays the mean and SE of the baseline and post-training state transition occurrences. Within the repeated measures ANOVA framework, pre-defined pair-wise comparisons showed that the MBT+tDCS group exhibited more state transitions compared to the Cont+Sham group ($p = 0.02$, $\eta_p^2 = 0.19$). However there were no differences post-training relative to baseline in the MBT+tDCS group ($p = 0.54$). There were also no baseline groups differences ($p = 0.89$).

Figure 33: Mean, SE and statistical comparisons on the occurrences of state transitions.

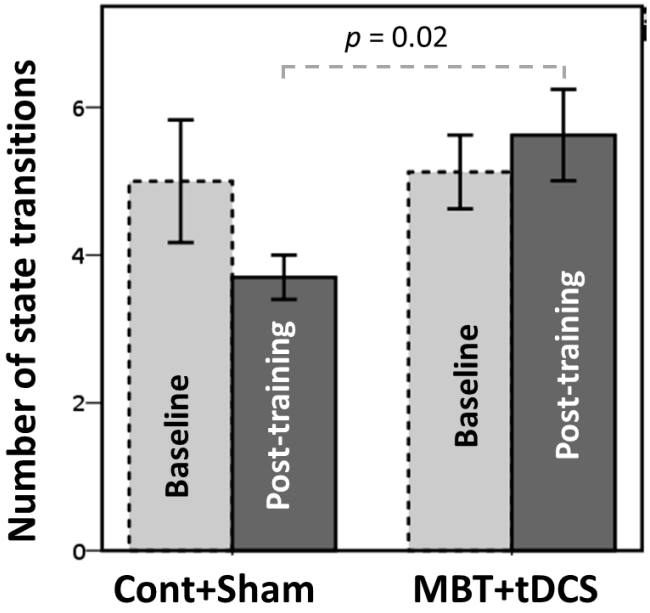

After training, the MBT+tDCS group exhibited more state transitions compared to the Cont+Sham group.

Examining whether dFNC measures relate to individual differences in performance and personality trait measures

In order to evaluate whether individual differences in performance measures (e.g., S-span, O-span, ravens, etc.) and personality measures (e.g., BIS, BFI, and MWS) were related to dFNC metrics (e.g., state dwell times and state transition occurrences), Pearson correlations were computed on baseline and post-training data. There were no associations observed between dFNC and performance measures (*p's* > 0.45). However, collapsed across both groups, there were several interesting relationships observed. First, for the baseline state transitions only, there was a significant correlation between MWS $r(26) = -0.74$, $p = 0.001$, which was also related to the attention sub-score of the BIS, $r(26) = -0.73$, $p < 0.001$. This finding suggest that the more a subject exhibited state transitions at baseline, the less they endorsed mind-wandering and problems with concentration. This relationship was observed within both groups (*p's* < 0.002), but was not present after training (*p's* > 0.37). Furthermore, there was a significant correlation between dwell time in state 5 and the attention sub-score within the BIS, which was present only after training in the Cont+Sham group, $r(10) = 0.66$, $p = 0.03$ and not in the MBT+tDCS group (p=0.78). The direction of this relationship may demonstrate that increases in the dynamic connectivity patterns that constitute state 5 may be predictive of attention related problems.

Training dose-related relationships with relative changes scores in transfer tasks and dFNC measures

In order to examine the number of MBT sessions and the number of tDCS sessions was related to gains in transfer tasks, personality traits, and the dFNC outcome variables. As described in the previous EEG section, Pearson correlations were computed on the relative change scores for each variable. The only significant correlation observed was between the relative change scores in S-span performance the number of MBT sessions, $r(16) = 0.51$, $p = 0.04$. Note: a similar correlation was observed in the EEG sample, where there was a 44% overlap in the participants included in this fMRI sample.

CHAPTER 5: DISCUSSION ON WORKING MEMORY CAPACITY AND ELECTROPHYSIOLOGICAL CHANGES ASSOCIATED WITH MBT+tDCS

The present study examined the effects of a novel mindfulness-based training (MBT) with right frontal stimulation using tDCS (MBT+tDCS) protocol. The impetus for this combined intervention was to enhance domain-general cognitive abilities that could potentially transfer to real-world cognition. That is, while MBT was employed to train and refine one's attentional control abilities, tDCS was used to accelerate the neurophysiological mechanisms responsible for neuroplastic change during the state-dependency of MBT, specifically targeting the right-lateralized cognitive control network. Thus, given that MBT's target the primary "focus" of one's own attention, a mechanism similar, if not isomorphic, to the "central executive" of WM, the present

study examined aspects of WM performance, their electrophysiological signatures, and the extent that they correlated with near and far transfer tasks.

Training-related gains in working memory performance

Consistent with our first hypothesis ($H_{01.1}$), the MBT+tDCS group demonstrated training-related improvements in working memory load, evinced by increased 3-back accuracy relative to baseline performance and compared to post-training 3-back performance in the active control with sham stimulation (Cont+Sham) group. Given that the observed increases in hit rate were specific to the most demanding WM load condition in this study, the observed training-related increase in accuracy may reflect an alteration in the range of capacity limits (Cowan, 2001) in the MBT+tDCS group. This enhancement in capacity is further evinced by quicker responses across WM load conditions after training in MBT+tDCS group compared to the Cont+Sham group, with the most robust effects observed in the 2- and 3-back WM load conditions. Altogether, these results suggest that the MBT+tDCS group improved in processing speeds and accuracy in the more demanding WM load conditions.

However, variations in RT are generally thought to reflect state-dependent measures of arousal and attentional states (Broadbent, 1971), a measure not reported on in previous studies that investigated the MBT effects on WM (Jha et a., 2010; Mrazek et al., 2013; Zeidan et al., 2010). Nonetheless, the examination of both variables of WM performance revealed that increased accuracy during the 3-back condition was observed without the predicted tradeoff for slower RTs, which is the typical response pattern when

there is a compromise between the incompatible demands for maximum accuracy and minimum RT (Wood and Jennings, 1976). More specifically, within the sequential sampling framework, shifts in the speed-accuracy tradeoff are presumed functionally identical to threshold shifts in the amount of information that can be accumulated prior to a decision or response mapping (see Hietz, 2014, for review). Although speculative, it is possible that the combined effects of tDCS on MBT may affect this threshold for simultaneously performing more accurately without losing efficiency in processing speed given its reliable effects on RTs during WM training (Brunoni et al., 2014). However, it remains unclear what mechanisms may alter this threshold. It could be an increase in overall arousal, capacity, or even motivation to perform better. Further research is needed to examine whether the speed-accuracy tradeoff is influenced more by tDCS or MBT alone. Altogether, the present results demonstrated an overall increase in the MBT+tDCS group's WM capacity constraints and state-dependent information processing.

More generally, the current findings are consistent with previous MBT studies that examined the effects of MBT on WM performance (Jha et al., 2010; Zeidan et al., 2010; Mrazek et al., 2013). For example, Zeidan et al. (2010) implemented a relatively short MBT protocol (4 days of training, 20 mins each) and tested adaptive 2-back performance before and after training and showed improvements in the MBT group. This study found increased performance on extended hit rate accuracy, i.e., the number of accurate and consecutive working memory discriminations. The authors concluded that the MBT group was able to maintain focus and accurately retrieve information from

working memory under conditions that required rapid stimulus processing. Although the n-back task used in this study was different than the one used in the current study, both studies provide additional evidence that MBT enhances similar executive control processes subsumed by WM processing, which may narrow down the possible mechanisms that MBT target and may transfer to other real-world applications.

Impact of MBT+tDCS on transfer tasks

Central to the context of learning and the methods by which to evaluate cognitive training interventions is the concept of transfer (Cormier and Hagman, 1987; Klingberg, 2010). In the present study, in order to evaluate whether there were near-transfer effects within WM, complex WM performance was assessed as it engages the attentional control aspect within WM (Engle, 2003). Although there are some controversies regarding the utility of the n-back in comparison to the complex WM tasks, (in that the n-back is typically conceived as measuring WM updating while complex span tasks specifically measure WM capacity in the face of distraction), a recent latent variable analysis showed that these tasks loaded on a similar factor, suggesting that each task family does indeed measure the same construct (Schmiedek et al., 2009). Thus, in the current study, complex WM span tasks were used as near-transfer task to the n-back task.

Consistent with our hypothesis that MBT+tDCS would produce transfer effects ($H_{02.1}$), a significant increase in S-span performance was observed in the MBT+tDCS group compared to the Cont+Sham group. Furthermore, relative (to baseline) increases in the 3-back was correlated with relative increases in S-span performance in the

MBT+tDCS group only, further suggesting a general near transfer effect produced by this protocol. This is an important finding as it is the first study to examine more than one measure of WM and establish a transfer relation between 3-back and S-span performance. Thus, to this extent, the current results suggest that MBT+tDCS broadly improves a common WM ability involved in building, maintaining, and updating arbitrary bindings (Miller & Cohen, 2001). Overall, this finding provides additional support for MBT+tDCS producing improvements specific to the top-down guidance of the executive attention component of WM (Chow and Conway, 2015), which are important for higher-order cognitive activities (Unsworth et al., 2009).

However, the present study did not find a statistically significant difference in O-span performance, which was unexpected, as previous studies that tested the effect of MBT on O-span performance reported only modest effect sizes (Jha et al., 2010; Mrazek et al., 2013). At the same time, however, these previous studies did not test for training-related differences on S-span performance, thereby making it impossible to determine if the current null results on O-span performance is an issue of statistical power. Despite the lack of difference in O-span performance, however, there were significant correlations between relative change scores in the O-span and relative change scores in the MWS, such that, less mind wandering after training was associated with better O-span performance. To this end, there is some evidence that O-span performance is linked to functional outcomes in the MBT+tDCS group.

Nonetheless, there were no overall O-span performance gains within the MBT+tDCS group. The most likely explanation to the current findings in complex WM performance is the methodological difference between the tasks and the nature of the MBT+tDCS protocol utilized in the current study. While S-span and O-span performance is significantly correlated (r = 0.57; Redick et al., 2012), there is still ~67% of unexplained variance between these two metrics, suggesting that each task measures a unique attribute of WM. The primary difference between these two span tasks is that one requires spatial reasoning whereas the other requires more verbal, arithmetic and serial information processing. Confirmatory factor analyses that included the S-span and O-span, among other WM measures, revealed that domain-differentiated models (verbal vs spatial) yielded better fits than models involving domain-general constructs, providing evidence for the need to distinguish verbal and spatial working memory abilities (Hale et al., 2011). Accordingly, there is mounting evidence from neuroimaging studies that show unique lateralized activations within each domain of WM; that is, a left-lateralized frontal-parietal network is engaged more for verbal WM tasks, while a right-lateralized frontal-parietal network subserves visuospatial WM tasks (Smith & Jonides, 1998; Reuter-Lorenz et al., 2000).

Taken together, it is plausible that the right frontal stimulation applied during MBT in the current study biased an enhancement of right-hemispheric visuospatial WM abilities by strengthening the local neuronal connections subserving a larger, distributed spatial WM network. This is consistent with prior evidence demonstrating that a single

session of tDCS is sufficient to change functional connectivity within and between large-scale intrinsic networks (Clemens et al., 2014; Hunter et al., 2015). Thus, given that right frontal regions are more involved in spatial-location monitoring (Owen et al., 2005) and that tDCS can improve performance on a visuospatial WM performance (Jeon & Han, 2012), the observed domain-specific improvement (i.e., increases in S-span, but not O-span performance) in the MBT+tDCS group may be attributed to the combined effect of MBT with the application of right frontal tDCS.

This hypothesis is further evinced by an observed correlation between the number of tDCS sessions and the relative performance gains in S-span performance in the MBT+tDCS group, which was not observed for the O-span or n-back relative change scores. Furthermore, based on responses obtained from our Exit Questionnaire (see Appendix A), the MBT+tDCS group reported specific improvements in "pattern recognition" and "analyzing puzzles", which is consistent with the abilities required to perform well on the S-span task.

With respect to domain-specific effects, the interpretation of the current findings could also be applied to the results obtained by Jha et al., 2014, who found increased O-span performance after 8-weeks of MBT in a sample of military personal. This improvement was also linked to the amount of time spent training, suggesting that greater practice time corresponded to greater WMC. Thus, it is possible that MBT alone may target verbal WM abilities, but when paired with tDCS, MBT may be biased more toward spatial abilities in a dose-dependent fashion, observed in the current study as enhanced S-

span performance. This observation may have particular relevance for training protocols that intend to preferentially target verbal vs spatial WM abilities. For example, a recent study found faster rates of cognitive decline in the spatial WM domain compared to verbal WM, suggesting that the spatial domain may be more demanding on neuronal resources and may underlie similar neural pathways associated with decline, thereby making the current MBT+tDCS protocol a primary target for this population.

Furthermore, it is also important to note that the null effect in O-span performance may also be influenced by a restricted range in O-span variability, since the current sample was derived from a young, high-functioning population. This is supported by a previous study that found a difference in the zero-order correlations between these span tasks as a function of college education, with lower correlations observed within samples with higher mean performance. The authors of this study suggested that the verbal domain vs spatial domain nature of WMC is uniquely different in high performing samples (Redick et al., 2012).

Future studies are needed to examine whether there are specific effects (as opposed to global benefits across all measures) associated with the amount of MBT and whether domain-specific WM abilities are modulated preferentially by left and right frontal stimulation in the context of MBT. Nonetheless, as it relates to this combined approach, more work is needed to test the additive effects of tDCS on MBT. In conclusion, the current findings suggest that the combined MBT+tDCS protocol may

facilitate the implementation of attentional control processing during working memory tasks.

Training-induced modulations on frontal and parietal P3 magnitude

In the present study, the canonical P3 ERP component was evaluated as an attention-related biomarker of neuroplastic change. The P3 represents a family of ERPs related to different aspects of global attentional processing and evaluation (Linden, 2005 Polich, 2007). Furthermore, P3 amplitude—in the context of updating in WM and/or inhibiting a dominant response in sustained attention tasks, is interpreted as an index for integrating information into existing networks (Kok, 2001; Polich, 2007). In the present study, P3 amplitude was obtained after each target ("match") in each of the WM load conditions in the n-back task, which was compared relative to baseline and between groups after training, as well as to task transfer gains within the MBT+tDCS group.

Consistent with previous studies, P3 amplitude to targets in the current study decreased as a function of WM load, indicating more efficient neural processing resulting from greater resource allocation during more demanding WM load conditions (Gevins and Cutillo, 1993; Polich, 1995; Cabeza et al. 2002; Gaspar et al., 2011; Saliasi et al., 2013). After training, the MBT+tDCS group displayed an increase in posterior P3 amplitude for the less demanding WM load conditions compared to the Cont+Sham group. Consistent with our hypothesis ($H_{01.2}$), the MBT+tDCS group also exhibited a simultaneous decrease in P3 amplitude across all WM load conditions at the frontal electrode sites (i.e., Fz and F10), particularly for the most demanding WM load condition

(i.e., 3-back). These results suggest a differential P3 response pattern in the distribution of EEG topology, where a heightened posterior response was preferred during low-demand WM load conditions, and a diminished P3 frontal response was preferred during high WM load conditions.

Previous studies have found this reversal in P3 magnitude may be due to the functional distinction between these two regions at varying levels of WM demands. That is, previous studies investigating the P3 response across WM load conditions suggest that an intensified posterior response during low-demand WM load conditions reflects an EEG topology associated with high performing individuals who achieve better performance by paying more attention to the task (Lakey et al., 2011). Indeed, posterior P3 activity during low demand WM performance is more involved in basic stimulus matching, requiring less resource allocation (Gevins and Cutillo, 1993; Vogel et al,. 2005). Thus, the current finding suggest that MBT+tDCS may further improve information processing by enhancing concentrative focus skills during tasks that require minimal resources.

However, during high cognitive load conditions, a neural system may recruit a more widely distributed network with reciprocal connections between frontal and parietal association areas (Kok, 2001; Fehr, 2013). Thus, the observed decrease in post-training P3 at the frontal electrodes in the MBT+tDCS group, specifically in the context of high WM load demands, may reflect the activation of widespread frontal-parietal and ACC networks involved in attentional capacity invested in the categorization of task relevant

events (Gaspar et al., 2011). Furthermore, given the observed frontal decreases in P3 amplitude, Vogel et al. (2005) found that high capacity performance reflects more efficiency by representing only the relevant items compared to low capacity performance, which is more characterized by inefficient encoding and maintenance of WM on irrelevant items. Thus, the current findings provide evidence that MBT+tDCS may expand WM load capacity constraints by efficiently recruiting multiple brain networks to efficiently allocate attention to relevant information.

Furthermore, in support of the hypothesis that decreased frontal P3 amplitude affords greater neural efficiency and capacity, the present study also found that there was a MBT+tDCS group-specific relationship between gains in S-span performance and relative decrease in P3 amplitude during 3-back performance in the F10 electrode site. This finding suggests that those in the MBT+tDCS group who showed the largest training-related gains within the S-span also exhibited the largest relative decrease in P3 amplitude at the F10 electrode site during the high WM load condition. Furthermore, the relative change scores in the attention sub-scale within the BIS was also significantly correlated with relative change scores in P3 amplitude during the 3-back condition at the F10 electrode. This finding indicates that for those who endorsed improvements in attention and concentration abilities relative to baseline also showed the largest decrease in 3-back P3 amplitude at electrode site F10 relative to baseline.

However, it is important to interpret the frontal changes in P3 with caution as there is evidence that the largest EEG contributor to the stimulus-locked P3 positivity at

Fz is volume-conducted from the same parietal (P3 cluster) sources, which casts doubt on the specificity of peak amplitude at Fz for indexing frontal function (Makeig et al., 2004). This is further evinced within the current sample as a subtle mean difference in Fz amplitude when using a mastoid reference vs average reference; however, these small mean difference were not statistically significant (see Appendix C).

Furthermore, it is important to highlight that the current gain score relationships were not observed at electrode site Fz or Pz, suggesting a spatial localization of transfer effects to right IFG, the target location of anodal tDCS in the current protocol. Altogether, it is possible that tDCS may facilitate task transfer of MBT abilities, specifically in the context of spatial WM abilities and to self-endorsements of improved attention and concentration.

Modulations on sustained frontal and parietal P3 theta power

Power-based measures of theta oscillatory activity estimate the amount of energy in a specific frequency band at a specific interval of time, providing valuable information about neuronal resource allocation during various cognitive load conditions. Frontal and parietal theta oscillations (4–8 Hz) are thought to serve as the temporal code that coordinates neuronal populations involved in implementing attentional control and WM load in the healthy brain (Berka et al., 2007; Reinhart et al., 2015). In the current study, sustained theta power in the P3 range (300 – 900 ms) was obtained after each target ("match") in all of the WM load conditions in the n-back task, which was compared

relative to baseline and between groups after training, as well as to task transfer gains within the MBT+tDCS group.

Consistent with previous studies investigating the relation between WM load and theta power in healthy populations, the current time-frequency analysis revealed increased frontal theta power as a function of WM load prior to training (Klimesch et al., 1997; Onton et al., 2005; Sauseng et al., 2005; Massonnier et al., 2012). This observed increase in sustained frontal theta activity (300 – 900 ms) during higher WM load conditions is thought to reflect efficient use of WM active maintenance (of WM items) and general continual cognitive engagement (Massonnier et al., 2012).

After training, the MBT+tDCS group exhibited a decrease in mid-line frontal theta power during the 3-back condition only, which was inconsistent with our initial hypothesis ($H_{01.3.1}$). Furthermore, the MBT+tDCS group also displayed a simultaneous increase in posterior theta power, with the largest difference observed during the 3-back condition. The current results provide evidence for a redistribution of theta power magnitude at frontal and posterior electrode sites.

Although the observed decrease in frontal theta power in the MBT+tDCS group appear inconsistent with previous MBT studies (and more specifically with our initial hypothesis; $H_{01.3.1}$), where frontal mid-line theta is typically increased, there are a number of methodological differences to consider. The majority of previous MBT studies examining the effects of MBT on theta oscillatory activity observed an increase in frontal midline theta power (for review, see Lomas, Ivtzan, Fu, 2015). However, each of these

studies either examined frontal theta during mediation, during rest (i.e., in the absence engaging task-related networks), or assessed immediate (same day) pre/post differences using a short-term mediation practice, all of which, suggest alterations in state-related changes in theta power. To the author's knowledge, there are no other published studies that examined the changes in theta power as function of cognitive load outside the context of state-related changes during mediation. Thus, the present study differs substantially from previous literature in that the current differences in theta power reflects alterations on task-related networks affect by a combined intervention designed to induce long-term neuroplastic changes outside the context of state-related mediations changes.

To this end, the observed decrease in midline frontal theta power in the MBT+tDCS group during the high-demand WM load condition may indicate enhanced neural efficiency. The neural efficiency hypothesis postulates that a higher cognitive capacity level is associated with more efficient brain functioning (Neubauer and Fink, 2009). For instance, individuals who score high on difficult tasks tend to rely on frontal cortex less as they gain mastery of a cognitive skill (Gevins and Smith, 2000). Using source localization methodology, synchronous field activity in the theta range has been localized to dorsal anterior cingulate cortex (Onton et al., 2005), which is one of the primary brain regions activated during MBT and most susceptible to functional reconfiguration. Accordingly, Allen et al. (2012) specifically found that MBT follows a nonlinear dosage–response curve, such that, early skill training may reflect different activation patterns compared to later phases of training and/or more advanced practices.

Thus, the observed post-training functional reconfiguration of the frontal electrode sites in the present study may contribute to improved WM capacity by affording more neural efficiency.

Moreover, there is empirical evidence that also emphasizes the global efficiency among the functional connectivity between frontal and parietal cortices, which operate efficiency more rapidly during more demanding aspect of a WM task (see Deary and Caryl, 1997). Consistent with the neural efficiency hypothesis, the MBT+tDCS group also exhibited an increase in theta power at the midline posterior electrode site, suggesting the recruitment of the frontal-parietal network to afford better WM performance. Indeed, relative increases in Pz theta power was correlated with relative performance gains during the 3-back condition. This result suggest that those who showed the largest training-related gains in 3-back performance in the MBT+tDCS group also exhibited the largest relative change in power in the Pz electrode, further suggesting that increased theta power in Pz may be beneficial for engaging (or recruiting) more efficient attention-related processes.

Furthermore, metabolic studies have indicated that the parietal regions tend to play an important role in attentional allocation and manipulations (Coull and Nobre, 1998; Zacks et al., 1999). The current results thus may indicate that the MBT+tDCS group learned to exploit these capabilities of the posterior cortex in order to perform the tasks more efficiently. Given that previous studies have found increased frontal-parietal theta coherence as a function of WM demands (Gevins and Smith, 2000; Sauseng et al.,

2005; Raghavachari et al., 2006), it is also possible that MBT+tDCS group identified strategies that make more optimal use of the wide array of the cortical resources.

To this end, the observed increase in posterior theta synchronization may enhance the dynamic, long-range communications of task-relevant brain areas within WM networks (Sauseng et al., 2005; Klimesch et al., 2008; Kawasaki et al., 2010). Interestingly, the observed large effect size in midline posterior theta power in the MBT+tDCS group may indicate an overall enhancement in the reactivity of cortico-hippocampal interactions required to perform well across all WM load conditions, particularly in the high-demand WM load condition (Newman and Grace, 1999). An increase in sustained theta activity serving a cortico-hippocampal interaction may help solidify memory traces, serving as a visual WM "sketchpad", "rehearsal loop", or "sensory storage buffer" for comparing external stimuli with internal representations (Kok, 2001; Kawasaki et al., 2010). Thus, it is possible that the observed training-induced alterations in posterior theta power may further be influenced by mechanisms that underlie a form of neural adaptation in polysynaptic association cortices within the context of MBT+tDCS on WM processes. Indeed, theta band activity has been shown to be highly effective at inducing LTP in the hippocampus and polysynaptic activations in association cortices *in vitro* (Werk and Chapman, 2003). Furthermore, these findings provide evidence for a possible "mindful transfer" effect on domain-general, associative, and polymodal neural architecture, which may bridging the necessary connection from near to far transfer gains.

CHAPTER 6: DISCUSSION ON VISUAL ODDBALL EEG AND BOLD TRAINING-REALTED CHANGES ASSOCIATED WITH MBT+TDCS

In addition to producing changes in WM ability, mindfulness training with tDCS was hypothesized to produce enhancements in core cognitive processes involved in sustained attention. Given that the ability to focus one's attention over an extended period of time while resisting distraction is a necessary condition for sustained attention and general tonic levels of arousal during mindfulness training (Malinoski, 2013), changes in the corresponding neuroelectric and BOLD responses specific to attentional engagement and disengagement were expected. In the present study, the three-stimulus oddball task was used to evaluate training-related effects on its reliable P3 representations and BOLD responses of the sustained attention brain circuit (Polich and Criado, 2006). In particular, evoked P3 amplitude and BOLD responses were obtained after each target ("hit") and after the presentation of distractor and standard stimuli, which was compared relative to baseline and between groups after training, as well as to task transfer gains within the MBT+tDCS group.

Training-related changes in P3 amplitude during visual oddball processing

With respect to the testing overall performance in the oddball task in the current EEG study (i.e., $H_{02.1}$), participants in both groups responded quicker after training (compared to baseline), suggesting a general practice effect across both groups. However, it was only the MBT+tDCS group who produced quicker RTs after training that were

statistically significant, indicating a training-specific increase in target detection on a task that requires sustained attention resources.

Consistent with previous studies that examined P3 amplitude during the visual three-stimulus oddball task, the present ERP analysis produced similar stimulus-specific spatial topographies and waveforms (see Polich, 2007 for review). For the target stimuli, P3 topology was dominated by increases in central-parietal electrodes, indicating a response elicited by contextually relevant information, which was generally stronger in magnitude than the responses elicited by the distractor and standard responses. The distractor stimuli generated a more focal temporal-parietal response along with a broad right frontal topology, which is thought to reflect the maintenance of stimulus information and processing in-frequent distractor stimuli. The standard stimuli produced a weaker P3 occipital-parietal topology, reflecting maintenance of visual information.

Group comparisons, testing $H_{03.3.1}$, revealed a statistically significant decrease in P3 amplitude in the MBT+tDCS group at the frontal midline electrode compared to the Cont+Sham group. Recent studies that employed the three-stimulus oddball task before and after meditation practice found consistent training-related findings across studies (Lutz et al., 2009; Slagter et al., 2009; Cahn and Polich, 2009; Cahn, Delorme, Polich, 2013). For instance, within MBT protocols, a consistent finding is a reduced (overall) P3 amplitude during attention-related task performance compared to control groups; that is, MBT subjects typically exhibit a reduction in P3 amplitude in response to rare stimuli, which is thought to co-vary with self-reported gains in trait mindfulness (Cahn & Polich,

2009). Overall, the current result is consistent with the neural efficiency hypothesis by which less attentional effort is required for the MBT+tDCS group, indexed by less resource allocation within the context of sustained attention (Cahn & Polich, 2009; Slagter et al., 2007).

However, inconsistent with our initial hypothesis, there were no group differences observed in P3 amplitude during distractor processing. Previous studies reported a reduction in P3 amplitude to distractor stimuli, which is thought to reflect state-dependent decreases in automated reactivity and evaluative processing of task irrelevant attention (Cahn and Polich, 2009). Further research is needed to examine possible training-related effects using multiple distractor stimuli, making the distractors more difficult to distinguish at varying ISIs.

Changes in alpha and theta oscillatory activity during visual oddball processing

The neuroelectric architecture of the P3 phenomenon during oddball processing is thought to reflect transient event-related changes in power of the theta and alpha frequency bands (among others), contributing more broadly to the distinction between phasic and tonic activity. In the present study, alpha and theta phase consistency and power was obtained after each target ("hit"), and after the presentation of distractor and standard stimuli, which was compared relative to baseline and between groups after training, as well as to task transfer gains within the MBT+tDCS group.

Phase-locked activity (averaged) across trials is thought to serve as the bases of functional configuration within a particular task. In order to test whether there were

significant group differences in phasic activity (i.e., $H_{03.4}$), the current study found that, relative to baseline, the MBT+tDCS group displayed a decrease in alpha phase consistency during distractor stimulus presentation at midline and right frontal electrodes, which is thought to be associated with a decrease in automated attentional engagement (Cahn and Polich, 2006) and consistent with our initial hypothesis. Moreover, there were significant associations between the relative change scores in S-span and frontal alpha-band ITPC during the distractor trials within the MBT+tDCS group only. These findings suggest that alterations to midline frontal alpha ITPC during distractor trials may be an important neuroplastic change to infrequent distractor stimuli that may lead to transfer of basic attentional skills to executive control of attention in the context of WM gains in performance.

Furthermore, relative to baseline, there was an increase in posterior alpha power (i.e., synchronization) during standard stimulus presentation within both groups, suggesting an enhancement of stimulus representation of the habituated standard stimuli. Research has shown that during the inter-stimulus "baseline" interval preceding each task event, tonic arousal states are reflected by alpha synchronization over posterior EEG sites as the participant anticipates the presentation of the next stimulus (Klimesch, 1999), or a "readiness" to process the next event, or perform a new task (Klimesch et al., 2007). It is possible that the active engagement of training in the posterior brain regions may enhance general sustained visual processing that is not specific to controlling attention per se, but rather associated with practice-related effects.

Furthermore, the MBT+tDCS displayed a de-synchronization of alpha specifically during the standard stimuli at the midline electrode, while the Cont+Sham group exhibited a similar de-synchronization of alpha power at F10. This regionally differential response may suggest a difference in the de-synchronization of frontal alpha between groups. It is possible that these findings indicate a frontal preference in the reduction in inhibitory and arousal processes that may be specific to the ACC for the MBT+tDCS group and to the right frontal control network in the control group. However, further research is needed to test this pattern of alpha suppression with other experimental groups under repetitive series of stimuli over time as alpha suppression has been associated with more efficient brain functioning across tasks that distinguish between expertise levels (Grabner, Neubauer, Stern, 2006).

Analyses on theta-band activity within the MBT+tDCS group revealed an interesting pattern of results. During the infrequent targets, there was an increase in theta ITPC at the posterior midline electrode site and also an increase during the infrequent distractors at the midline frontal electrode site. These results suggest a training-induced region-specific increase in theta-band neural entrainment indicative of effective attentional allocation in the MBT+tDCS group only. While the targets recruited more theta clustering, the distractors elicited more frontal theta clustering both of which are require more attentional demands on this sustained attention task.

In addition, while both groups displayed a decreased in theta power to distractors at the midline electrode, there was a reversal in power magnitude between groups for the

distractors at the F10 electrode, such that the MBT+tDCS group decreased theta power, the Cont+Sham group recruited more theta power. This result is consistent with the neural efficiency hypothesis of neural plastic change in the MBT+tDCS group who recruited less theta power, while the Cont+Sham group recruited more theta power, which in comparison to the MBT+tDCS group, suggesting an inefficient use of theta power in the control group relative to the MBT+tDCS group. That is, the Cont+Sham group required more neural energy in the theta-band to implement inhibitory control of these processes.

Training-related changes in BOLD responses during visual oddball processing

The neuroelectric architecture of the P3 phenomenon during oddball processing has also been extensively studied using event-related fMRI in order to examine the specific anatomic locations of brain regions involved in attention-related processes that is required during stimulus processing of targets, distractors and standard stimuli (Clark et al., 2000; Bledowski et al., 2004). In the present study, BOLD responses modeled from each stimulus onset was obtained, which was compared relative to baseline and between groups after training. As expected (according to ($H_{02.2}$), the current study revealed group differences in gross BOLD changes in anatomical regions involved in MBT+tDCS, namely in ACC, insula, DLPFC, hippocampus, and rIFG. There were also additional regions that showed a training-related effect, which included the cerebellum, caudate, putamen, and bilateral PCC.

Consistent with previous studies, the infrequent target condition elicited a distributed network of brain regions involved in attention, such as the right insula, inferior frontal gyrus, inferior parietal cortex, thalamus, extrastriate, and cerebellum. Although there was no hypothesized difference in BOLD activations in the parietal regions within the MBT+tDCS group, decreases in the target BOLD response were observed in the medial frontal gyrus (BA 9) and head of the caudate relative to baseline. These two specific brain regions represent a parallel frontal–subcortical circuit, which originates in BA 9 and 10 and projects to the dorsolateral head of the caudate nucleus (Tekin and Cummings, 2002).

In the context of sustained attention, a study found that brain regions underlying fast RTs during a psychomotor vigilance task included bilateral putamen, inferior parietal cortex, and several medial frontal and motor regions (Drummound et al., 2005), suggesting that frontal and putamen circuitry work in concert to produce fast RTs during a vigilance task (Alexander, Crutcher and Delong, 1990). Thus, the current results suggest that the MBT+tDCS group rely less on this circuit for target detection after training given the decrease in BOLD activity, indicating a possible neuroplastic change in the neural circuitry involved in more efficient attentional engagement (Neubauer, 2009).

Furthermore, it is important to consider a possible interaction of excitatory neurotransmission that may underlie this change in BOLD response in the MBT+tDCS group. The fibers originating from the frontal lobe are mediated by excitatory glutamatergic neurotransmission (Tekin and Cummings, 2002), which project to striatum

(includes caudate and putamen). Thus, given the role of tDCS on modulating glutamatergic neurotransmission on functional connectivity (Hunter et al., 2013; Clemens et al., 2014), it is possible that tDCS may have influenced the change in BOLD activity between these brain regions via glutamatergic signaling pathways (Hunter et al., 2015), which may further facilitate long-term effects of MBT.

Furthermore, relative to the post-training activations in the Cont+Sham group, the MBT+tDCS group exhibited an increased target BOLD response in the left culmen of the cerebellum. The cerebellum has been shown to play a role in a number of different cognitive and motor abilities, such as planning, initiation, stability, organization, and long-term memory of movements (Schmahmann and Caplan, 2006; Miall et al., 2007). In particular, the left culmen of the cerebellum, along with other brain regions (e.g., bilateral insulae, thalamus, and parietal cortex), has been associated with target detection to rare targets during a visual oddball task, which was thought to be associated with motor response and salience processing (Clark et al., 2000; Tegelbeckers et al., 2015). Thus, the observed increase of BOLD activity in the cerebellum may be due to increased cortical representation of target button responses (Enriquez-Geppert et al., 2013 for review). Furthermore, this increase in BOLD activity may also be influenced by the current distribution produced by the tDCS montage used in this study. Indeed, given that the cathode was placed on the left upper arm, the current flow may have directed current to (or near) the cerebellum, thereby affecting the BOLD signal.

Consistent with previous studies, the distractor condition produced a distributed network of brain regions, such as, bilateral extrastriate, left precentral gyrus, right insula, right IFG and inferior parietal cortex, as well as medial frontal gyrus (Clark et al., 2000). For the distractor BOLD response comparisons, although there was no hypothesized decreases in BOLD activations in frontal regions within the MBT+tDCS group, BOLD responses to distractors were increased in regions that may be involved in active encoding and inhibition of attentional engagement to irrelevant stimuli. In particular, relative to the Cont+Sham group, the MBT+tDCS group displayed an increase in BOLD response to distractors in parietal cortex and bilateral insulae. This particular finding of the contributions of the insula to distractor processing (i.e., the generation of the P3a) converges on a crucial role for these brain regions in producing an early cognitive control signal that disengages the DMN and activates task-specific, executive control networks (Ham et al., 2013).

Additionally, within the MBT+tDCS group only, BOLD responses to distractors were significantly increased relative to baseline in left and right post-central gyri and left parahippocampal gyrus. These results may indicate an overall increase in salience-related and general encoding processing after training in the MBT+tDCS group. Indeed, the parahippocampal formation in particular has been shown to increase in BOLD signal during mediation, while the pre- and post-central gyri and hippocampal formation increased in BOLD response as a function of practice (Lazar et al., 2000). Furthermore, the left hippocampus has been shown to mediate some of the benefits of meditation

modulation specific to cortical arousal and responsiveness (Hölzel et al., 2011) and trait mindfulness (Doll et al., 2015). Thus, the current results provide further evidence for the MBT-related effects on these brain regions within the context of processing distractor stimuli.

Given the close proximity of the anode electrode to right IFG and INS in the present study, the observed increase in BOLD signal in these regions (among others) may further establish an enhancement of the casual outflow from the right insula and IFG to other nodes that anchor the salience network for enabling the recruitment of contextually relevant brain regions (Sridharan et al. 2008). Thus, MBT+tDCS may operate by enhancing the network activity within bilateral insulae, parietal cortex, parahippocampal gyrus and post-central gyrus during sustained attention, particularly at the initial phase of processing irrelevant (distractor) information. Its effects may also have an impact on integrating external stimuli with one's internal homeostatic context (Seeley et al., 2007, Singer et al., 2009, Menon and Uddin, 2010 and Seth et al., 2012).

Lastly, standard stimuli produced a distributed network of brain regions, including bilateral visual cortex, left pre- and post-central gyrus, right insula, right IFG, as well as the right parahippocampal gyrus. Compared to the Cont+Sham group, the MBT+tDCS group exhibited an increase in BOLD to standards in posterior cingulate cortex (PCC), suggest an enhanced response to frequent stimuli, reflecting enhanced stimulus representation. Previous studies also found that the PCC is involved in self-awareness (Vanhaudenhuyse et al., 2010; Manna et al., 2010), cognitive switching (Menon and

Uddin, 2010; Liang et al., 2014) and mindfulness disposition (Prakash et al., 2013). Furthermore, within the MBT+tDCS group there was a decrease in BOLD response in left putamen and right IFG, which may suggest enhanced neural efficiency to frequent standard response during a relatively easy task.

Overall, these results point to the involvement of distinct attentional subsystems in target and distractor processing (Clark et al., 2000; Bledowski et al., 2004), which involve brain regions that are relevant for attentional processing during mindfulness practice. This pattern of results was interpreted as the MBT group exhibiting greater resource allocation and more efficient processing during tasks requiring attentional control (Cahn & Polich, 2009; Slagter et al., 2007).

CHAPTER 7: DISCUSSION ON DYNAMIC NETWORK CONNECTIVITY

The present study also evaluated the dynamic resting-state network connectivity patterns before and after training in order to investigate gross changes in network adaptation and integration. Given that large-scale functional brain networks are continuously engaged in MBT, the intrinsic connectivity among these networks may be strengthened (or weakened), resulting in training-related modifications to the intrinsic architecture of functionally-relevant large-scale networks. The present study utilized the analytical techniques developed to model the dynamical relation between resting-state networks, providing a canonical set of descriptors of time-varying, but reoccurring, patterns of coupling among brain regions, i.e., the chronnectome (Calhoun et al., 2014). Within this analytical framework, brain dynamics are assumed to be intrinsic

nonstationarities, in contrast to traditional functional connectivity analyses that assume brain dynamics are stationary, that is, remaining static, or unchanging, over time.

In particular, dynamic functional network connectivity (dFNC) analyses provide a method for evaluating quasi-stable intrinsic brain organization by revealing information about functional connectivity states (i.e., dynamic pattern of functional connectivity among networks over time), how long a person resides in such states (i.e., state dwell time), and how flexible these states transitions from one to another (see Allen et al., 2012). In the present study, the dynamic network properties of the default-mode network (DMN), cognitive control network (CCN), and the salience network (SN) were identified and assessed for any possible training-related reconfigurations in the chronnectome of these networks. The dynamic relationships among the DMN, CCN, and SN have received much attention in recent literature (Cocchi et al. 2014), and are thought to be engaged during MBT (Malinowski, 2013; Doll et al., 2015).

Training-specific changes in dFNC state dwell times

Consistent with previous studies examining the dynamic network patterns of DMN, SAL and CCNs (among other RSNs), there were connectivity states distinguished by a general positive dynamic connectivity pattern within the DMN network and a simultaneous antagonistic ("anti-correlation") between the DMN and the networks grouped within the CCN and SAL networks. In the present study, this distinct pattern of connectivity states was most apparent in state 1. Group comparisons on the amount of time spent in each state showed that the MBT+tDCS group spent more time in state 1

compared to the Cont+Sham group. This result suggest that increases in the amount of dwell time in states that are distinguished by inter-network interactions (i.e., dFNC) between the DMN and SAL and CCNs may reflect a stable change in states that correspond to a decoupling of the DMN and an improvement in focus-related processing.

Previous research has shown that the DMN is unique in that it reflects an intrinsic 'idling' of the brain that may be tightly coupled with attentional processes (Gusnard et al., 2001). The "coupling" between the dynamics of the DMN and attentional networks (e.g., frontal-parietal networks) can be described as the so-called anti-correlation between the two networks, which suggests distinct attentional processes (Fransson, 2005). Thus, it's hypothesized that the interplay between the DMN and task-related networks can significantly impact behavioral performance (Uddin et al., 2008). Furthermore, Hampson et al. (2006) reported that greater connectivity between the posterior cingulate and medial prefrontal nodes of the DMN correlated with better performance on a working memory task, suggesting that deactivation of a brain area may require increased (rather than decreased) connectivity with the DMN.

Consistent with our initial hypothesis ($H_{03.1.1}$), follow-up group comparisons on the cell nodes within state 1 revealed that the MBT+tDCS group exhibited increased *positive* dynamic connectivity between the precuneus RSN and bilateral inferior parietal RSN, and also between the "frontal" DMN and the right-lateralized frontal RSN. The observed increase in dynamic connectivity among the right-lateralized frontal RSN and the frontal node of the DMN may correspond to a readiness to regulate a cognitive

control network. Furthermore, the MBT+tDCS group showed *less antagonism* between the precuneus RSN and the right-lateralized frontal RSN, and between the posterior cingulate RSN and the bilateral inferior parietal RSN. This result may indicate more independence among the right frontal RSN and posterior That is, the observed increases in the amount of dwell time in states that are distinguished by inter-network interactions between the SAL network and the CCN, and a decrease in the dFNC among SAL and CCN and the DMN, indicating an enhancement of attentional control circuitry.

The current dFNC analysis also revealed connectivity states distinguish by less dynamic connectivity patterns within the DMN and more inter-grouping dynamic connectivity patterns; in particular, state 5 exhibited a mixture of positive and antagonistic connectivity patterns between the DMN and the SAL networks. Group comparisons showed that the MBT+tDCS group spent less time in state 5 compared to the Cont+Sham group. Furthermore, there was a significant correlation between dwell time in state 5 and the attention sub-score within the BIS, which was present only after training in the Cont+Sham group, but not in the MBT+tDCS group. The direction of this relationship may demonstrate that increases in the dynamic connectivity patterns that constitute state 5 may be predictive of attention related problems.

Follow-up comparisons on the cell nodes within state 5 revealed that the MBT+tDCS group showed increased positive dynamic connectivity between the precuneus RSN and the canonical "salience" RSN and the precuneus RSN and the bilateral inferior parietal RSN. Furthermore, the MBT+tDCS group also displayed a

decrease in positive dynamic connectivity between the precuneus RSN and the posterior cingulate RSN, the "frontal" DMN and the LH frontal–parietal network, and between the "salience" RSN and the right-lateralized frontal RSN. Both long-term meditators and individuals who have completed 2 weeks of mindfulness training show reduced activation of the default network (Brefczynski-Lewis et al., 2007; Brewer et al., 2011; Tang et al., 2009). Given that the default network has been repeatedly associated with markers of mind wandering (Christoff, Gordon, Smallwood, Smith, & Schooler, 2009; Mason et al., 2007), future research should directly test whether mindfulness training reduces mind wandering by dampening activation of the default network.

Post-training increase in dFNC state transitions

The current study also obtained the number of state transitions from one state to another and found that after training, the MBT+tDCS group increased the number of state transition occurrence compared to the Cont+Sham group, which is consistent with our initial hypothesis (i.e., $H_{03.1.3}$). This particular finding may indicate an enhancement in cognitive flexibility. A previous study comparing state transition in healthy controls compared to patients with schizophrenia found that patients made fewer state transitions compared to the control group (Rashid et al., 2014; Damaraju et al., 2014), suggesting a functional advantage for increased state transitions during the resting-state.

However, it is important to note that the post-training difference between groups was partly influenced by a decrease in state transitions within the Cont+Sham group. There have been no published studies to the author's knowledge that examined the

behavioral correlates of state transitions. To this end, the current study found that baseline state transitions were correlated with less endorsements of mind wandering and less concentration problems (sub-score of the BIS). However, these relationships were not observed after training in either group, suggesting change in variance resulting from training that the current metrics could not detect. Future studies are needed to examine the functional significance of an increase vs decrease in the number of state transitions before and after cognitive training and brain stimulation protocols.

CHAPTER 7: LIMITATIONS AND DELIMITATIONS

A limitation of this dissertation project is the recruitment inclusion criteria set forth by our funding agency, which included "high-functioning" individuals. Although this very specific sample may limit the generalizability of the current results to a more diverse population, it may have a direct application in the sample population studied: individuals who operate in potentially high-stress and challenging work environments. To this end, however, this limitation may also be a strength, as any enhancements observed within this "high-functioning" population – who presumably may be performing near ceiling for some of the tasks in this study, this same intervention may have an even larger effect on those with more room to improve their cognitive control abilities.

Another limitation is the collection of only two time points to assess neuroplastic changes due to training. An optimal design would include at least 3 to 4 time points to ascertain the incremental changes induced by the training. Also, although the performance measures obtained within this study are reliable and well-studied metrics of

cognitive control, they have limited ecological validity. Nonetheless, the WM measures used for this study have been associated with reading ability, GRE scores, and various other real-world metrics of cognitive ability outside the research laboratory. Nevertheless, future studies are needed to address this issue by including novel ways to collect such performance measures that overlap with tasks outside of the laboratory, or within other "real-world" contexts.

Lastly, another limitation of this study design is that it does not have the necessary group to test the additive effects of tDCS; that is, there was no group that received sham tDCS with mindfulness training. The reason for this limitation was outside of the experimenters control because the groups were selected from the larger MIRACLE study, which had its own time line and funding restrictions set forth by the funding agency. Nonetheless, the evaluation of the practical utility of this overall combined intervention effects is very useful for developing future studies that aim to examine the incremental effects produced by MBT or tDCS alone. To this end, the control training with sham tDCS group was chosen for this dissertation project as it serves as the best "baseline" group by which to compare the combined effects of MBT and active tDCS. Future studies should be conducted to assess the effects of active tDCS and MBT separately using similar (if not identical) methods proposed in this dissertation project.

CHAPTER 8: GENERAL CONCLUSIONS

The scope of this dissertation spans multiple domains. First is the feasibility and efficacy of a combined mindfulness training with tDCS intervention to enhance cognitive control abilities in a high-functioning population. Second is the assessment of analytical methods that could track the neuroplastic changes associated with any type of training intervention. Importantly, the methods developed within this dissertation project could then be used to guide future cognitive training studies assessing the combined effects of MBT with tDCS. Altogether, given the scope of this dissertation project, future studies can be developed to better understand the additive effects of tDCS on mindfulness practice, along with identifying the most optimal tDCS parameters (electrode montage, current intensity, and selection of frequency bands for alternating current, etc.) in various healthy and clinical populations.

To the author's knowledge, this is the first published work that examined the effects of a novel combined mindfulness-based training with right frontal tDCS intervention compared to an active control group with sham stimulation. Given that mindfulness practice stimulates and pushes one's core (domain-general) cognitive control capacity limits, tDCS was hypothesized to facilitate the ongoing neural patterns of functional connectivity toward long-lasting neuroplastic changes. The current study found an enhancement in working memory (WM) performance using a n-back task and the complex WM symmetry span task (S-span), suggesting a possible modification to the range of cognitive capacity limits. Furthermore, changes in the attention-sensitive P3

component and its theta oscillatory profiles revealed a pattern of results consistent with neural efficiency hypothesis within the right frontal and parietal sites. Furthermore, it is possible that right frontal (anodal) stimulation may bias an enhancement of lateralized WM ability, observed in the current study as enhanced right-hemispheric visuospatial WM activity and self-endorsements of improved attention and concentration.

In addition, training-induced alterations observed using event-related fMRI may be influenced by mechanisms that underlie a form of neural encoding and adaptation in domain-general, associative, and polymodal neural architecture, which may bridge the necessary connection from near to far transfer gains. Furthermore, training-related reconfigurations in the chronnectome of large-scale resting-state networks was observed and may reflect a stable change in states that correspond to a decoupling of the DMN and an improvement in focus-related processing.

Altogether, the assessment of cognitive control abilities and their corresponding brain patterns of activation using EEG and fMRI, along with individual differences on various personality traits and intrinsic connectivity, this dissertation study provided important contributions to the development of methods for conducting experiments on neural and cognitive plasticity. Advancements in this particular domain of research will ultimately guide future studies with the goal of tailoring a neuroplasticity-based interventions that maximize an individual's cognitive capacity, specifically by expanding his or her skill sets and abilities that can be transferred to various aspects of real-world cognition.

APPENDIX A: EXIT QUESTIONNAIRE

Appendix A contains a copy of the Exit Questionnaire developed by Michael Hunter, Vincent Clark, Katie Witkiewitz, and Greg Lieberman at the University of New Mexico. This survey was designed to collect information regarding the participant's experience on the effectiveness of the cognitive training and tDCS components in the study. Also, in order to ask evaluate far transfer from the participant's personal experience, this questionnaire ascertained data on the participant's level of confidence as to whether they experienced improvements in general aspects of daily living, e.g., college and work performance.

Two-sample t-tests were obtained to compare responses between groups, with the results displayed in Appendix A Table 1 (below). In short, the MBT+tDCS group rated the MBT portion of the study as effective in helping them perform better on the cognitive tests used in the study relative to the Cont+Sham group ($p = 0.02$). Furthermore, the MBT+tDCS reported higher levels of confidence in which they believed that the MBT+tDCS training improved general aspects of daily performance ($p = 0.02$). The confidence levels provided by each subject was summed to give an overall score of endorsed far transfer. Participant examples within the MBT+tDCS group included: "solve work tasks", "planning daily work tasks", "clarity in thought process", "concentration on school assignments", "attention span increased during class", "troubleshooting problems with equipment", "remember vocabulary in Japanese class", "breathe awareness", "remembering list when grocery shopping", "short-term memory retention", "pattern

recognition", "analyzing puzzles", "comprehension of new ideas during lectures and conversation", "improved overall sense of well-being", "self-awareness", "noticed mind wandering more", "less stress when driving", "calmer in stressful situations", etc.

Likewise, although our Cont+Sham protocol was used as an active "control" group, participants in this group also provided examples of general daily improvements in performance. Examples included: "retention of reading", "playing video games", "slightly quicker to come up with new ideas", "playing video games", "writing papers for school", and "focus with fewer breaks while working on a project".

The groups did not differ on ratings related to the effectiveness of tDCS on task performance, nor on ratings to whether participants' felt "smarter" after training. Further research is needed to further explore perceived benefits from a combined MBT and tDCS protocol.

Appendix A Table 1. Mean (SD) and corresponding statistics on Exit Questionnaire.

	Control+sham	**MBT+tDCS**	**Comparisons[a]**
Effectiveness of *training* on task performance	0.18 (2.7)	2.4 (1.6)	*t= 2.48, p = 0.02*
Effectiveness of *tDCS* on task performance	-0.1 (3.6)	0.36 (1.8)	*t= 0.43, p = 0.67*
Feel *"smarter"* after overall training	-0.45 (3.4)	0.21 (2.6)	*t= 0.55, p = 0.58*
Level of confidence that overall training improved aspects of *daily performance*	6.0 (7.8)	16.6 (13.2)	*t= 2.34, p = 0.03*

[a.] **Two-sample t-tests** were computed to test any differences between groups on numerical data obtained from the Exit Questionnaire.

EXIT QUESTIONNAIRE

SUBJECT ID_____ Date_____ RA_____

INSTRUCTIONS: Now that you have completed our study, we would like to ask you a few questions about your experience with the brain-training games or meditation, as well as your experience with tDCS. Please answer the questions below and do not hesitate to provide us with additional information about your thoughts and experience.

1.1). In your own words, how *effective* was the brain-training game play or meditation in helping you perform today's tasks?

1.2). Please circle the number that best reflects your opinion on the following statement:

"Based on my experience, the brain-training *game play or meditation was effective in helping me perform today's tasks."*

-5	-4	-3	-2	-1	0	1	2	3	4	5
Strongly Disagree					**Neutral No Opinion**					**Strongly Agree**

2.1). In your own words, how *effective* was tCS in helping you perform the brain-training games or meditation?

2.2). Using the scale provided, please circle the number that best reflects your opinion on the following statement:

"Based on my experience, brain stimulation was effective in helping me perform the training."

-5	-4	-3	-2	-1	0	1	2	3	4	5
Strongly Disagree					**Neutral No Opinion**					**Strongly Agree**

3.1). Do you feel any *smarter* now than before you enrolled into our study?

3.2). Using the scale provided, please circle the number that best reflects your opinion on the following statement:

"I feel smarter now than before I enrolled into the study".

-5	-4	-3	-2	-1	0	1	2	3	4	5
Strongly Disagree					**Neutral No Opinion**					**Strongly Agree**

4). If possible, please provide any specific examples (one per line in the spaces provided below) where you noticed *improvement* or *decline* in any aspect of your daily life, or work/school settings, which you believe were due or related to the brain-training games or meditation training, and rate how *confident* you

are in your improvement in each area on a scale from 0 to 10, with 0 being completely unsure and 10 being certain of your improvement.

WRITE SCALE NUMBER HERE

1. _____

2. _____

3. _____

4. _____

5. _____

6. _____

7. _____

---

5). If possible, please provide any specific or general comments or concerns you have regarding your experience with the brain-training games, meditation, and/or tDCS.

THANK YOU FOR COMPLETING OUR STUDY

APPENDIX B: SENSATION QUESTIONNAIRE

Appendix B contains a copy of the tDCS Sensation Questionnaire, which was developed in our lab and used in previous studies. This survey was designed to collect information regarding the participant's sensation during and after the application of tDCS. In particular, participants were asked to describe their physical sensations at approximately 1, 5, and 30 minutes after the start of tDCS to monitor participant ratings for itching, tingling, and heat/burning on a 10-point Likert scale (see below). Note: in order to avoid interrupting the MBT session, sensation data were acquired only at the first and last time points for the MBT+tDCS group.

Results comparing sensation ratings collapsed across the 8 tDCS sessions are reported in Appendix B Figure 1. In short, repeated measures ANOVA showed that there were no statistically significant differences between groups on any of the sensation ratings.

Appendix B. Figure 1: Mean, SE and statistical comparisons on tDCS sensations collapsed across sessions.

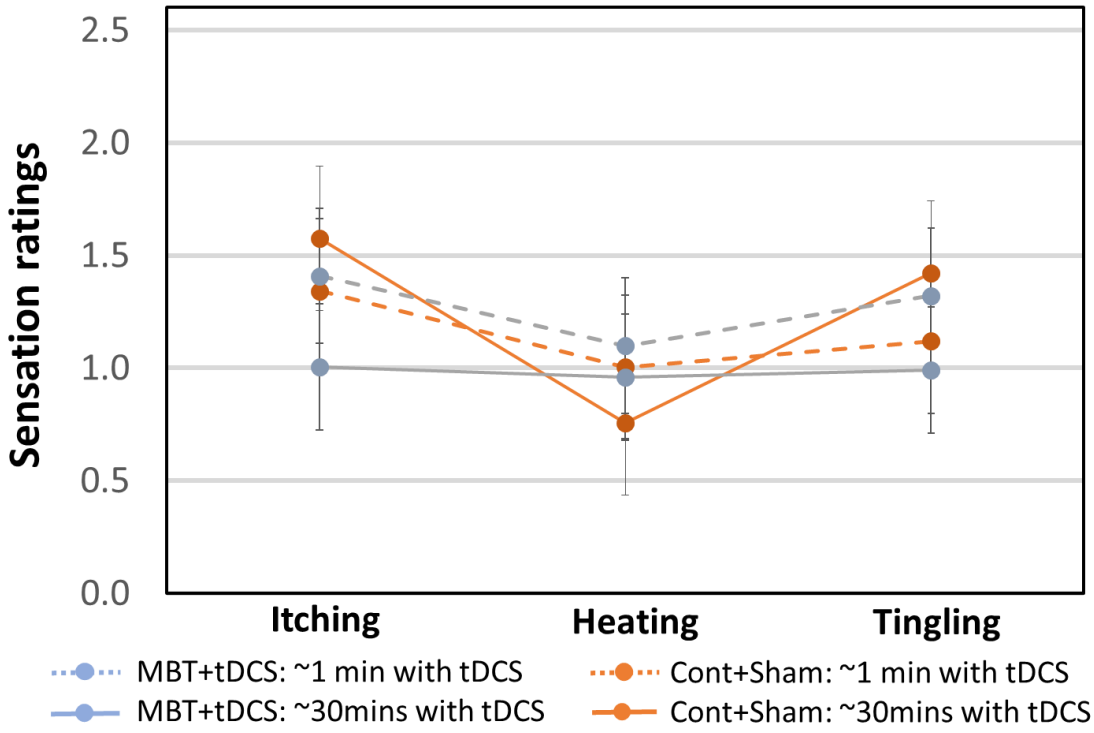

Mean sensation ratings averaged across all tDCS sessions at ~1 minute after tDCS was "turned on" and again after the tDCS session, which was ~30 mins. The sensation rating scale ranged from 0-10, where 0 indicates no sensation and 10 the most extreme. There were no statistical differences observed between groups (*p's* > 0.10).

In order to examine sensation ratings across all sessions within the MBT+tDCS group only, Appendix B Figure 2 displays the mean, SE and within-subject statistical comparisons on sensation ratings. In short, there were no statistical differences observed across sessions.

Appendix B. Figure 2: Mean, SE and statistical comparisons at each of the tDCS sensations within the MBT+tDCS group.

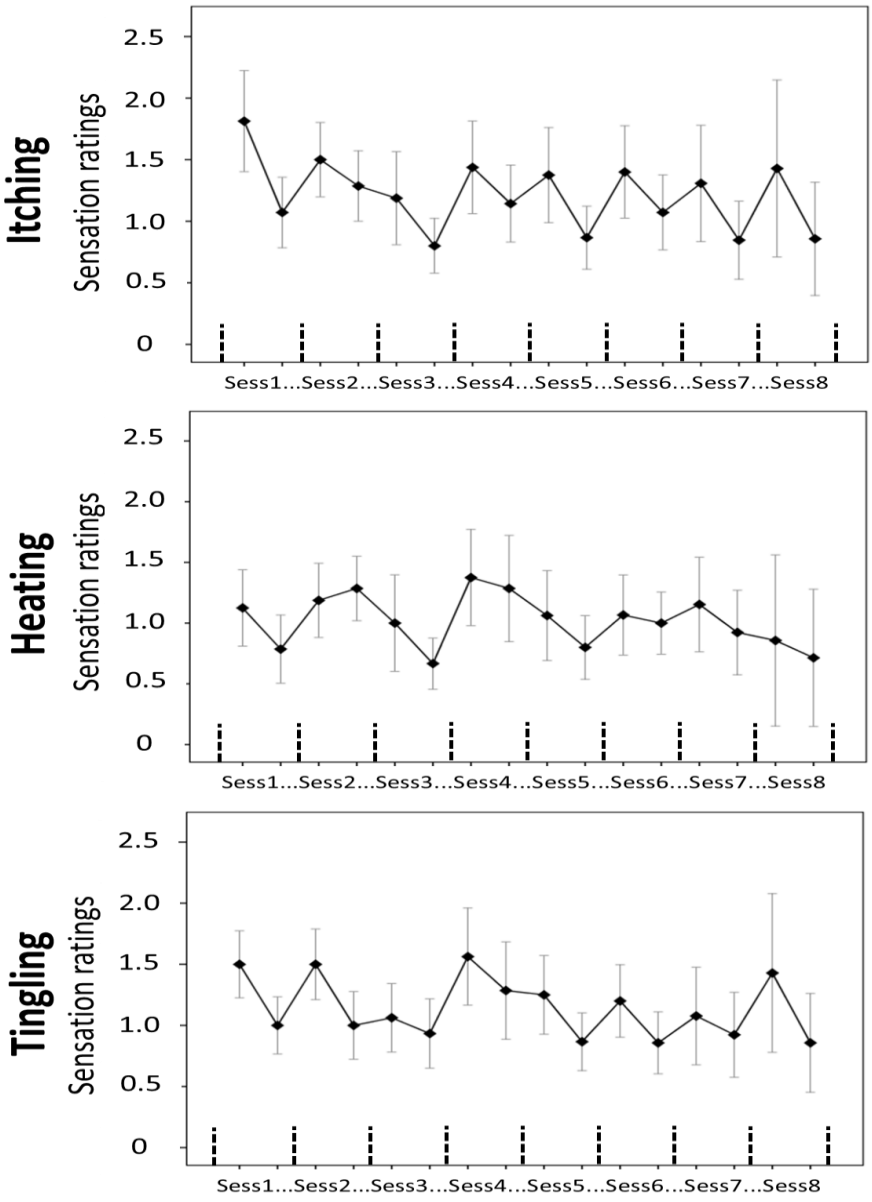

For the MBT+tDCS group, there were 2 time points at which sensation data were acquired within each tDCS session: 1st data point was acquired ~1 minute with tDCS and the 2nd after training (~30 mins with tDCS). Note: the sensation rating scale ranged from 0-10, where 0 indicates no sensation and 10 is the most extreme. Within-subject comparisons showed no differences across sessions (*p's* > 0.26).

In order to examine sensation ratings across all sessions within the Cont+Sham group only, Appendix B Figure 3 displays the mean, SE and within-subject statistical comparisons on sensation ratings. In short, within-subject comparisons showed that across sessions there was an overall difference in ratings for itching only (p=0.04), with the largest difference between session 1 and 2.

Appendix B Fig 3. Mean, SE and statistical comparisons at each of the tDCS sensations within the Cont+Sham group.

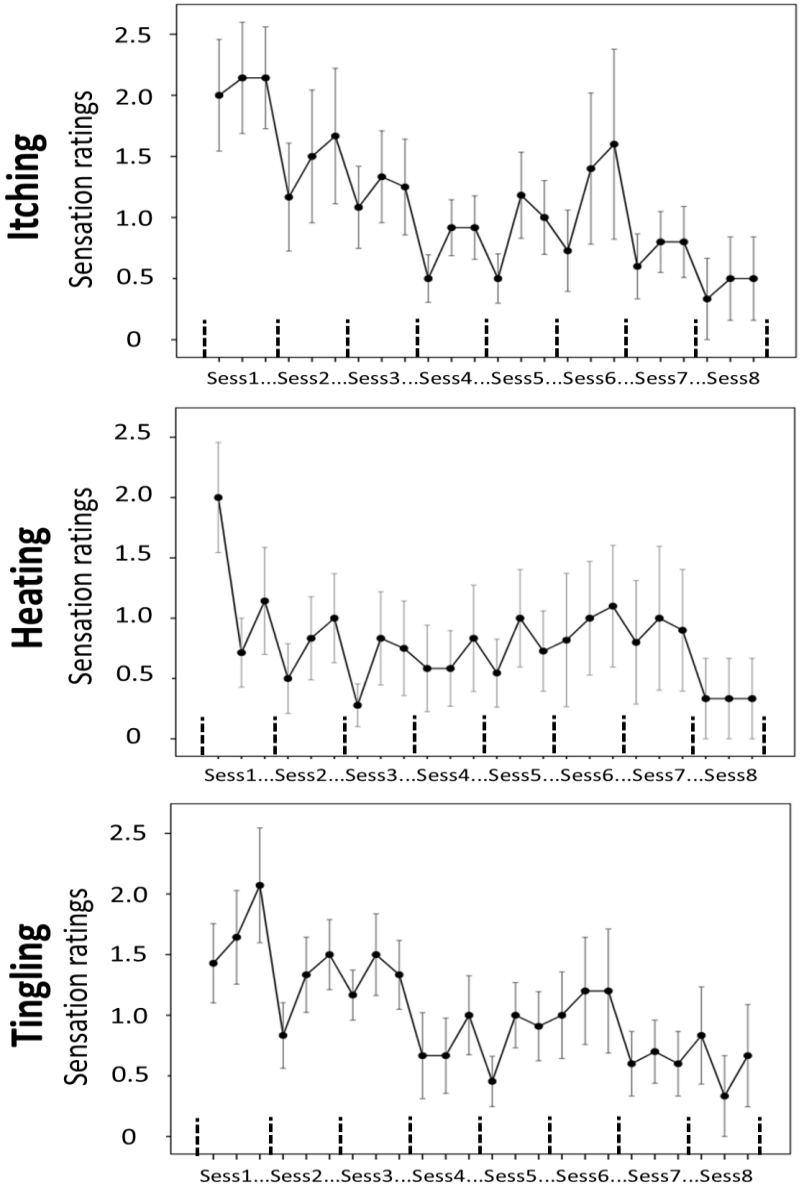

For the Cont+Sham group, there were 3 time points at which sensation data were acquired within each tDCS session: 1st data point was acquired ~1 minute after "stimulation", 2nd after 5 minutes, and the 3rd at the very end of the tDCS session (~30 mins with sham tDCS). Within-subject comparisons showed that across sessions there was an overall difference in ratings for itching only (p=0.04), with the largest difference between session 1 and 2.

URSI_____________________ Date_____________ RA________________

tCS Sensation Questionnaire

cle the number which best describes what you are feeling for the following descriptors using the following scale:

SCALE

0	1	2	3	4	5	6	7	8	9	10
None					**Moderate**					**Excessive**

Circle the number that best describes what you are feeling for the following descriptors:

Itching

0	1	2	3	4	5	6	7	8	9	10

Heat/Burning

0	1	2	3	4	5	6	7	8	9	10

Tingling

0	1	2	3	4	5	6	7	8	9	10

Other Sensations you are feeling:

____

Time Point____ Time____________

Circle the number that best describes what you are feeling for the following descriptors:

Itching

0	1	2	3	4	5	6	7	8	9	10

Heat/Burning

0	1	2	3	4	5	6	7	8	9	10

Tingling

0	1	2	3	4	5	6	7	8	9	10

Other Sensations you are feeling:

____

Time Point____ Time____________

Circle the number that best describes what you are feeling for the following descriptors:

Itching

0	1	2	3	4	5	6	7	8	9	10

Heat/Burning

0	1	2	3	4	5	6	7	8	9	10

Tingling

0	1	2	3	4	5	6	7	8	9	10

Other Sensations you are feeling:

____

Time Point____ Time____________

APPENDIX C: COMPARISONS OF RE-REFERENCING METHODS

Given that structure of EEG data depends on the reference electrode, which affects voltages, power amplitudes and phase angels (Yuval-Greenburg et al., 2008; Michel, 2009), the average-referenced EEG n-back data was compared to scalp distributions using a mastoid reference (the average between left and right electrodes over each mastoid bone). The ERP waveforms corresponding to the pre-defined electrode locations (Pz, Fz, and F10) are displayed in Appendix Figure 1 (below).

Appendix C: Figure 1. Baseline group-level ERP waveforms for Pz, Fz, and F10 as a function of working memory load (target hits) for each re-referencing method.

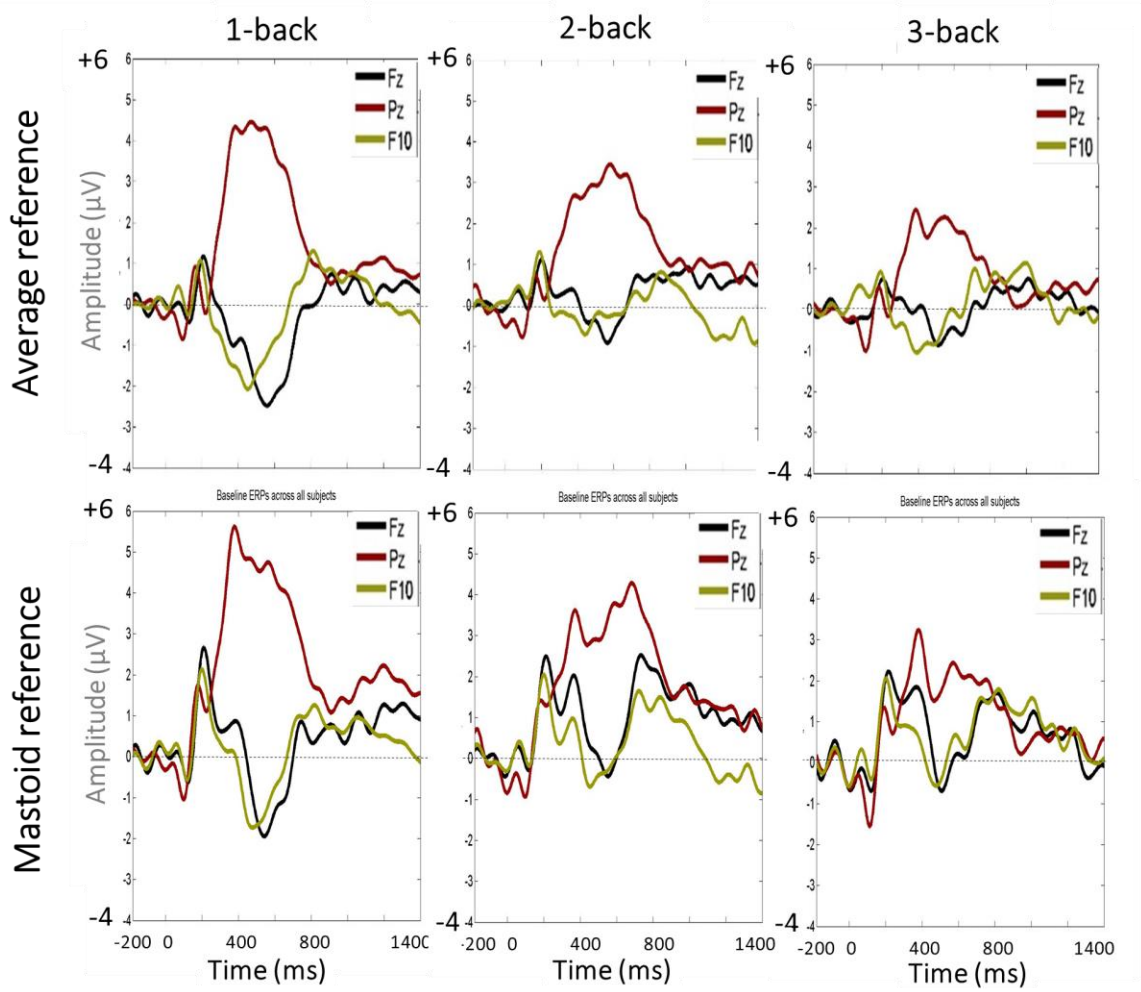

Comparison between re-referencing methods. Top row: EEG scalp distribution re-referenced using average of scalp electrodes. Bottom row: data re-referenced using average of left and right mastoids. Electrode-specific P3 activity was averaged between 350 – 650 ms. Compared to the average-reference data, the mastoid-referenced data showed subtle qualitative differences in the shape of the waveforms but were statistically non-significant in amplitude across all three electrode locations. Appendix C: Figure 3 displays the means and statistical comparisons between these two re-referencing methods.

In short, compared to the average-reference data, the mastoid-referenced data showed subtle qualitative differences in the shape of the waveforms. Similar results can be inferred for the entire scalp topology, which is shown in Appendix Figure 2 (below).

Appendix C: Figure 2: Baseline group-level ERPs and mean P3 topology as a function of working memory load for each re-referencing method.

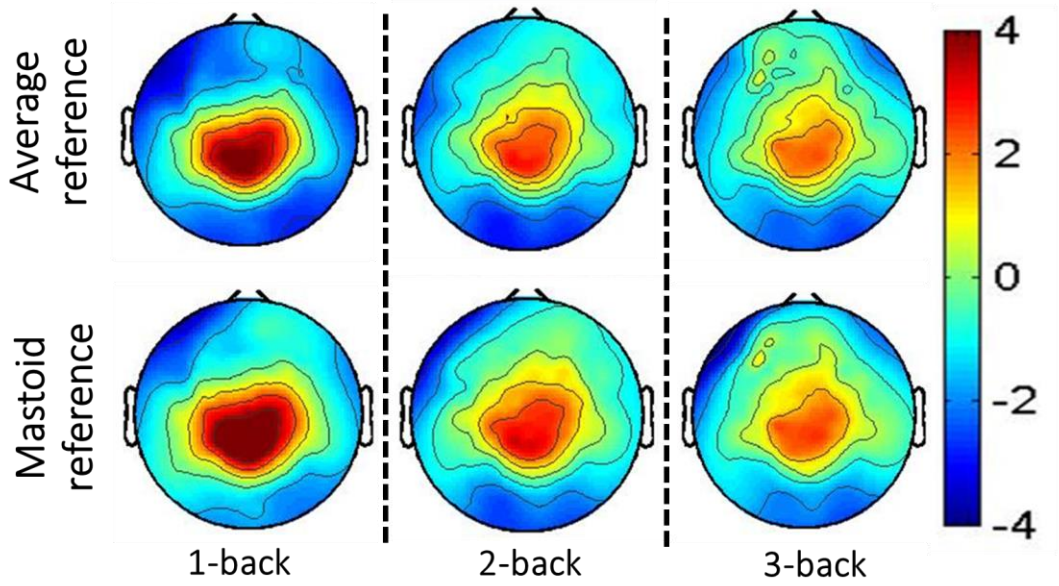

Comparison between re-referencing methods on scalp topology. Top row: EEG scalp distribution re-referenced using average of all scalp electrodes. Bottom row: data re-referenced using average of left and right mastoids. P3 activity was averaged between 350 – 650 ms. Compared to the average-reference data, the mastoid-referenced data showed subtle broad increases in the frontal electrodes, but these differences were statistically non-significant for Fz and F10. Appendix C: Figure 3 displays the means and statistical comparisons between these two re-referencing methods for Pz, Fz, and F10 electrode sites.

Finally, for the time-domain data, Appendix C Figure 3 displays the means and statistical comparisons between the two re-referencing methods.

Appendix C: Figure 3. Baseline mean, SE and statistical comparisons of P3 amplitude for all WM load conditions and electrode sites of interest at baseline (n = 29) for each re-referencing method.

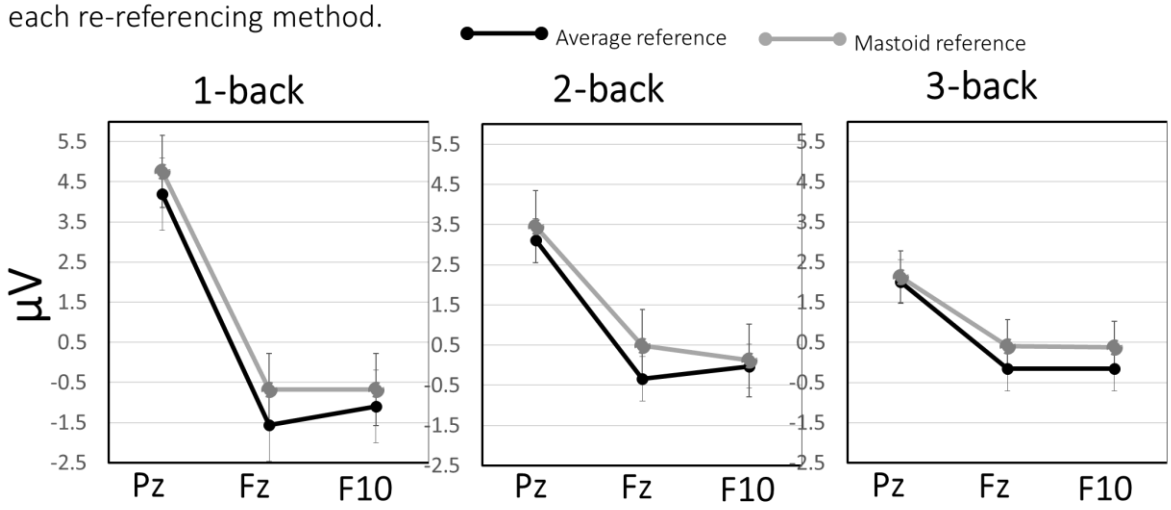

Pair-wise within-subject comparisons showed no statistically significant differences between re-referencing methods in electrode locations across any of the n-back conditions (*p's* > 0.14). Average-referenced data are represented by black bold lines and mastoid-referenced data by gray solid lines for each WM load condition. P3 activity was computed as the average between 350 – 650 ms.

Although the average-reference data showed subtle qualitative differences in the shape of the waveforms compared to the mastoid-referenced data, there were no statistically significant differences in amplitude across all WM load conditions and the three electrode locations (*p's* > 0.14).

Comparisons between re-referencing methods for the frequency-domain data are shown as time-frequency maps displayed in Appendix Figure 4 (below)

Appendix C: Figure 4. Comparison between referencing method on baseline group-level sustained theta power time-frequency maps for each n-back condition and electrode site of interest.

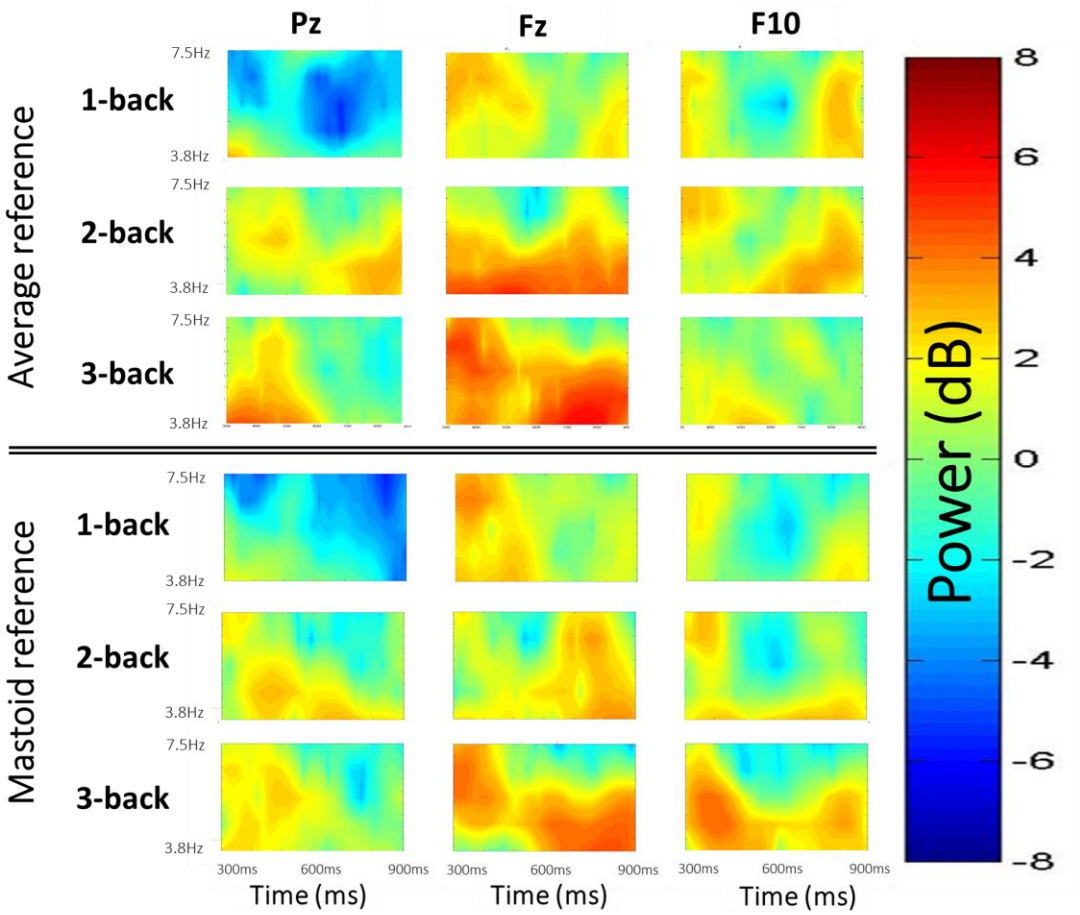

Comparisons between re-referencing methods on power (dB) in the sustained P3 power range (300 – 900 ms). Top 3 rows: Average-referenced time-frequency maps for each WM load condition (1-3). Bottom 3 row: Mastoid-referenced time-frequency maps. Theta power (3.8 – 7.5 H, log spaced) was decibel scaled, baseline corrected from -200 to 0 ms. Compared to the average-reference data, the mastoid-referenced data showed a broad decrease in power across all WM load conditions. However, these differences were statistically non-significant. Appendix C: Figure 5 displays the means and statistical comparisons between these two re-referencing methods.

The time-frequency maps also showed qualitative differences between re-referencing methods. However, as displayed in Appendix Figure 5, within-subject comparisons showed that these subtle mean differences in the P3 range were statistically non-significant (*p's* > 0.24).

Appendix C: Figure 5. Baseline mean, SE and statistical comparisons of power (P3 range) for all WM load conditions and electrode sites of interest at baseline (n = 29) for each re-referencing method.

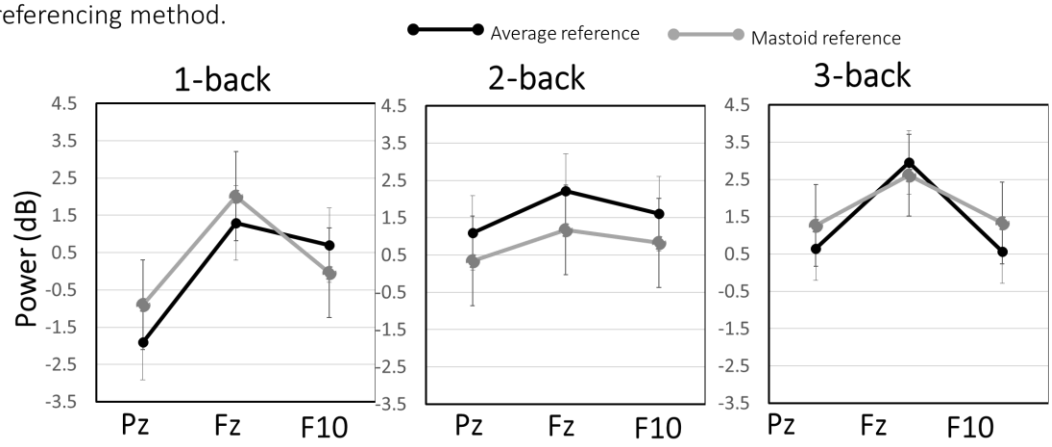

Pair-wise within-subject comparisons showed no statistically significant differences in power between re-referencing methods in electrode locations across any of the n-back conditions (*p's* > 0.19). Average-referenced data are represented by black bold lines and mastoid-referenced data by gray solid lines for each WM load condition and electrode site. Sustained P3 theta (3.8 – 7.5 Hz) power was averaged between 300 and 900 ms and was decibel scaled, baseline corrected from -200 to 0 ms.

Overall, it is important to note that although the potential values, phase, and power amplitudes at the electrodes change based on the pre-selected re-referencing procedure, the potential differences *between electrodes* are not affected because this mathematical transformation is linear across electrodes (Michel, 2009; Cohen, 2014; Luck, 2014). Accordingly, the same (average) re-referencing procedure was implemented on both time- and frequency-domain data in all reported data.

APPENDIX D: MINDFULNESS TRAINING FAQs HANDOUT

FREQUENTLY ASKED QUESTIONS

What is meditation?
Meditation is the act of focusing your attention on a specific object. It is a practice anyone can do. There are many ways to meditate.

What is mindfulness?
Mindfulness is the ability to bring full awareness to the present moment. It means to be attentive and conscious about what's happening - to be aware.

What are the benefits of practicing mindfulness?
The benefits are numerous. Studies have shown that people who regularly practice mindfulness have experienced

- improved health and overall quality of life
- reduction in anxiety and depression
- increased concentration, and:
- a stronger ability to cope more effectively with stress in daily life.

Health benefits include enhanced immune function, improved blood pressure and healthier cardiac functioning. Studies also show people who practice mindfulness have increased motivation to make lifestyle changes, decreased perception of pain and increased ability to tolerate pain.

Do I have to stop my thoughts?
No, but that is a common misconception. People often think that meditating correctly means clearing all thought from the mind. We are not trying to stop or control our thoughts, we're simply noticing them. It's when we get caught up in those thoughts that we lose mindfulness.

Why is daily practice important?
Recent research shows that regular practice reshapes the brain, which changes how we respond to and perceive situations that are difficult or stressful. And, as with any lifestyle change, it requires consistent practice to gain results.

No time to practice?
You can work mindfulness into your daily life in an informal way (such as by walking from your car to the store or waiting in line) by simply being mindful of your thoughts, emotions and body sensations.

Where should I meditate?
You can practice mindfulness almost anywhere. It is ideal to create a supportive environment for practice, one that is comfortable, quiet and uncluttered.

What if I am a skeptic?
Skepticism is a great place to start. Mindfulness is a practice where you test ideas and techniques for yourself and notice results. Try it for a while. As with many changes, such as exercising regularly and eating healthier, it requires some degree of patience and the benefits of practice continue to build over time.

Is mindfulness a religion?
No, mindfulness is not a system of beliefs. It is a practice that brings full awareness to the present moment.

How should I sit in meditation?

There are two important principles that you need to bear in mind in setting up a suitable posture for meditation.

- your posture has to allow you to relax and to be comfortable.
- your posture has to allow you to remain alert and aware.

Both of these are vitally important. If you're uncomfortable you'll not be able to meditate because of discomfort. If you can't relax then you won't be able to enjoy the meditation practice and, just as importantly, you won't be able to let go of the underlying emotional conflicts that cause your physical tension.

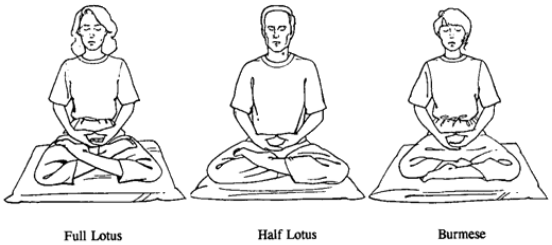

Full Lotus Half Lotus Burmese

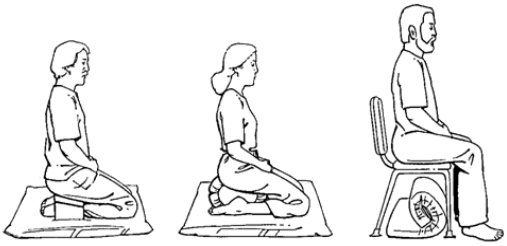

On a stool Sciza On a Chair

Many people who experience back and/or knee pain find that sitting in a chair is the most comfortable position. Others with back pain find that kneeling on a cushion or pillow (the "Seiza" position in the picture) is most comfortable.

If sitting in a chair, it is easier to stay upright and alert on a chair if you sit closer to the front edge and hold your own spine up instead of leaning against the chair back. If you sit with your pelvis against the back of the chair, you can use a cushion behind you to help keep your back straight. The hips should be slightly higher than the knees, this keeps you from slouching. It helps to keep feet flat on the floor. You can use a cushion under the feet if shorter, or under the buttocks if taller.

REFERENCES

Alexander, G. E., Crutcher, M. D., & DeLong, M. R. (1990). Basal ganglia-thalamocortical circuits: parallel substrates for motor, oculomotor, "prefrontal" and "limbic" functions. *Progress in Brain Research*, *85*, 119–146.

Allen, E. A., Damaraju, E., Plis, S. M., Erhardt, E. B., Eichele, T., & Calhoun, V. D. (2012). Tracking Whole-Brain Connectivity Dynamics in the Resting State. Cerebral Cortex, bhs352.

Anicha, C. L., Ode, S., Moeller, S. K., & Robinson, M. D. (2012). Toward a cognitive view of trait mindfulness: distinct cognitive skills predict its observing and nonreactivity facets. Journal of Personality, 80(2), 255–285.

Avila, E., van der Geest, J. N., Kengne Kamga, S., Verhage, M. C., Donchin, O., Frens, M. A., … Frens, M. A. (2015). Cerebellar Transcranial Direct Current Stimulation Effects on Saccade Adaptation, Cerebellar Transcranial Direct Current Stimulation Effects on Saccade Adaptation. *Neural Plasticity, Neural Plasticity*, *2015*, *2015*, e968970.

Baer, R. A., Smith, G. T., Hopkins, J., Krietemeyer, J., & Toney, L. (2006). Using self-report assessment methods to explore facets of mindfulness. Assessment, 13(1), 27–45.

Baijal, S., & Srinivasan, N. (2009). Theta activity and meditative states: spectral changes during concentrative meditation. Cognitive Processing, 11(1), 31–38.

Barriga-Paulino, C. I., Rodríguez-Martínez, E. I., Rojas-Benjumea, M. Á., & Gómez, C. M. (2014). Slow wave maturation on a visual working memory task. Brain and Cognition, 88, 43–54.

Barry, R. J., Clarke, A. R., McCarthy, R., & Selikowitz, M. (2002). EEG coherence in attention-deficit/hyperactivity disorder: a comparative study of two DSM-IV types. Clinical Neurophysiology: Official Journal of the International Federation of Clinical Neurophysiology, 113(4), 579–585.

Ben-Soussan, T. D., Glicksohn, J., Berkovich-Ohana, A., Ben-Soussan, T. D., Glicksohn, J., & Berkovich-Ohana, A. (2015). From Cerebellar Activation and Connectivity to Cognition: A Review of the Quadrato Motor Training. *BioMed Research International, BioMed Research International*, *2015, 2015*, e954901.

Berka, C., Levendowski, D. J., Lumicao, M. N., Yau, A., Davis, G., Zivkovic, V. T., … Craven, P. L. (2007). EEG Correlates of Task Engagement and Mental Workload in Vigilance, Learning, and Memory Tasks. Aviation, Space, and Environmental Medicine, 78(5), B231–B244.

Bikson, M., Rahman, A., Datta, A., Fregni, F., & Merabet, L. (2012). High-resolution Modeling Assisted Design of Customized and Individualized Transcranial Direct Current Stimulation Protocols. Neuromodulation : Journal of the International Neuromodulation Society, 15(4), 306–315.

Biswal, B., Zerrin Yetkin, F., Haughton, V. M., & Hyde, J. S. (1995). Functional connectivity in the motor cortex of resting human brain using echo-planar mri. Magnetic resonance in medicine, 34 (4), 537–541.

Blais, C., Stefanidi, A., & Brewer, G. A. (2014). The Gratton effect remains after controlling for contingencies and stimulus repetitions. Frontiers in Psychology, 5.

Bledowski, C., Prvulovic, D., Hoechstetter, K., Scherg, M., Wibral, M., Goebel, R., & Linden, D. E. J. (2004). Localizing P300 generators in visual target and distractor processing: a combined event-related potential and functional magnetic resonance imaging study. The Journal of Neuroscience: The Official Journal of the Society for Neuroscience, 24(42), 9353–9360.

Borghini, G., Astolfi, L., Vecchiato, G., Mattia, D., & Babiloni, F. (2014). Measuring neurophysiological signals in aircraft pilots and car drivers for the assessment of mental workload, fatigue and drowsiness. Neuroscience and Biobehavioral Reviews, 44, 58–75.

Braver, T. S. (2012). The variable nature of cognitive control: a dual mechanisms framework. Trends in Cognitive Sciences, 16(2), 106–113.

Bridwell, D. A., Wu, L., Eichele, T., & Calhoun, V. D. (2013). The spatiospectral characterization of brain networks: Fusing concurrent EEG spectra and fMRI maps. NeuroImage, 69, 101–111.

Brink, R. L., Wynn, S. C., & Nieuwenhuis, S. (2014). Post-Error Slowing as a Consequence of Disturbed Low-Frequency Oscillatory Phase Entrainment. The Journal of Neuroscience, 34(33), 11096–11105.

Brown, K. W., & Ryan, R. M. (2003). The benefits of being present: mindfulness and its role in psychological well-being. Journal of Personality and Social Psychology, 84(4), 822–848.

Brunoni, A. R., & Vanderhasselt, M.-A. (2014). Working memory improvement with non-invasive brain stimulation of the dorsolateral prefrontal cortex: a systematic review and meta-analysis. Brain and Cognition, 86, 1–9.

Bürki, C. N., Ludwig, C., Chicherio, C., & de Ribaupierre, A. (2014). Individual differences in cognitive plasticity: an investigation of training curves in younger and older adults. Psychological Research, 78(6), 821–835.

Buzsáki, G., & Draguhn, A. (2004). Neuronal Oscillations in Cortical Networks. Science, 304(5679), 1926–1929.

Cabeza, R., & Nyberg, L. (2000). Imaging Cognition II: An Empirical Review of 275 PET and fMRI Studies. Journal of Cognitive Neuroscience, 12(1), 1–47.

Cahn, B. R., & Polich, J. (2006). Meditation states and traits: EEG, ERP, and neuroimaging studies. Psychological Bulletin, 132(2), 180–211.

Cahn, B. R., & Polich, J. (2009). Meditation (Vipassana) and the P3a event-related brain potential. International Journal of Psychophysiology, 72(1), 51–60.

Cahn, B. R., Delorme, A., & Polich, J. (2013). Event-related delta, theta, alpha and gamma correlates to auditory oddball processing during Vipassana meditation. Social Cognitive and Affective Neuroscience, 8(1), 100–111.

Calhoun, V. D., Adali, T., Pearlson, G. D., & Kiehl, K. A. (2006). Neuronal chronometry of target detection: Fusion of hemodynamic and event-related potential data. NeuroImage, 30(2), 544–553.

Calhoun, V. D., Adali, T., Pearlson, G. D., & Pekar, J. J. (2001). A method for making group inferences from functional MRI data using independent component analysis. Human brain mapping, 14(3), 140–151.

Calhoun, V. D., Miller, R., Pearlson, G., & Adalı, T. (2014). The Chronnectome: Time-Varying Connectivity Networks as the Next Frontier in fMRI Data Discovery. *Neuron*, *84*(2), 262–274.

Carter, C. S., & van Veen, V. (2007). Anterior cingulate cortex and conflict detection: An update of theory and data. Cognitive, Affective, & Behavioral Neuroscience, 7(4), 367–379.

Carter, C. S., Braver, T. S., Barch, D. M., Botvinick, M. M., Noll, D., & Cohen, J. D. (1998). Anterior cingulate cortex, error detection, and the online monitoring of performance. Science (New York, N.Y.), 280(5364), 747–749.

Cattell, R. B. (1963). Theory of fluid and crystallized intelligence: A critical experiment. Journal of Educational Psychology, 54(1), 1–22.

Cavanagh, J. F., & Frank, M. J. (2014). Frontal theta as a mechanism for cognitive control. Trends in Cognitive Sciences, 18(8), 414–421.

Cavanagh, J. F., Cohen, M. X., & Allen, J. J. B. (2009). Prelude to and Resolution of an Error: EEG Phase Synchrony Reveals Cognitive Control Dynamics during Action Monitoring. The Journal of Neuroscience, 29(1), 98–105.

Chan, D., & Woollacott, M. (2007). Effects of Level of Meditation Experience on Attentional Focus: Is the Efficiency of Executive or Orientation Networks Improved? The Journal of Alternative and Complementary Medicine, 13(6), 651–658.

Chapman, S. B., Aslan, S., Spence, J. S., Hart, J. J., Bartz, E. K., Didehbani, N., … Lu, H. (2013). Neural Mechanisms of Brain Plasticity with Complex Cognitive Training in Healthy Seniors. Cerebral Cortex, bht234. http://doi.org/10.1093/cercor/bht234

Chein, J. M., & Morrison, A. B. (2010). Expanding the mind's workspace: Training and transfer effects with a complex working memory span task. Psychonomic Bulletin & Review, 17(2), 193–199.

Chen et al. Vertes, R. P., & Jr, R. W. S. (Eds.). (2011). Current Source Density Analysis of Ongoing Neural Activity: Theory and Application - Springer. Humana Press.

Cheyne, J. A., Carriere, J. S. A., & Smilek, D. (2006). Absent-mindedness: Lapses of conscious awareness and everyday cognitive failures. Consciousness and Cognition, 15(3), 578–592.

Chiesa, A., Serretti, A., & Jakobsen, J. C. (2013). Mindfulness: top-down or bottom-up emotion regulation strategy? Clinical Psychology Review, 33(1), 82–96.

Chow, M., & Conway, A. R. A. (2015). The scope and control of attention: Sources of variance in working memory capacity. Memory & Cognition.

Cicchetti, D., & Blender, J. A. (2006). A Multiple-Levels-of-Analysis Perspective on Resilience. Annals of the New York Academy of Sciences, 1094(1), 248–258.

Cieslik, E. C., Zilles, K., Caspers, S., Roski, C., Kellermann, T. S., Jakobs, O., … Eickhoff, S. B. (2013). Is There "One" DLPFC in Cognitive Action Control? Evidence for Heterogeneity From Co-Activation-Based Parcellation. Cerebral Cortex, 23(11), 2677–2689.

Clark, V. P., & Parasuraman, R. (2014). Neuroenhancement: Enhancing brain and mind in health and in disease. NeuroImage, 85, Part 3, 889–894.

Clark, V. P., Coffman, B. A., Mayer, A. R., Weisend, M. P., Lane, T. D. R., Calhoun, V. D., … Wassermann, E. M. (2012). TDCS guided using fMRI significantly accelerates learning to identify concealed objects. NeuroImage, 59(1), 117–128.

Clark, V. P., Fannon, S., Lai, S., Benson, R., & Bauer, L. (2000). Responses to Rare Visual Target and Distractor Stimuli Using Event-Related fMRI. Journal of Neurophysiology, 83(5), 3133–3139.

Clemens, B., Jung, S., Mingoia, G., Weyer, D., Domahs, F., & Willmes, K. (2014). Influence of Anodal Transcranial Direct Current Stimulation (tDCS) over the Right Angular Gyrus on Brain Activity during Rest. *PLoS ONE*, *9*(4), e95984.

Cocchi, L., Halford, G. S., Zalesky, A., Harding, I. H., Ramm, B. J., Cutmore, T., … Mattingley, J. B. (2014). Complexity in relational processing predicts changes in functional brain network dynamics. Cerebral Cortex (New York, N.Y.: 1991), 24(9), 2283–2296.

Cohen, J. D., Aston-jones, G., & Gilzenrat, M. S. (2004). A systems-level perspective on attention and cognitive control: Guided activation, adaptive gating, conflict monitoring, and exploitation vs. exploration, chapter 6. In M. I. Posner (Ed.), Cognitive, 71–90.

Cohen, M. X., & Cavanagh, J. F. (2011). Single-Trial Regression Elucidates the Role of Prefrontal Theta Oscillations in Response Conflict. Frontiers in Psychology, 2. http://doi.org/10.3389/fpsyg.2011.00030

Cohen, M. X., & Donner, T. H. (2013). Midfrontal conflict-related theta-band power reflects neural oscillations that predict behavior. Journal of Neurophysiology, 110(12), 2752–2763.

Cohen, M.X. (2014). Analyzing Neural Time Series Data: Theory and Practice. Cambridge: MIT Press.

Colom, R., Román, F. J., Abad, F. J., Shih, P. C., Privado, J., Froufe, M., … Jaeggi, S. M. (2013). Adaptive n-back training does not improve fluid intelligence at the construct level: Gains on individual tests suggest that training may enhance visuospatial processing. Intelligence, 41(5), 712–727.

Colzato, L. S., Sellaro, R., Samara, I., & Hommel, B. (2015). Meditation-induced cognitive-control states regulate response-conflict adaptation: Evidence from trial-to-trial adjustments in the Simon task. Consciousness and Cognition, 35, 110–114.

Corbetta, M., & Shulman, G. L. (2002). Control of goal-directed and stimulus-driven attention in the brain. Nature Reviews Neuroscience, 3(3), 201–215.

Cormier, S.M., and Hagman, J.D. (1987). The transfer of learning: contemporary research and applications. New York: Academic Press; Singley, M.K., and Anderson, J.R.

Cowan, N., Elliott, E. M., Scott Saults, J., Morey, C. C., Mattox, S., Hismjatullina, A., & Conway, A. R. A. (2005). On the capacity of attention: its estimation and its role in working memory and cognitive aptitudes. Cognitive Psychology, 51(1), 42–100.

Crespo-Garcia, M., Pinal, D., Cantero, J. L., Díaz, F., Zurrón, M., & Atienza, M. (2013). Working memory processes are mediated by local and long-range synchronization of alpha oscillations. Journal of Cognitive Neuroscience, 25(8), 1343–1357.

Damaraju, E., Allen, E. A., Belger, A., Ford, J. M., McEwen, S., Mathalon, D. H., … Calhoun, V. D. (2014). Dynamic functional connectivity analysis reveals transient states of dysconnectivity in schizophrenia. NeuroImage : Clinical, 5, 298–308.

Damoiseaux, J. S., Rombouts, S. a. R. B., Barkhof, F., Scheltens, P., Stam, C. J., Smith, S. M., & Beckmann, C. F. (2006). Consistent resting-state networks across healthy subjects. Proceedings of the National Academy of Sciences, 103(37), 13848–13853.

De Vibe, M., Solhaug, I., Tyssen, R., Friborg, O., Rosenvinge, J. H., Sørlie, T., … Bjørndal, A. (2015). Does Personality Moderate the Effects of Mindfulness Training for Medical and Psychology Students? Mindfulness, 6(2), 281–289.

Deary, I. J., Penke, L., & Johnson, W. (2010). The neuroscience of human intelligence differences. Nature Reviews Neuroscience, 11(3), 201–211.

Di Fabio, A., & Palazzeschi, L. (2009). An in-depth look at scholastic success: Fluid intelligence, personality traits or emotional intelligence? Personality and Individual Differences, 46(5–6), 581–585.

Dieckhöfer, A., Waberski, T. D., Nitsche, M., Paulus, W., Buchner, H., & Gobbelé, R. (2006). Transcranial direct current stimulation applied over the somatosensory cortex – Differential effect on low and high frequency SEPs. Clinical Neurophysiology, 117(10), 2221–2227.

Doll, A., Hölzel, B. K., Boucard, C. C., Wohlschläger, A. M., & Sorg, C. (2015). Mindfulness is associated with intrinsic functional connectivity between default mode and salience networks. Frontiers in Human Neuroscience, 461.

Dosenbach, N. U. F., Fair, D. A., Cohen, A. L., Schlaggar, B. L., & Petersen, S. E. (2008). A dual-networks architecture of top-down control. Trends in Cognitive Sciences, 12(3), 99–105.

Drew, T. W., McCollough, A. W., & Vogel, E. K. (2006). Event-related potential measures of visual working memory. Clinical EEG and Neuroscience, 37(4), 286–291.

Driel, J., Ridderinkhof, K. R., & Cohen, M. X. (2012). Not All Errors Are Alike: Theta and Alpha EEG Dynamics Relate to Differences in Error-Processing Dynamics. The Journal of Neuroscience, 32(47), 16795–16806.

Engle, R. (2003). Executive Attention, Working Memory Capacity, and a Two-Factor Theory of Cognitive Control. Psychology of Learning and Motivation, 44, 145–199.

Enriquez-Geppert, S., Huster, R. J., & Herrmann, C. S. (2013). Boosting brain functions: Improving executive functions with behavioral training, neurostimulation, and neurofeedback. International Journal of Psychophysiology: Official Journal of the International Organization of Psychophysiology, 88(1), 1–16.

Farb, N. A. S., Segal, Z. V., Mayberg, H., Bean, J., McKeon, D., Fatima, Z., & Anderson, A. K. (2007). Attending to the present: mindfulness meditation reveals distinct neural modes of self-reference. Social Cognitive and Affective Neuroscience.

Fehr, T. (2013). A hybrid model for the neural representation of complex mental processing in the human brain. *Cognitive Neurodynamics*, *7*(2), 89–103. http://doi.org/10.1007/s11571-012-9220-2

Feldman, G., Hayes, A., Kumar, S., Greeson, J., & Laurenceau, J.-P. (2006). Mindfulness and Emotion Regulation: The Development and Initial Validation of the Cognitive and Affective Mindfulness Scale-Revised (CAMS-R). Journal of Psychopathology and Behavioral Assessment, 29(3), 177–190.

Fox, M. D., Corbetta, M., Snyder, A. Z., Vincent, J. L., & Raichle, M. E. (2006). Spontaneous neuronal activity distinguishes human dorsal and ventral attention systems. Proceedings of the National Academy of Sciences, 103(26), 10046–10051.

Fransson, P. (2005). Spontaneous low-frequency BOLD signal fluctuations: An fMRI investigation of the resting-state default mode of brain function hypothesis. Human Brain Mapping, 26(1), 15–29.

Freunberger, R., Werkle-Bergner, M., Griesmayr, B., Lindenberger, U., & Klimesch, W. (2011). Brain oscillatory correlates of working memory constraints. Brain Research, 1375, 93–102.

Friston, K. J. (1994). Functional and effective connectivity in neuroimaging: a synthesis. Human Brain Mapping, 2 (1-2), 56–78.

Gaspar, P. A., Ruiz, S., Zamorano, F., Altayó, M., Pérez, C., Bosman, C. A., & Aboitiz, F. (2011). P300 amplitude is insensitive to working memory load in schizophrenia. BMC Psychiatry, 11, 29.

Gazzaley, A., Cooney, J. W., Rissman, J., & D'Esposito, M. (2005). Top-down suppression deficit underlies working memory impairment in normal aging. Nature Neuroscience, 8(10), 1298–1300.

Gevins, A., & Cutillo, B. (1993). Spatiotemporal dynamics of component processes in human working memory. Electroencephalography and Clinical Neurophysiology, 87(3), 128–143.

Gevins, A., & Smith, M. E. (2000). Neurophysiological measures of working memory and individual differences in cognitive ability and cognitive style. Cerebral Cortex (New York, N.Y.: 1991), 10(9), 829–839.

Gold, D. P., Andres, D., Etezadi, J., Arbuckle, T., Schwartzman, A., & Chaikelson, J. (1995). Structural equation model of intellectual change and continuity and predictors of intelligence in older men. Psychology and Aging, 10(2), 294–303.

Grabner, R. H., Neubauer, A. C., & Stern, E. (2006). Superior performance and neural efficiency: The impact of intelligence and expertise. Brain Research Bulletin, 69(4), 422–439.

Gray, J. A. (1970). The psychophysiological basis of introversion–extraversion. Behavioral Research and Therapy, 8, 249–266.

Gray, J. R., & Braver, T. S. (2002). Personality predicts working-memory—related activation in the caudal anterior cingulate cortex. Cognitive, Affective, & Behavioral Neuroscience, 2(1), 64–75.

Greicius, M. D., Krasnow, B., Reiss, A. L., & Menon, V. (2003). Functional connectivity in the resting brain: a network analysis of the default mode hypothesis. Proceedings of the National Academy of Sciences, 100 (1), 253.

Gulbinaite, R., van Rijn, H., & Cohen, M. X. (2014). Fronto-parietal network oscillations reveal relationship between working memory capacity and cognitive control. Frontiers in Human Neuroscience, 8, 761.

Gully, S. M., Payne, S. C., Koles, K. L. K., & Whiteman, J.-A. K. (2002). The impact of error training and individual differences on training outcomes: An attribute-treatment interaction perspective. Journal of Applied Psychology, 87(1), 143–155.

Gusnard, D. A., Raichle, M. E., Raichle, M. E., & others. (2001). Searching for a baseline: functional imaging and the resting human brain. Nature Reviews Neuroscience, 2(10), 685–694.

Hale, S., Rose, N. S., Myerson, J., Strube, M. J., Sommers, M., Tye-Murray, N., & Spehar, B. (2011). The structure of working memory abilities across the adult life span. Psychology and Aging, 26(1), 92–110.

Hampshire, A., Chamberlain, S. R., Monti, M. M., Duncan, J., & Owen, A. M. (2010). The role of the right inferior frontal gyrus: inhibition and attentional control. NeuroImage, 50(3), 1313–1319.

Hampson, M., Driesen, N. R., Skudlarski, P., Gore, J. C., & Constable, R. T. (2006). Brain connectivity related to working memory performance. The Journal of Neuroscience, 26(51), 13338–13343.

Harrison, T. L., Shipstead, Z., Hicks, K. L., Hambrick, D. Z., Redick, T. S., & Engle, R. W. (2013). Working memory training may increase working memory capacity but not fluid intelligence. Psychological Science, 24(12), 2409–2419.

Hertzog, C., & Dunlosky, J. (2012). Metacognitive approaches can promote transfer of training: Comment on McDaniel and Bugg. Journal of Applied Research in Memory and Cognition, 1(1), 61–63.

Hill, N. L., Kolanowski, A. M., Fick, D., Chinchilli, V. M., & Jablonski, R. A. (2014). Personality as a Moderator of Cognitive Stimulation in Older Adults at High Risk for Cognitive Decline. Research in Gerontological Nursing, 7(4), 159–170.

Hofmann, W., Schmeichel, B. J., & Baddeley, A. D. (2012). Executive functions and self-regulation. Trends in Cognitive Sciences, 16(3), 174–180.

Hölzel, B. K., Carmody, J., Vangel, M., Congleton, C., Yerramsetti, S. M., Gard, T., & Lazar, S. W. (2011). Mindfulness practice leads to increases in regional brain gray matter density. Psychiatry Research, 191(1), 36–43.

Huepe, D., & Salas, N. (2013). Fluid intelligence, social cognition, and perspective changing abilities as pointers of psychosocial adaptation. Frontiers in Human Neuroscience, 7.

Hunter, M. A., Coffman, B. A., Gasparovic, C., Calhoun, V. D., Trumbo, M. C., & Clark, V. P. (2015). Baseline effects of transcranial direct current stimulation on glutamatergic neurotransmission and large-scale network connectivity. Brain Research, 1594, 92–107.

Hunter, M. A., Coffman, B. A., Trumbo, M. C., & Clark, V. P. (2013). Tracking the neuroplastic changes associated with transcranial direct current stimulation: a push for multimodal imaging. *Frontiers in Human Neuroscience*, *7*.

Jaeggi, S. M., Buschkuehl, M., Shah, P., & Jonides, J. (2014). The role of individual differences in cognitive training and transfer. Memory & Cognition, 42(3), 464–480.

Jafri, M. J., Pearlson, G. D., Stevens, M., & Calhoun, V. D. (2008). A method for functional network connectivity among spatially independent intrinsic components in schizophrenia. Neuroimage, 39(4), 1666–1681.

James, W. (1890). The principles of psychology. New York : Holt. Retrieved from http://archive.org/details/theprinciplesofp01jameuoft

Jausovec, N., & Jausovec, K. (2003). Spatiotemporal brain activity related to intelligence: a low resolution brain electromagnetic tomography study. Brain Research. Cognitive Brain Research, 16(2), 267–272.

Jha, A. P., Morrison, A. B., Dainer-Best, J., Parker, S., Rostrup, N., & Stanley, E. A. (2015). Minds “at attention”: mindfulness training curbs attentional lapses in military cohorts. PloS One, 10(2), e0116889.

Jha, A. P., Stanley, E. A., Kiyonaga, A., Wong, L., & Gelfand, L. (2010). Examining the protective effects of mindfulness training on working memory capacity and affective experience. Emotion, 10(1), 54–64.

Johnson, W., Logie, R. H., & Brockmole, J. R. (2010). Working memory tasks differ in factor structure across age cohorts: Implications for dedifferentiation. Intelligence, 38(5), 513–528.

Jorgenson, L. A., Newsome, W. T., Anderson, D. J., Bargmann, C. I., Brown, E. N., Deisseroth, K., … Wingfield, J. C. (2015). The BRAIN Initiative: developing technology to catalyse neuroscience discovery. Philosophical Transactions of the Royal Society B: Biological Sciences, 370(1668).

Kabat-Zinn, J., Lipworth, L., & Burney, R. (1985). The clinical use of mindfulness meditation for the self-regulation of chronic pain. Journal of Behavioral Medicine, 8(2), 163–190.

Kane, M. J., & Engle, R. W. (2002). The role of prefrontal cortex in working-memory capacity, executive attention, and general fluid intelligence: An individual-differences perspective. Psychonomic Bulletin & Review, 9(4), 637–671.

Kawasaki, M., Kitajo, K., & Yamaguchi, Y. (2014). Fronto-parietal and fronto-temporal theta phase synchronization for visual and auditory-verbal working memory. *Frontiers in Psychology*, *5*.

Keeser, D., Meindl, T., Bor, J., Palm, U., Pogarell, O., Mulert, C., … Padberg, F. (2011). Prefrontal transcranial direct current stimulation changes connectivity of resting-state

networks during fMRI. The Journal of Neuroscience: The Official Journal of the Society for Neuroscience, 31(43), 15284–15293.

Kerns, J. G., Cohen, J. D., MacDonald, A. W., Cho, R. Y., Stenger, V. A., & Carter, C. S. (2004). Anterior cingulate conflict monitoring and adjustments in control. Science (New York, N.Y.), 303(5660), 1023–1026.

Klimesch, W. (1999). EEG alpha and theta oscillations reflect cognitive and memory performance: a review and analysis. Brain Research. Brain Research Reviews, 29(2-3), 169–195.

Klimesch, W. (2012). Alpha-band oscillations, attention, and controlled access to stored information. Trends in Cognitive Sciences, 16(12), 606–617.

Klimesch, W., Sauseng, P., & Hanslmayr, S. (2007). EEG alpha oscillations: The inhibition–timing hypothesis. Brain Research Reviews, 53(1), 63–88.

Klingberg, T. (2010). Training and plasticity of working memory. Trends in Cognitive Sciences, 14(7), 317–324.

Kok, A. (2001). On the utility of P3 amplitude as a measure of processing capacity. Psychophysiology, 38(3), 557–577.

Kolb, B., & Muhammad, A. (2014). Harnessing the power of neuroplasticity for intervention. Frontiers in Human Neuroscience, 8.

Lakey, C. E., Berry, D. R., & Sellers, E. W. (2011). Manipulating Attention via Mindfulness Induction Improves P300-based Brain-Computer Interface Performance. *Journal of Neural Engineering*, *8*(2), 025019.

Langer, E. J. (2000). Mindful Learning. Current Directions in Psychological Science, 9(6), 220–223.

Larson, M. J., Steffen, P. R., & Primosch, M. (2013). The impact of a brief mindfulness meditation intervention on cognitive control and error-related performance monitoring. Frontiers in Human Neuroscience, 7.

Lawlor-Savage, L., & Goghari, V. M. (2014). Working memory training in schizophrenia and healthy populations. Behavioral Sciences (Basel, Switzerland), 4(3), 301–319.

Lazar, S. W., Bush, G., Gollub, R. L., Fricchione, G. L., Khalsa, G., & Benson, H. (2000). Functional brain mapping of the relaxation response and meditation. Neuroreport, 11(7), 1581–1585.

Leech, R., Kamourieh, S., Beckmann, C. F., & Sharp, D. J. (2011). Fractionating the Default Mode Network: Distinct Contributions of the Ventral and Dorsal Posterior Cingulate Cortex to Cognitive Control. The Journal of Neuroscience, 31(9), 3217–3224.

Lewis, C. M., Baldassarre, A., Committeri, G., Romani, G. L., & Corbetta, M. (2009). Learning sculpts the spontaneous activity of the resting human brain. Proceedings of the National Academy of Sciences of the United States of America, 106(41), 17558–17563.

Liang, X., Zou, Q., He, Y., & Yang, Y. (2015). Topologically Reorganized Connectivity Architecture of Default-Mode, Executive-Control, and Salience Networks across Working Memory Task Loads. Cerebral Cortex, bhu316.

Lippelt, D. P., Hommel, B., & Colzato, L. S. (2014). Focused attention, open monitoring and loving kindness meditation: effects on attention, conflict monitoring, and creativity – A review. Frontiers in Psychology, 5.

Lomas, T., Ivtzan, I., & Fu, C. H. Y. (2015). A systematic review of the neurophysiology of mindfulness on EEG oscillations. *Neuroscience and Biobehavioral Reviews*, *57*, 401–410.

Lövdén, M., Bäckman, L., Lindenberger, U., Schaefer, S., & Schmiedek, F. (2010). A theoretical framework for the study of adult cognitive plasticity. Psychological Bulletin, 136(4), 659–676.

Luck, S. J. (2014). An Introduction to the Event-Related Potential Technique. MIT Press.

Lustig, C., Shah, P., Seidler, R., & Reuter-Lorenz, P. A. (2009). Aging, training, and the brain: a review and future directions. Neuropsychology Review, 19(4), 504–522.

Lutz, A., Slagter, H. A., Dunne, J. D., & Davidson, R. J. (2008). Attention regulation and monitoring in meditation. Trends in Cognitive Sciences, 12(4), 163–169.

MacDonald, A. W., Cohen, J. D., Stenger, V. A., & Carter, C. S. (2000). Dissociating the Role of the Dorsolateral Prefrontal and Anterior Cingulate Cortex in Cognitive Control. Science, 288(5472), 1835–1838.

Makeig, S., Delorme, A., Westerfield, M., Jung, T.-P., Townsend, J., Courchesne, E., & Sejnowski, T. J. (2004). Electroencephalographic Brain Dynamics Following Manually Responded Visual Targets. *PLoS Biology*, *2*(6).

Malinowski, P. (2013). Neural mechanisms of attentional control in mindfulness meditation. Frontiers in Neuroscience, 7, 8.

Manna, A., Raffone, A., Perrucci, M. G., Nardo, D., Ferretti, A., Tartaro, A., … Romani, G. L. (2010). Neural correlates of focused attention and cognitive monitoring in meditation. Brain Research Bulletin, 82(1–2), 46–56.

Martin, D. M., Liu, R., Alonzo, A., Green, M., & Loo, C. K. (2014). Use of transcranial direct current stimulation (tDCS) to enhance cognitive training: effect of timing of stimulation. Experimental Brain Research, 1–7.

Mason, M. F., Norton, M. I., Van Horn, J. D., Wegner, D. M., Grafton, S. T., & Macrae, C. N. (2007). Wandering minds: the default network and stimulus-independent thought. Science, 315(5810), 393–395.

McCabe, D. P., Roediger, H. L., McDaniel, M. A., Balota, D. A., & Hambrick, D. Z. (2010). The Relationship Between Working Memory Capacity and Executive Functioning: Evidence for a Common Executive Attention Construct. Neuropsychology, 24(2), 222–243.

Melby-Lervag, M., & Hulme, C. (2013). Is working memory training effective? A meta-analytic review. Developmental Psychology, 49(2), 270.

Menon, V., & Uddin, L. Q. (2010). Saliency, switching, attention and control: a network model of insula function. Brain Structure & Function, 214(5-6), 655–667.

Mercado, E. (2008). Neural and cognitive plasticity: from maps to minds. Psychological Bulletin, 134(1), 109–137.

Michel, C. M., Koenig, T., Brandeis, D., Gianotti, L. R. R., & Wackermann, J. (2009). Electrical Neuroimaging. Cambridge University Press.

Milham, M. P., & Banich, M. T. (2005). Anterior cingulate cortex: an fMRI analysis of conflict specificity and functional differentiation. Human Brain Mapping, 25(3), 328–335.

Miller, E. K., & Cohen, J. D. (2001). An Integrative Theory of Prefrontal Cortex Function. Annual Review of Neuroscience, 24(1), 167–202.

Missonnier, P., Herrmann, F. R., Zanello, A., Bâ, M. B., Curtis, L., Canovas, D., … Merlo, M. C. G. (2012). Event-related potentials and changes of brain rhythm oscillations during working memory activation in patients with first-episode psychosis. Journal of Psychiatry & Neuroscience : JPN, 37(2), 95–105.

Miyake, A., Friedman, N.P., 2012. The nature and organization of individual differences in executive functions: four general conclusions. Current Directions in Psychological Science 21, 8–14.

Moore, A., & Malinowski, P. (2009). Meditation, mindfulness and cognitive flexibility. Consciousness and Cognition, 18(1), 176–186.

Morrison, A. B., Goolsarran, M., Rogers, S. L., & Jha, A. P. (2014). Taming a wandering attention: Short-form mindfulness training in student cohorts. Frontiers in Human Neuroscience, 7, 897.

Mõttus, R., Realo, A., Allik, J., Esko, T., Metspalu, A., & Johnson, W. (2015). Within-Trait Heterogeneity in Age Group Differences in Personality Domains and Facets: Implications for the Development and Coherence of Personality Traits. PLoS ONE, 10(3).

Mrazek, M. D., Franklin, M. S., Phillips, D. T., Baird, B., & Schooler, J. W. (2013). Mindfulness Training Improves Working Memory Capacity and GRE Performance While Reducing Mind Wandering. Psychological Science, 0956797612459659.

Murias, M., Webb, S. J., Greenson, J., & Dawson, G. (2007). Resting state cortical connectivity reflected in EEG coherence in individuals with autism. Biological Psychiatry, 62(3), 270–273.

Neubauer, A. C., & Fink, A. (2009). Intelligence and neural efficiency. Neuroscience and Biobehavioral Reviews, 33(7), 1004–1023.

Neubauer, A. C., Fink, A., & Schrausser, D. G. (2002). Intelligence and neural efficiency: The influence of task content and sex on the brain–IQ relationship. Intelligence, 30(6), 515–536.

Nitsche, M. A., & Paulus, W. (2000). Excitability changes induced in the human motor cortex by weak transcranial direct current stimulation. The Journal of Physiology, 527(3), 633–639.

Oelhafen, S., Nikolaidis, A., Padovani, T., Blaser, D., Koenig, T., & Perrig, W. J. (2013). Increased parietal activity after training of interference control. Neuropsychologia, 51(13), 2781–2790.

Oken, B. S., Salinsky, M. C., & Elsas, S. M. (2006). Vigilance, alertness, or sustained attention: physiological basis and measurement. Clinical Neurophysiology : Official Journal of the International Federation of Clinical Neurophysiology, 117(9), 1885–1901.

Onton, J., Delorme, A., & Makeig, S. (2005). Frontal midline EEG dynamics during working memory. NeuroImage, 27(2), 341–356.

Overbeek, T. J. M., Nieuwenhuis, S., & Ridderinkhof, K. R. (2005). Dissociable Components of Error Processing: On the Functional Significance of the Pe Vis-à-vis the ERN/Ne. Journal of Psychophysiology, 19(4), 319–329.

Owen, A. M., McMillan, K. M., Laird, A. R., & Bullmore, E. (2005). N-back working memory paradigm: a meta-analysis of normative functional neuroimaging studies. Human Brain Mapping, 25(1), 46–59.

Patton, J. H., Stanford, M. S., & Barratt, E. S. (1995). Factor structure of the Barratt impulsiveness scale. Journal of Clinical Psychology, 51(6), 768–774.

Peña-Gómez, C., Sala-Lonch, R., Junqué, C., Clemente, I. C., Vidal, D., Bargalló, N., … Bartrés-Faz, D. (2012). Modulation of large-scale brain networks by transcranial direct current stimulation evidenced by resting-state functional MRI. Brain Stimulation, 5(3), 252–263.

Peña-Gómez, C., Vidal-Piñeiro, D., Clemente, I. C., Pascual-Leone, Á., & Bartrés-Faz, D. (2011). Down-Regulation of Negative Emotional Processing by Transcranial Direct Current Stimulation: Effects of Personality Characteristics. PLoS ONE, 6(7), e22812.

Perkins and Salomon, 1992.Transfer of learning. International Encyclopedia of Education, Second Edition Oxford, England: Pergamon Press.

Petersen, S. E., & Posner, M. I. (2012). The attention system of the human brain: 20 years after. Annual Review of Neuroscience, 35, 73–89.

Pfurtscheller, G., Stancák Jr., A., & Neuper, C. (1996). Event-related synchronization (ERS) in the alpha band — an electrophysiological correlate of cortical idling: A review. International Journal of Psychophysiology, 24(1–2), 39–46.

Plewnia, C., Zwissler, B., Längst, I., Maurer, B., Giel, K., & Krüger, R. (2013). Effects of transcranial direct current stimulation (tDCS) on executive functions: influence of COMT Val/Met polymorphism. Cortex; a Journal Devoted to the Study of the Nervous System and Behavior, 49(7), 1801–1807.

Polanía, R., Nitsche, M. A., & Paulus, W. (2011). Modulating functional connectivity patterns and topological functional organization of the human brain with transcranial direct current stimulation. Human Brain Mapping, 32(8), 1236–1249.

Polich, J. (2007). Updating P300: An Integrative Theory of P3a and P3b. Clinical Neurophysiology : Official Journal of the International Federation of Clinical Neurophysiology, 118(10), 2128–2148.

Polich, J., & Criado, J. R. (2006). Neuropsychology and neuropharmacology of P3a and P3b. International Journal of Psychophysiology, 60(2), 172–185.

Power, J. D., Cohen, A. L., Nelson, S. M., Wig, G. S., Barnes, K. A., Church, J. A., … Petersen, S. E. (2011). Functional Network Organization of the Human Brain. Neuron, 72(4), 665–678.

Prakash, R. S., De Leon, A. A., Patterson, B., Schirda, B. L., & Janssen, A. L. (2014). Mindfulness and the aging brain: a proposed paradigm shift. Frontiers in Aging Neuroscience, 6, 120.

Raghavachari, S., Lisman, J. E., Tully, M., Madsen, J. R., Bromfield, E. B., & Kahana, M. J. (2006). Theta Oscillations in Human Cortex During a Working-Memory Task: Evidence for Local Generators. *Journal of Neurophysiology*, *95*(3), 1630–1638.

Raichle, M. E., MacLeod, A. M., Snyder, A. Z., Powers, W. J., Gusnard, D. A., & Shulman, G. L. (2001). A default mode of brain function. Proceedings of the National Academy of Sciences of the United States of America, 98 (2), 676–682.

Raisman, G. 1969. Neuronal plasticity in the septal nuclei of the adult rat. Brain Research, vol. 14, no. 1, pp. 25–48, 1969.

Rammstedt, B., & John, O. P. (2007). Measuring personality in one minute or less: A 10-item short version of the Big Five Inventory in English and German. Journal of Research in Personality, 41(1), 203–212.

Rashid, B., Damaraju, E., Pearlson, G. D., & Calhoun, V. D. (2014). Dynamic connectivity states estimated from resting fMRI Identify differences among Schizophrenia, bipolar disorder, and healthy control subjects. *Frontiers in Human Neuroscience*, *8*, 897.

Ravizza, S. M., Behrmann, M., & Fiez, J. A. (2005). Right parietal contributions to verbal working memory: Spatial or executive? Neuropsychologia, 43(14), 2057–2067.

Redick, T. S., Shipstead, Z., Harrison, T. L., Hicks, K. L., Fried, D. E., Hambrick, D. Z., … Engle, R. W. (2013). No evidence of intelligence improvement after working memory training: A randomized, placebo-controlled study. Journal of Experimental Psychology: General, 142(2), 359–379.

Reinhart, R. M. G., Zhu, J., Park, S., & Woodman, G. F. (2015). Synchronizing theta oscillations with direct-current stimulation strengthens adaptive control in the human brain. Proceedings of the National Academy of Sciences, 201504196.

Ridderinkhof, R. K. (2002). Micro- and macro-adjustments of task set: activation and suppression in conflict tasks. Psychological Research, 66(4), 312–323.

Roux, F., & Uhlhaas, P. J. (2014). Working memory and neural oscillations: α-γ versus θ-γ codes for distinct WM information? Trends in Cognitive Sciences, 18(1), 16–25.

Sahdra, B. K., MacLean, K. A., Ferrer, E., Shaver, P. R., Rosenberg, E. L., Jacobs, T. L., … Saron, C. D. (2011). Enhanced response inhibition during intensive meditation training predicts improvements in self-reported adaptive socioemotional functioning. Emotion (Washington, D.C.), 11(2), 299–312.

Saliasi, E., Geerligs, L., Lorist, M. M., & Maurits, N. M. (2013). The Relationship between P3 Amplitude and Working Memory Performance Differs in Young and Older Adults. PLoS ONE, 8(5), e63701.

Sarnthein, J., Petsche, H., Rappelsberger, P., Shaw, G. L., & von Stein, A. (1998). Synchronization between prefrontal and posterior association cortex during human working memory. Proceedings of the National Academy of Sciences of the United States of America, 95(12), 7092–7096.

Sauseng, P., Klimesch, W., Schabus, M., & Doppelmayr, M. (2005). Fronto-parietal EEG coherence in theta and upper alpha reflect central executive functions of working memory. *International Journal of Psychophysiology*, *57*(2), 97–103.

Schaie, K. W., Willis, S. L., & Caskie, G. I. L. (2004). The Seattle Longitudinal Study: Relationship Between Personality and Cognition. Neuropsychology, Development, and Cognition. Section B, Aging, Neuropsychology and Cognition, 11(2-3), 304–324.

Schmiedek, F., Hildebrandt, A., Lövdén, M., Wilhelm, O., & Lindenberger, U. (2009). Complex span versus updating tasks of working memory: The gap is not that deep. Journal of Experimental Psychology: Learning, Memory, and Cognition, 35(4), 1089–1096.

Semple, R. J. (2010). Does Mindfulness Meditation Enhance Attention? A Randomized Controlled Trial. Mindfulness, 1(2), 121–130.

Shapiro, S. L., Brown, K. W., Thoresen, C., & Plante, T. G. (2011). The moderation of Mindfulness-based stress reduction effects by trait mindfulness: Results from a randomized controlled trial. Journal of Clinical Psychology, 67(3), 267–277.

Shipley, W.C., Gruber, C.P., Martin, T.A., & Klein, A.M. (2009). Shipley-2 manual. Los Angeles, CA: Western Psychological Services

Shipstead, Z., Redick, T. S., & Engle, R. W. (2012). Is working memory training effective? Psychological Bulletin, 138(4), 628.

Slagter, H. A., Lutz, A., Greischar, L. L., Francis, A. D., Nieuwenhuis, S., Davis, J. M., & Davidson, R. J. (2007). Mental Training Affects Distribution of Limited Brain Resources. *PLoS Biol*, *5*(6), e138.

Soltani, M., & Knight, R. T. (2000). Neural origins of the P300. Critical Reviews in Neurobiology, 14(3-4), 199–224.

Steriade, M. (2006). Grouping of brain rhythms in corticothalamic systems. Neuroscience, 137(4), 1087–1106.

Stiles, J. (2000). Neural plasticity and cognitive development. Developmental Neuropsychology, 18(2), 237–272.

Studer-Luethi, B., Jaeggi, S. M., Buschkuehl, M., & Perrig, W. J. (2012). Influence of neuroticism and conscientiousness on working memory training outcome. Personality and Individual Differences, 53(1), 44–49.

Takahashi, T., Murata, T., Hamada, T., Omori, M., Kosaka, H., Kikuchi, M., … Wada, Y. (2005). Changes in EEG and autonomic nervous activity during meditation and their association with personality traits. International Journal of Psychophysiology, 55(2), 199–207.

Tang, Y.-Y., Hölzel, B. K., & Posner, M. I. (2015). The neuroscience of mindfulness meditation. Nature Reviews Neuroscience, 16(4), 213–225.

Tang, Y.-Y., Lu, Q., Geng, X., Stein, E. A., Yang, Y., & Posner, M. I. (2010). Short-term meditation induces white matter changes in the anterior cingulate. Proceedings of the National Academy of Sciences, 107(35), 15649–15652.

Tang, Y.-Y., Ma, Y., Fan, Y., Feng, H., Wang, J., Feng, S., … Fan, M. (2009). Central and autonomic nervous system interaction is altered by short-term meditation. Proceedings of the National Academy of Sciences of the United States of America, 106(22), 8865–8870.

Tegelbeckers, J., Bunzeck, N., Duzel, E., Bonath, B., Flechtner, H.-H., & Krauel, K. (2015). Altered salience processing in attention deficit hyperactivity disorder. *Human Brain Mapping*, *36*(6), 2049–2060.

Tekin, S., & Cummings, J. L. (2002). Frontal-subcortical neuronal circuits and clinical neuropsychiatry: an update. *Journal of Psychosomatic Research*, *53*(2), 647–654.

Tenke, C. E., Kayser, J., Abraham, K., Alvarenga, J. E., & Bruder, G. E. (2015). Posterior EEG alpha at rest and during task performance: Comparison of current source density and field potential measures. International Journal of Psychophysiology, 97(3), 299–309.

Teper, R., & Inzlicht, M. (2013). Meditation, mindfulness and executive control: the importance of emotional acceptance and brain-based performance monitoring. Social Cognitive and Affective Neuroscience, 8(1), 85–92.

Thatcher, R. W., North, D., & Biver, C. (2005). EEG and intelligence: Relations between EEG coherence, EEG phase delay and power. Clinical Neurophysiology, 116(9), 2129–2141.

Thelen, E., & Smith, L. B. (1996). A dynamic systems approach to the development of cognition and action. MIT press.

Thompson, E., & Varela, F. J. (2001). Radical embodiment: neural dynamics and consciousness. Trends in Cognitive Sciences, 5(10), 418–425. http://doi.org/10.1016/S1364-6613(00)01750-2

Thompson, T. W., Waskom, M. L., Garel, K.-L. A., Cardenas-Iniguez, C., Reynolds, G. O., Winter, R., … Gabrieli, J. D. E. (2013). Failure of Working Memory Training to Enhance Cognition or Intelligence. PLoS ONE, 8(5), e63614.

Tuladhar, A. M., Huurne, N. ter, Schoffelen, J.-M., Maris, E., Oostenveld, R., & Jensen, O. (2007). Parieto-occipital sources account for the increase in alpha activity with working memory load. Human Brain Mapping, 28(8), 785–792.

Uddin, L. Q., Clare Kelly, A. m., Biswal, B. B., Xavier Castellanos, F., & Milham, M. P. (2009). Functional connectivity of default mode network components: Correlation, anticorrelation, and causality. Human Brain Mapping, 30(2), 625–637.

Uhlhaas, P. J., Haenschel, C., Nikolić, D., & Singer, W. (2008). The Role of Oscillations and Synchrony in Cortical Networks and Their Putative Relevance for the Pathophysiology of Schizophrenia. Schizophrenia Bulletin, 34(5), 927–943.

Unsworth, N., Fukuda, K., Awh, E., & Vogel, E. K. (2014). Working memory and fluid intelligence: Capacity, attention control, and secondary memory retrieval. Cognitive Psychology, 71, 1–26.

Unsworth, N., Redick, T. S., Spillers, G. J., & Brewer, G. A. (2012). Variation in working memory capacity and cognitive control: goal maintenance and microadjustments of control. Quarterly Journal of Experimental Psychology (2006), 65(2), 326–355.

Vaidya, C. J., & Gordon, E. M. (2013). Phenotypic Variability in Resting-State Functional Connectivity: Current Status. Brain Connectivity, 3(2), 99–120. http://doi.org/10.1089/brain.2012.0110

Valentine, E. R., & Sweet, P. L. G. (1999). Meditation and attention: A comparison of the effects of concentrative and mindfulness meditation on sustained attention. Mental Health, Religion & Culture, 2(1), 59–70.

Van Den Heuvel, M. P., Mandl, R. C. W., Kahn, R. S., & Hulshoff Pol, H. E. (2009). Functionally linked intrinsic networks reflect the underlying structural connectivity architecture of the human brain. Human brain mapping, 30(10), 3127–3141.

Vanderhasselt, M.-A., Raedt, R. D., & Baeken, C. (2009). Dorsolateral prefrontal cortex and Stroop performance: Tackling the lateralization. Psychonomic Bulletin & Review, 16(3), 609–612.

Vanhaudenhuyse, A., Demertzi, A., Schabus, M., Noirhomme, Q., Bredart, S., Boly, M., … Laureys, S. (2010). Two Distinct Neuronal Networks Mediate the Awareness of Environment and of Self. Journal of Cognitive Neuroscience, 23(3), 570–578.

Varela, F., Lachaux, J.-P., Rodriguez, E., & Martinerie, J. (2001). The brainweb: Phase synchronization and large-scale integration. Nature Reviews Neuroscience, 2(4), 229–239.

Vogel, E. K., McCollough, A. W., & Machizawa, M. G. (2005). Neural measures reveal individual differences in controlling access to working memory. Nature, 438(7067), 500–503.

Von Stein, A., & Sarnthein, J. (2000). Different frequencies for different scales of cortical integration: from local gamma to long range alpha/theta synchronization. International Journal of Psychophysiology, 38(3), 301–313.

Wass, S. V., Scerif, G., & Johnson, M. H. (2012). Training attentional control and working memory – Is younger, better? Developmental Review, 32(4), 360–387.

Weissman, D. H., Roberts, K. C., Visscher, K. M., & Woldorff, M. G. (2006). The neural bases of momentary lapses in attention. Nature Neuroscience, 9(7), 971–978.

Weldon, R. B., Mushlin, H., Kim, B., & Sohn, M.-H. (2013). The effect of working memory capacity on conflict monitoring. Acta Psychologica, 142(1), 6–14.

Werk, C. M., & Chapman, C. A. (2003). Long-term potentiation of polysynaptic responses in layer V of the sensorimotor cortex induced by theta-patterned tetanization in the awake rat. *Cerebral Cortex (New York, N.Y.: 1991)*, *13*(5), 500–507.

Witkiewitz, K., Lustyk, M. K. B., & Bowen, S. (2013). Re-Training the Addicted Brain: A Review of Hypothesized Neurobiological Mechanisms of Mindfulness-Based Relapse Prevention. Psychology of Addictive Behaviors : Journal of the Society of Psychologists in Addictive Behaviors, 27(2), 351–365.

Wood, C. C., & Jennings, J. R. (1976). Speed-accuracy tradeoff functions in choice reaction time: Experimental designs and computational procedures. Perception & Psychophysics, 19(1), 92–102.

Woodworth, R.S., & Thorndike, E.L. (1901). The influence of improvement in one mental function upon the efficiency of other functions. (I). Psychological Review, 8(3), 247–261.

Yerkes, R.M. and Dodson, J.D.. (1908). The relation of strength of stimulus to rapidity of habit-formation. Journal of Comparative Neurology and Psychology, 18, 459-482.

Yuval-Greenberg, S., Tomer, O., Keren, A. S., Nelken, I., & Deouell, L. Y. (2008). Transient Induced Gamma-Band Response in EEG as a Manifestation of Miniature Saccades. Neuron, 58(3), 429–441.

Zeidan, F., Johnson, S. K., Diamond, B. J., David, Z., & Goolkasian, P. (2010). Mindfulness meditation improves cognition: Evidence of brief mental training. Consciousness and Cognition, 19(2), 597–605.

Zheng, Z., Zhu, X., Yin, S., Wang, B., Niu, Y., Huang, X., … Li, J. (2015). Combined Cognitive-Psychological-Physical Intervention Induces Reorganization of Intrinsic Functional Brain Architecture in Older Adults. Neural Plasticity, 2015.